Probing CHO cells metabolism using metabolomics and fluxomics tools

Tiago Martins da Costa Duarte

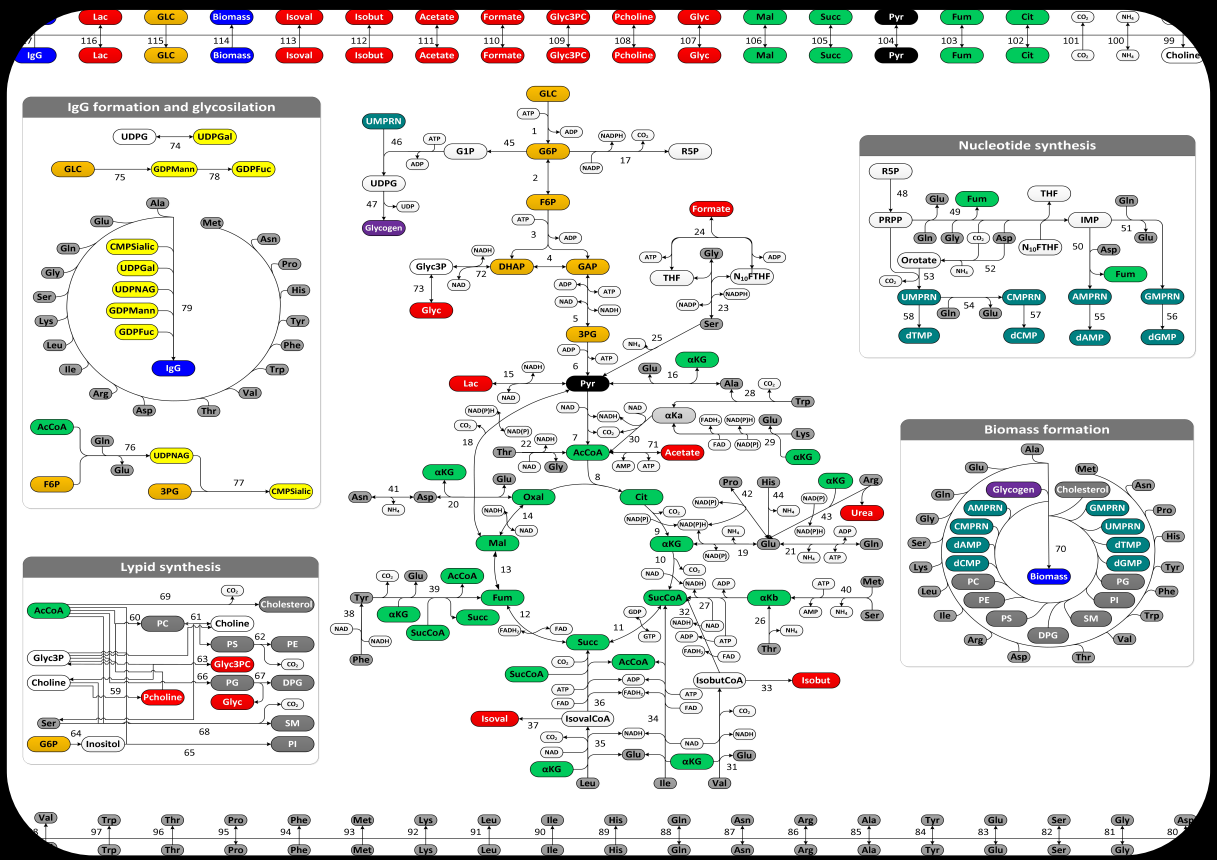

Dissertation presented to obtain the Ph.D degree in Technological and Engineering Sciences, specialization in Systems Biology

Instituto de Tecnologia Química e Biológica António Xavier | Universidade Nova de Lisboa

Oeiras,
June, 2016

UNIVERSIDADE NOVA DE LISBOA

Probing CHO cells metabolism using metabolomics and fluxomics tools

Tiago Martins da Costa Duarte

Dissertation presented to obtain the Ph.D degree in Technological and Engineering Sciences, specialization in Systems Biology

Instituto de Tecnologia Química e Biológica António Xavier | Universidade Nova de Lisboa

Oeiras, June, 2016

Brief Contents

ACKNOWLEDGEMENTS

I would like to express my deepest gratitude to the people who have contributed directly or indirectly to the content of this thesis.

To my supervisor Prof. Paula Alves, for the opportunity to carry out my thesis in your group, for your encouraging words and for your commitment to make the Animal Cell Technology Unit a place to do high quality research.

To my co-supervisor Dr. Ana Teixeira, for your vision and guidance throughout this journey. For always pushing me to overcome myself and my limitations.

To Prof. Manuel Carrondo, for your words on leadership, hard work and resilience.

To Dr. Nuno Carinhas, for your important contributions to this work, for sharing your insights in metabolic flux analysis and your solid scientific writing style.

To Laura Barreiro, for your important contribution to this work during your research training and for your high spirit inside and outside the lab.

To my colleagues at the ACTU, former and present, especially to Marcos Sousa for your support in bioprocesses and for the camaraderie in the lab, to Dr. Ana Barbas for our fruitful discussions about antibodies, to Dr. Cristina Peixoto for your help in purifying those antibodies, and to Daniel Pais for being such a curious and enthusiast colleague and helping me with my last experiments in the lab.

To the iBET Analytical Services Unit, to António Ferreira, Dr. Rosário Bronze, Cláudia Duarte, and especially to Cláudio Almeida, for sharing your knowledge and expertise with GC-MS.

To the Centro de Ressonância Magnética António Xavier (CERMAX) team, Dr. Pedro Lamosa, Dr. Helena Matias, Dr. Ana Rute Neves and Dr. Manolis Matzapetakis for your support and for our fruitful discussions concerning NMR.

To the Cell Systems Engineering group at TU Delft, especially to Prof. Joseph Heijnen for being such a good host, to Dr. Aljoscha Wahl and Dr. Reza Seifar for your support and guidance during my stay, to Angela ten Pierick and Cor Ras for teaching me the tips and tricks of mass spectrometry.

To a particular bunch who made my life and work better every day, especially for your warm welcome at the "Insects Team", Fabiana Fernandes, João Vidigal and Mafalda Dias.

To Dr. Francisca Monteiro and Dr. Filipa Rodrigues for your endless help and our always interesting discussions about science and philosophy.

To my Science Runners team, (besides the ones mentioned above) Sofia Rebelo, Daniel Simão, Marta Silva, Catarina Pinto, Marta Estrada, João Sá, Rita Costa, Ana Oliveira and Paulo Fernandes, who still give me every day the motivation to always go faster and further to reach my goals – in life as well as in running.

To the InTeraQB team for giving me an excuse to make funny paper hats and to interact with awesome people and scientists across ITQB and beyond.

To the financial support provided by Fundação para a Ciência e a Tecnologia (FCT) (SFRH/BD/81553/2011 and PTDC/BBB-BSS/0518/2012). The NMR spectrometers are part of the National NMR Facility supported by FCT (RECI/BBB-BQB/0230/2012).

To my friends for our discussions about engineering, arts and life, in particular, João Henriques, Ana Espiga and João Chaves. To Cecília and Rita for you continuous support. To an inspiring Iron(wo)man and "office" partner, Ranna, in sports and in business. To my second encouraging "office" partner, Laura Moya. To a team of advisors who helped me in the last stage of my PhD, preparing me for the Viva: Francisca Monteiro, João Dias and Rodolfo Marques.

To my family for your support and for handling all the twists and turns inherent to this journey, especially my father Leonel, mother Graça, brother Leonel, and Tia Manuela. To my cousins Pedro and Fernando for your continuous support and encouragement. To James Lanham, for being my special advisor.

With special jubilation, to my beloved wife Ana.

FCT Fundação para a Ciência e a Tecnologia
MINISTÉRIO DA CIÊNCIA, TECNOLOGIA E ENSINO SUPERIOR

CERMAX
Centro de Ressonância Magnética António Xavier

From left to right: Dr. Rosário Bronze, Dr. Rui Oliveira, Dr. Ana Teixeira, Tiago Duarte, Dr. Paula Alves, Dr. Joana Azeredo, Dr. Arménia Carrondo, Dr. Pedro Cruz.

JURY

Prof. Rui Oliveira, Associate Professor with Habilitation, Chemistry Department at Faculdade de Ciências e Tecnologia, Universidade Nova de Lisboa, Caparica, Portugal

Prof. Joana Azeredo, Associate Professor with Habilitation, Biological Engineering Department at Universidade do Minho, Braga, Portugal

Prof. Maria do Rosário Bronze, Associate Professor at Faculdade de Farmácia, Universidade de Lisboa, Lisboa, Portugal

Dr. Pedro Cruz, Chief Scientific Officer (CSO) at ECBio, Oeiras, Portugal

Prof. Paula Marques Alves, Principal Investigator and Head of the the Animal Cell Technology Unit at IBET/ITQB-NOVA, Chief Executive Officer (CEO) at IBET, Oeiras, and Invited Associated Professor at Faculdade de Ciências e Tecnologia, Universidade Nova de Lisboa, Caparica, Portugal (Supervisor)

Dr. Ana Palma Teixeira, Auxiliary Investigator and Head of the Bioengineering & Systems Biology Lab at the Animal Cell Technology Unit, IBET/ITQB-NOVA, Oeiras, Portugal (Co-Supervisor)

“We are drowning in information but starved for knowledge.”

John Naisbitt

CONTENTS

LIST OF FIGURES

LIST OF TABLES

LIST OF ABBREVIATIONS AND ACRONYMS

αKG	α-ketoglutarate
3PG	3-phosphoglycerate
6PG	6-phosphogluconate
6PGDH	6-phosphogluconate dehydrogenase
AcCoA	acetyl coenzyme A
ADCC	antibody-dependent cellular cytotoxicity
Ala	alanine
Amm	ammonia
Arg	arginine
Asn	asparagine
Asp	aspartate
ATP	adenosine-3-phosphate
BHK	baby hamster kidney
But	butyrate-treated
CHO	chinese hamster ovary
Cit	citrate
CO_2	carbon dioxide
Cys	cysteine
DHAP	dihydroxyacetone-phosphate
DHFR	dihydrofolate reductase
DMF	dimethylformamide
DMSO	dimethylsulfoxide
DNA	deoxyribonucleic acid
DoE	design of experiment
DSS-d_6	deuterated 3-(trimethylsilyl)-1-propanesulfonic acid sodium salt, 2,2-Dimethyl-2-silapentane-5-sulfonate-d_6 sodium salt
EPO	erythropoietin
F6P	fructose-6-phosphate
FBA	flux balance analysis
FSH	follicle-stimulating hormone
Fum	fumarate
G6P	glucose-6-phosphate
GC	gas chromatography
GEM	genome-scale model
GIDH	glutamate dehydrogenase
Glc	glucose
GLDH	glutamate dehydrogenase
Gln	glutamine
Glu	glutamate
GLUT5	fructose transporter
Gly	glycine
Glyc3PC	glycerol-3-phosphocholine
GOI	gene of interest

GS	glutamine synthetase
HDAC	histone deacetylases
HEK	human embryonic kidney
His	histidine
HP	high producer
hPRL	human prolactin
IgG	immunoglobulin
Ile	isoleucine
INST	isotopically non-stationary
Lac	lactate
LC	liquid chromatography
LDH-A	lactate dehydrogenase A
Leu	leucine
LP	low producer
Lys	lysine
mAb	monoclonal antibody
Mal	malate
MDH II	malate dehydrogenase II
ME	malic enzymes
Met	methionine
MFA	metabolic flux analysis
MID	mass isotopomer distributions
miRNA	micro RNA
MOX	O-methoxyamine hydrochloride
mRNA	messenger RNA
MS	mass spectrometry
MSTFA	N-Methyl-N-(trimethylsilyl)trifluoroacetamide
MSX	methionine sulfoximine
MTBSTFA	N–Methyl-N-(t-Butyldimethylsilyl) trifluoroacetamide
MTX	methotrexate
NaBu	sodium butyrate
NAD^+/NADH	nicotinamide adenine dinucleotide
$NADP^+$/NADPH	nicotinamide adenine dinucleotide phosphate
NMR	nuclear magnetic resonance
O_2	oxygen
OAA	oxaloacetate
PC	pyruvate carboxylase
P_{CMV}	human cytomegalovirus promoter
PDH	pyruvate dehydrogenase
PEP	phosphoenol-pyruvate
PEPCK	phosphoenolpyruvate carboxykinase
Phe	phenylalanine
PPP	pentose phosphate pathway
Pro	proline
PYC2	pyruvate carboxylase

Pyr	pyruvate
R5P	ribose-5-phosphate
RNA	ribonucleic acid
SDS-PAGE	sodium dodecyl sulphate-polyacrylamide gel electrophoresis
SEAP	secreted alkaline phosphatase
Ser	serine
Suc	succinate
TCA	tricarboxylic acids
THF	tetrahydrofolate
Thr	threonine
TMB	tetramethylbenzidine
TMCS	tetramethylchlorosilane
tPA	tissue plasminogen activator
Tyr	tyrosine
Val	valine
ZFN	zinc-finger nuclease

THESIS PUBLICATIONS

Duarte, TM*, Carinhas, N*, Barreiro, LC, Carrondo, MJT, Alves, PM, Teixeira, AP, 2014, Metabolic responses of CHO cells to limitation of key amino acids. Biotechnol. Bioeng 111(10):2095–2106 *equal contributions

Carinhas N*, **Duarte TM***, Barreiro LC, Carrondo MJT, Alves PM, Teixeira AP, 2013, Metabolic signatures of GS CHO cell clones associated with butyrate treatment and culture phase transition, Biotechnol. Bioeng. 110(12):3244-3257 *equal contributions

Duarte TM, Seifar RM, Wahl AS, Alves PM, Teixeira AP, Exploring GS-CHO metabolism under control and butyrate-treated conditions through parallel ^{13}C-labeling experiments (manuscript in preparation)

BOOK CHAPTERS

Sá JV, **Duarte TM**, Carrondo MJT, Alves PM, Teixeira AP, 2014, Metabolic Flux Analysis: A Powerful Tool in Animal Cell Culture, Animal Cell Culture, Springer, Cell Engineering 9:521-539

Duarte TM, Carinhas N, Silva AC, Alves PM, Teixeira AP, 2013, ^{1}H-NMR protocol for exometabolome analysis of cultured mammalian cells, Animal Cell Biotechnology-Methods and Protocols, Springer, 3rd edition, Part III:237-247

OTHER PUBLICATIONS

Duarte TM, Carrondo MJT, Alves PM, Teixeira AP, 2011, Fluorescence-based tools to improve biopharmaceutical process development, BMC proceeding 5(Suppl 8):O5

Teixeira AP, **Duarte TM**, Carrondo MJT, Alves PM, 2011, Synchronous Fluorescence Spectroscopy as a Novel Tool to Enable PAT Applications in Bioprocess, Biotechnol. Bioeng 108(8):1852-61

Teixeira AP, **Duarte TM**, Oliveira R, Carrondo MJT, Alves PM, 2011, High-throughput analysis of animal cell cultures using two-dimensional fluorometry, J. Biotechnol 151(3):255-260

SUMMARY

Chinese hamster ovary (CHO) cells are preferred mammalian hosts for industrial production of therapeutic glycoproteins such as monoclonal antibodies (mAbs), used to treat cancer and immunological disorders. In these cells, the glutamine synthetase (GS) expression system has been widely used for efficient selection of high-yielding clones. However, fundamental knowledge on the metabolic behavior of GS-CHO cells in culture and its impact on product yields have not been yet systematized. The overall objective of this thesis was to comprehensively analyse the metabolome and fluxome of CHO cells exploring how the metabolism is affected by clonal variability and culture conditions. This information is then used to generate hypotheses on how metabolic wiring impacts mAb production.

We started by implementing a ^{1}H-NMR metabolomics platform to assess the metabolic footprints of two GS-CHO cell clones expressing IgG_4 under control and butyrate-treated conditions. With this method, we could accurately quantify the dynamic profiles of about 40 metabolites, including some not usually analyzed in mammalian cells cultures, such as acetate, pyruvate, formate, TCA cycle intermediates, lipid and nucleotide precursors. Noteworthy, several metabolic by-products accumulated in the cell supernatant over culture time, suggesting that different metabolic nodes could be targeted to decrease overflow metabolism. Overall, most carbon and nitrogen sources were consumed at higher rates during the exponential phase than during the stationary phase.

Then, the exometabolome data collected for the different clones and conditions was contextualized in a network model of 117 intracellular and transport reactions to estimate the corresponding fluxomes through metabolic flux analysis (MFA). While the two clones displayed generally similar specific metabolic fluxes, butyrate treatment had a marked effect on sustaining high nutrient consumption along culture time. This

resulted in a significantly increased energetic state and biosynthetic activity during the stationary phase compared to control conditions, coinciding with the largest effect on specific productivity. Furthermore, the intracellular concentration pools of most metabolites measured in butyrate-treated cultures were 2.5-fold higher (on average) when compared to control cultures. Higher differences were observed for glutamine, alanine and citrate (up to 4-fold), hence these metabolites should be further explored in future experiments to study the impact on recombinant protein production.

In order to have a more in-depth view of cell metabolism, namely the relative activities of parallel pathways and substrate contributions to intracellular metabolites, we next performed tracer studies using labelled versions of the three most consumed nutrients ([1,2-^{13}C]glucose, [U-^{13}C/^{15}N]asparagine and [U-^{13}C/^{15}N]serine). Upon incubation of a high producing GS-CHO cell clone with each isotopic tracer, we collected samples over the exponential growth phase to follow the transient labelling profiles of intracellular metabolites by GC-MS and LC-MS. The patterns produced from the [1,2-^{13}C]glucose tracer revealed a high diversion of glucose to the pentose phosphate pathway when compared to that previously published for non-producing CHO cells during the same growth phase, suggesting this route as an important source of NADPH for recombinant protein synthesis. Another potential source of NADPH is the flux through malic enzyme, the high activity of which was suggested by the labelling pattern of pyruvate after incubation with [U-^{13}C/^{15}N]asparagine. Noteworthy, asparagine was essential for replenishing TCA cycle intermediates as well as for glutamine synthesis in GS-CHO cells. Together with asparagine, serine was confirmed to be a significant nitrogen source in these cells, with ^{15}N from both amino acid tracers propagating to many non-essential amino acids.

Finally, with the goal of better evaluating the importance of asparagine and serine in GS-CHO metabolism, we modulated the availability of these amino acids by culturing cells in the absence, or maintaining a low concentration, of each amino acid. The absence of asparagine in the medium caused growth arrest, and was associated with a

dramatic increase in pyruvate uptake, a higher ratio of pyruvate carboxylation to dehydrogenation and an inability for *de novo* asparagine synthesis. The release of ammonia and amino acids such as aspartate, glutamate and alanine were deeply impacted. This confirms asparagine to be essential for GS-CHO cells as the main source of intracellular nitrogen as well as having an important anaplerotic role for TCA cycle activity. In turn, serine limitation also negatively affected culture growth while triggering its *de novo* synthesis, confirmed by label incorporation coming from pyruvate, and reduced glycine and formate secretion congruent with its role as a precursor in the metabolism of one-carbon units. The results obtained suggest that feeding schemes of asparagine or serine should be tightly tuned to minimize by-product formation while assuring biosynthetic needs.

Overall, the work performed in the scope of this thesis contributes to unfold important insights into the metabolic operation of the industrially relevant GS-CHO cell expression host. An in-depth study of the metabolic network of GS-CHO cells allowed to uncover potential targets for minimizing overflow metabolism, reduce the diversion of resources to by-product accumulation or minimize their impact on recombinant protein production. Also allowed to couple PPP and ME activities, important sources of NADPH, with a high productive phenotype in GS-CHO cells. We believe that these markers represent an opportunity for future cell engineering efforts aiming the improvement of the production of biopharmaceuticals.

RESUMO

As células do ovário de hamster chinês (CHO, do inglês *Chinese Hamster Ovary*) são o hospedeiro mamífero preferido para a produção industrial de glicoproteínas terapêuticas, tais como os anticorpos monoclonais (mAbs, do inglês *monoclonal antibodies*) usados para o tratamento de cancro e doenças imunológicas. Nestas células, o sistema de expressão através da glutamina sintetase (GS) tem sido frequentemente utilizado para a selecção eficiente de clones de alto rendimento produtivo. No entanto, o conhecimento fundamental sobre o comportamento metabólico de células GS-CHO em cultura e o seu impacto sobre o rendimento na produtividade não tem sido sistematizado. O objectivo geral desta tese foi o de fazer uma análise exaustiva do metaboloma e do fluxoma de células CHO, explorando a forma como o metabolismo é afectado pela variabilidade clonal e condições de cultura. A informação resultante poderá então ser utilizada para formular hipóteses sobre o impacto que determinados rearranjos metabólicos podem ter sobre a produção de mAbs.

Começámos por implementar uma plataforma baseada em metabolómica através de RMN de protão para avaliar os perfis metabólicos de dois clones GS-CHO com diferentes níveis de expressão de uma imunoglobulina (IgG_4) em condições controlo e tratada com butirato. Com este método, conseguimos quantificar rigorosamente os perfis dinâmicos de cerca de 40 metabolitos, incluindo alguns que normalmente não são analisados em culturas de células de mamífero, tais como o acetato, piruvato, formato, intermediários do ciclo dos ácidos tricarboxílicos (ATC), e precursores de lípidos e nucleótidos. De salientar, vários sub-produtos metabólicos foram acumulados no sobrenadante das culturas ao longo do tempo, indicando que vários centros metabólicos podem ser alvo de acção no decréscimo de um metabolismo exagerado. De uma forma geral, a maior parte das fontes de carbono e azoto foi consumida durante a fase exponencial de crescimento celular com taxas de consumo superiores às observadas na fase estacionária.

Posteriormente, os dados do exo-metaboloma, recolhidos das culturas controlo ou tratadas com butirato, foram integrados num modelo metabólico com 117 reacções intracelulares ou de transporte celular para se poder estimar os fluxomas correspondentes através de uma metodologia clássica de análise de fluxos metabólicos. Apesar de ambos os clones apresentarem fluxos metabólicos específicos semelhantes, o tratamento com butirato teve um efeito significativo na manutenção de um elevado consumo de nutrientes ao longo do tempo de cultura. Isto resultou num aumento significativo do estado energético e da actividade biossintética durante a fase estacionária, quando o efeito sobre a produtividade específica é igualmente superior. Para além disto, as concentrações intracelulares obtidas para os metabolitos analisados foram em média 2.5 vezes superiores quando comparadas com as culturas controlo. Diferenças mais substanciais foram detectadas para a glutamina, alanina e citrato (cerca de 4 vezes superiores), pelo que estes metabolitos deverão ser deverão ser explorados em experiências futuras no estudo dos seus efeitos na produção de proteínas recombinantes.

De forma a obter uma visão mais detalhada sobre o metabolismo celular, nomeadamente sobre as actividades relativas de vias metabólicas paralelas e a contribuição de certos substratos para vários metabolitos intracelulares, decidiu-se fazer estudos com a incubação de compostos marcados dos três metabolitos mais consumidos (glucose-[1,2-^{13}C], asparagina-[U-^{13}C/^{15}N] and serina-[U-^{13}C/^{15}N]). Após a incubação de culturas com o clone de células GS-CHO com mais elevada produtividade com cada um dos isótopos durante a fase exponencial do crescimento celular, recolhemos amostras ao longo do tempo para podermos seguir os perfis transientes de incorporação da marca nos metabolitos intracelulares por GC-MS e LC-MS. Os perfis obtidos através da incubação com [1,2-^{13}C]glucose, revelam um desvio significativo de glucose através da via das pentoses fosfatadas quando comparadas com culturas de células CHO não-produtivas durante a mesma fase de crescimento, sugerindo que esta via pode ser uma importante fonte de poder redutor (NADPH), necessário para a

síntese de proteínas recombinantes. Outra fonte de NADPH é o fluxo através da reacção das enzimas málicas, como sugerido pela incorporação de isótopos observada no piruvato obtido através da asparagina-[U-^{13}C/^{15}N]. De salientar, a asparagina foi essencial para o reabastecimento de intermediários do ciclo ATC, tal como para a síntese de glutamina em células GS-CHO. Juntamente com a asparagina, a serina foi confirmada como sendo uma fonte de nitrogénio importante nestas células, tendo-se observado azoto (^{15}N) derivado de ambas as fontes em vários amino ácidos não-essenciais.

Finalmente, com o objectivo de avaliar a importância da asparagina e da serina no metabolismo de células GS-CHO, foi feita uma análise da disponibilidade da asparagina e da serina: através da cultura de células na ausência de cada um dos amino ácidos, ou através da cultura de células na presença de cada amino ácido em baixas concentrações. A ausência de asparagina no meio basal interrompeu o crescimento celular, e foi associado a um aumento acentuado do consumo de piruvato, um elevado rácio entre as reacções de carboxilação e desidrogenação de piruvato, e à incapacidade das células para a síntese *de novo* de asparagina. A secreção de amónia e de amino ácidos como o aspartato, glutamato e alanina foi igualmente afectada. Isto confirma que a asparagina é essencial para as células GS-CHO como principal fonte de nitrogénio, assim como tendo uma função anaplerótica na actividade do ciclo ATC. Por outro lado, a limitação de serina também afectou negativamente o crescimento celular tendo despoletado a síntese de novo de serina, confirmada pela incorporação do isótopo observada no piruvato, e reduziu a secreção de glicina e formato, de acordo com o seu papel como precursor no metabolismo de unidades com um carbono unitário. Estes resultados sugerem que as estratégias de alimentação com asparagina ou serina devem ser rigorosamente reguladas para se poder reduzir a formação de sub-produtos, e ao mesmo tempo manter as necessidades biossintéticas.

Em suma, esta tese contribui para o desvendar de importantes fenómenos biológicos no metabolismo de células GS-CHO com alto relevo industrial. O estudo aprofundado da rede metabólica das células GS-CHO permitiu identificar alvos de estudo para minimizar o metabolismo exagerado, reduzir o consumo de recursos dirigidos para a acumulação de produtos secundários ou o impacto sobre a produção de proteínas recombinantes. Da mesma forma, permitiu associar as actividades da via das pentoses fosfatadas e das enzimas málicas, importantes fontes de NADPH, a um fenótipo de produção elevada em células GS-CHO. Julgamos que estes elementos representam uma oportunidade para esforços futuros em engenharia celular no sentido de melhorar a produção de produtos farmacêuticos.

Chapter 1

Introduction

CONTENTS

1.1 Mammalian cells as production factories of biopharmaceuticals

Mammalian cells are the dominant biological system for the production of recombinant therapeutic proteins mainly due to their ability to perform human-like post-translational modifications. The first therapeutic protein produced from recombinant mammalian cells, tissue plasminogen activator (tPA), obtained market approval thirty years ago (reviewed by Butler and Spearman 2014; Wurm 2004). Nowadays, monoclonal antibodies (mAbs) constitute the main class of biopharmaceuticals produced from mammalian cell cultures. The development of antibody-based products has increased significantly over the years, representing 27 % of all biologic products approved as of 2014 (Walsh 2014). Global sales revenue for all mAb products in 2013 was nearly US$75 billion, representing the most lucrative single product class (Ecker et

al. 2015). Table 1 summarizes the mAb-based products approved after 2010 in Europe and in the USA.

Among common targets of mAbs are various types of cancer, and several inflammatory and cardiovascular diseases. The high incidence of these diseases, associated to an increasing and aging worldwide population and the standard of living in emerging markets increases the pressure to develop more efficient bioprocesses (Ecker et al. 2015).

The prevalence of mammalian cells over other expression systems, such as insect cells or *Escherichia coli*, goes parallel with the increasing proportion of approved molecules that show post-translational modifications, in particular glycosylation. It is crucial that therapeutic proteins display human-like glycosylation patterns to ensure their optimal efficacy and higher stability in the human serum (Butler and Spearman 2014). Although several mammalian cell lines are used for production of complex biopharmaceuticals (such as murine myeloma cells (NS0 and SP2/0), human embryonic kidney (HEK)-293 and baby hamster kidney (BHK)), nearly 70 % of all recombinant therapeutic proteins are produced in Chinese hamster ovary (CHO) cells (Jayapal et al. 2007).

Table 1.1 Monoclonal antibody (mAb)-based biopharmaceuticals produced in mammalian cells, approved in the United States and Europe after 2010 (adapted from Walsh 2014)

Product	Cell line	Company	Target	Date approved
Entyvio	CHO	Takeda Parma (USA) Millenium (UK)	Ulcerative colitis, Crohn's disease	2014 (USA/EU)
Sylvant	CHO	Janssen Biotech (USA)	Multicentric Castleman's disease	2014 (USA/EU)
Cyramza	NS0	Eli Lilly	Gastric cancer	2014 (USA)
Gazyva (USA) **Gazyvaro (EU)**	CHO	Roche (Genentech) Roche	Chronic lymphocytic leukemia	2014 (EU)/ 2013 (USA)
Inflectra **Remsima**	Sp2/0	Hospira (UK)	Arthritis, colitis, Crohn's, psoriasis, ankylosing spondylitis	2013 (USA)
Kadcyla	CHO	Roche/Genentech (UK)	Breast cancer	2013 (EU/USA)
Simponi Aria	Sp2/0	Janssen Biotech	Rheumatoid arthritis	2013 (USA)
Perjeta	CHO	Roche/Genentech (UK)	Breast cancer	2013 (EU) 2012 (USA)
Abthrax	NS0	GSK Human Genome Sciences	Inhalational anthrax	2012 (USA)
Adcetris	CHO	Takeda Pharma (UK) Seattle Genetics (USA)	Lymphoma	2012 (EU) 2011 (USA)
Benlysta	NS0	Glaxo Group (UK) Human Genome Sciences (USA)	Lupus	2011 (USA/EU)
Xgeva	CHO	Amgen (NL)	Bone loss associated to cancer	2011 (EU) 2010 (USA)
Yervoy	CHO	Bristol-Meyers Squibb (UK)	Melanoma	2011 (USA/EU)
Actemra (USA) **RoActemra (EU)**	-	Roche (UK)	Rheumatoid arthritis	2010 (USA) 2009 (EU)
Arzerra	NS0	Navartis/Genmab (UK)	Chronic lymphocytic leukaemia	2010 (EU) 2009 (USA)
Prolia	CHO	Amgen (NL)	Osteoporosis	2010 (EU/USA)
Scintimun	Hybridoma	CIS Bio International (FR)	In vivo diagnosis/investigation of sites of inflammation/infection via scientigraphic imaging	2010 (EU)

1.2 The Chinese Hamster Ovary Cells

The initial CHO cell strain was isolated at the laboratory of Theodore Puck, after culturing cells derived from the ovarian tissue of a Chinese hamster (Puck et al. 1958). After an unknown amount of culture time the morphology of some cells changed and these underwent spontaneous immortalization (reviewed by Wurm 2013). Several laboratories across the world have propagated the number of CHO cell lines being manipulated, considerably increasing the genetic and phenotypic diversity of the CHO cell system.

CHO cells are not only used to produce biopharmaceutical products that generate over US$50 billion annually, but the pipelines of pharmaceutical companies are also full of CHO-derived products in different phases of clinical trials (Wurm 2013). The success of these cells is explained by i) their robustness to growth to high cell densities in serum-free, chemically-defined suspension cultures, ii) their safety profile (they are unable to replicate most human pathogenic viruses), iii) their capacity to easily integrate foreign genes, and iv) the powerful selection systems (such as dihydrofolate reductase (DHFR) and glutamine synthetase (GS)) (Durocher and Butler 2009).

From all CHO-derived cell lines, the CHO-DG44 with the DHFR selection system and the CHO-K1 in combination with the GS selection system are the two most used industrially. The CHO-DG44 cells are DHFR deficient, thus they are incapable of reducing dihydrofolate to tetrahydrofolate, a reaction that is crucial for the *de novo* synthesis of nucleotides. As a result, dhfr negative cells have to be cultured in medium containing hypoxanthine and thymidine (HT) in order to survive. Therefore, by transfecting these cells with a plasmid encoding the gene of interest (GOI) and a functional dhfr gene, successfully transfected cells can be selected in culture media without HT. Additional selection pressure can be introduced using stepwise increases in the concentration of methotrexate (MTX), an antagonist of DHFR, which results in amplified copies of the transfected dhfr gene together with the GOI, consequently increasing the productivity of the GOI (Hacker et al. 2009; Wurm 2013) (Fig. 1.1A).

GS-CHO-K1 cells are obtained from the transfection with a functional glutamine synthetase gene together with gene of interest on the same plasmid, followed by culture selection in medium without glutamine (Wurm 2013). Nevertheless, CHO cells possess endogenous GS activity which must be specifically inhibited by low levels of methionine sulphoximine (MSX) to ensure that any cell that survive on gln-deficient medium possess the GOI. Gene amplification can be achieved by further application of higher levels of MSX. However, as opposed to the DHFR amplification system, a single round of amplification is sufficient to achieve high expression levels of the GOI (Noh et

al. 2013) (Fig. 1.1B/C). Importantly, the GS-system has the advantage of reducing the accumulation of ammonia in the medium, a toxic byproduct resultant of glutaminolysis in other cell lines (Wurm 2013).

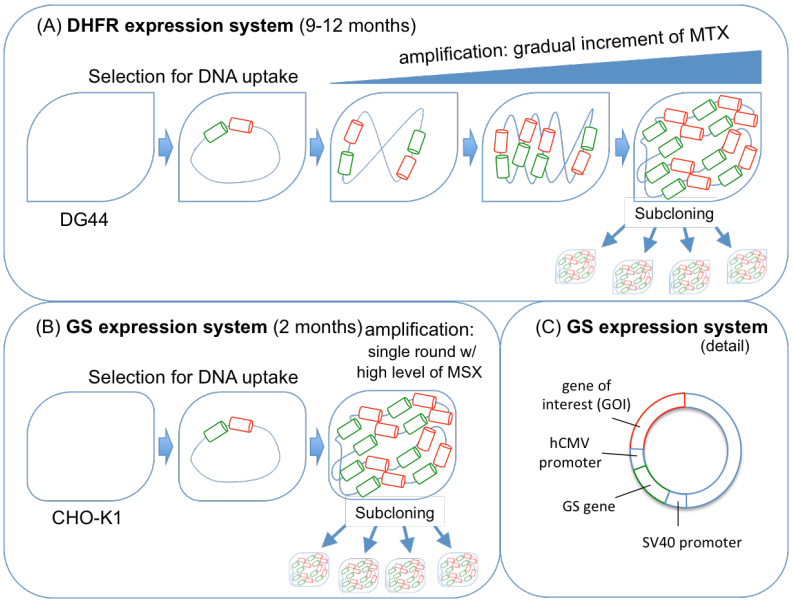

Figure 1.1 GS and DHFR expression systems. DHFR system (A) requires five to six fold more time to attain a high expression rate, when compared to the GS system (B); (C) detail of the GS-expression system (adapted from Noh et al. 2013).

The development and identification of a highly-productive cell line generally involves a high-throughput selection step, which is usually low efficient and thus generates large numbers of low and non-productive cells, like in the case of GS selection in CHO cell lines (Cacciatore et al. 2010). It has been supposed that the basal expression from the endogenous GS gene may decrease the GS-system selection stringency (Fan et al. 2012). In order to maximize the number of desirable and rare highly-productive candidates, which is to say improving selection stringency, while reducing timeline and costs, Fan and colleagues knocked out the endogenous CHO GS gene. This was achieved through specific zinc-finger nuclease (ZFN)-based technology, and translated into a six-fold efficiency increase in cell line generation, when compared to GS-CHO cells (expressing both endogenous GS activity and the GS system) (Fan et al. 2012). Posteriorly, the

same group used a weakened promoter to drive GS expression (an engineered version of the SV40), in combination with the GS-knockout CHO cells, resulting in improved productivities associated to higher selection efficiencies and eliminating the need to add MSX, a toxic and expensive chemical GS inhibitor, to the culture medium (Fan et al. 2013).

1.3 Performance of mammalian cell bioprocesses

In order to meet the growing demand for mAb products, there is a persistent need to develop robust, cost-effective and efficient cell culture processes (Sheikholeslami et al. 2013; Wurm 2004). The mammalian cell culture field has matured significantly over the years, and today it is possible to deliver gram per litre titres of product in fed-batch cultures, representing over 100-fold improvement since the 1980s (Mead et al. 2012). This yield improvement has been the result of better expression vector designs, improved host cell lines, development of medium composition and feeding regimes, and advanced screening techniques.

1.3.1 Culture medium and fed batch processes

Medium development for mammalian cells has progressed enormously since the first formulations that required serum supplementation (Bruhlmann et al. 2015). Fully chemically defined media consisting of amino acids, vitamins, trace elements, inorganic salts, lipids and insulin or insulin-like growth factors, have been developed for mAb production processes (Pasupuleti et al. 2008). In general, medium development is labor-intensive and time-consuming, and it is based in statistical design of experiment (DoE) (Kim and Lee 2009).

Not all antibody production cell lines can achieve high yield in chemically defined media. Therefore, the addition of non-animal hydrolysates (composed of amino acids, small peptides, carbohydrates, vitamins and minerals) became a common strategy in order to maximize cell density, culture viability and productivity (Kim and Lee 2009; Michiels et al. 2011). However, because of its composition complexity and lot-to-lot variations, hydrolysates can be a significant source of medium variability.

Bioreactors operating in fed-batch mode are the most common processes used to produce monoclonal antibodies (Wurm 2004). High yields of up to 10 g/L have been achieved through feeding optimization, which increase cell productivity, maintain cell viability, and extend culture longevity (Kim et al. 1998; Lee et al. 1999; Liu et al. 2001). Perfusion has been used also like fed-batch mode for the production of recombinant proteins in mammalian cell cultures. In fact, the highest volumetric productivities have been achieved using continuous stirred tank bioreactors in perfusion mode, using internal retention systems. However, due to the limited scalability of these systems, novel biopharmaceuticals have been produced in fed-batch cultures (Lee et al. 2012).
While the most common approach to develop a feed medium is to concentrate the basal medium, a sophisticated optimization of feed composition and feeding strategy would require to take into consideration: nutrient consumption, by-product accumulation and the balance between promoting growth versus volumetric productivity. Nevertheless, step-wise bolus addition of the feed solution to the production bioreactor is still the most widely used technique in the industry due to its simplicity and scalability (Li et al. 2014).

1.3.2 Classical approaches to improve specific productivity

Further strategies for process optimization often included modulations of temperature, or addition of chemicals (Fig 1.2). Temperature shifts from 37 °C to 30-34 °C allowed improvements in cell specific and volumetric productivity, protein folding and product quality (Al-Fageeh et al. 2006). For instance, Yoon et al showed a significant improvement in specific productivity of erythropoietin (EPO) and follicle-stimulating hormone (FSH) when decreasing culture temperature from 37 to 32 °C (Yoon et al. 2006). Several chemicals have been applied as productivity enhancers for recombinant protein production in cultured mammalian cells, including dimethylsulfoxide (DMSO) (Allen et al. 2008), sodium butyrate (NaBu) (Yee et al. 2008) and rapamycin (Balcarcel and Stephanopoulos 2001). In particular, sodium butyrate has been used to improve the production of tPA (Palermo et al. 1991), EPO (Wang et al. 2011), mAb (Mimura et al.

2001) and human prolactin (hPRL) (Goulart et al. 2010). NaBu has several effects on cultured cells, namely growth inhibition, induction or repression of gene expression and induction of apoptosis (Jiang and Sharfstein 2008). NaBu regulates gene transcription by improving gene accessibility through the inhibition of histone deacetylases (HDAC) (Jiang and Sharfstein 2008). When hyper acetylated histones become more relaxed complexes with DNA, genes are more accessible to regulatory factors and thus transcribed at higher rates.

Although these strategies managed to boost productivities and yields, they have to be optimized for each cell line, being time consuming and frequently with little or no understanding of the actual reasoning behind the improvements obtained (Selvarasu et al. 2012).

1.3.3 Cell line engineering

A significant amount of work has been done to genetically engineer host cells to improve their robustness, enhance their specific productivity or improve product quality (Le et al. 2015). Cell engineering efforts usually target the machinery of several cellular processes, such as: apoptosis, protein expression, cell proliferation, metabolism, cell cycle, protein secretion and post translational modifications (Balcarcel and Stephanopoulos 2001; Fischer et al. 2015; Le et al. 2015) (Fig. 1.2). Most common approaches include the knockout and downregulation of key genes that are involved in these mechanisms, or the introduction of other genes (Fischer et al. 2015). A lot of attention has been given to anti-apoptosis engineering as a main strategy of cell line development for protein production (Majors et al. 2007). Anti-apoptosis approaches rely, at a first instance, on the overexpression of anti-apoptotic genes held by mammalian cells. These genes encode for anti-death proteins that prevent the activation of the apoptosis cascade. Among these, with positive results in terms of cell density and protein titre are Bcl-2, Bcl-xL and 30Kc6 (Figueroa et al. 2007; Mastrangelo et al. 2000; Wang et al. 2011). A second approach to avoid apoptosis has been the inhibition of caspase expression, since the activation of members of the caspase family

is part of the cellular processes that lead to apoptosis (Laken and Leonard 2001; Mimura et al. 2000). Thirdly, the inhibition of cell cycle progression as this significantly increases cell density and productivity in mammalian cell cultures. These strategies led to a slower cell cycle that lead to an extended cell viability through time and, consequently, an increased specific mAb productivity (Balcarcel and Stephanopoulos 2001). Recently, Tan et al (2015) introduced heat shock protein 27 in CHO cells in order to improve cell density and viability with a 2.3-fold increase in mAb titre, affecting apoptosis signaling pathways and delaying caspase activities.

CHO cells and other continuous mammalian cell lines have low efficiency in completely oxidizing glucose to CO_2, producing high levels of lactate. This can cause acidification of culture medium and lead to high osmolarity and low viability due to the base added to control the medium pH. A significant amount of work has been performed to reduce lactate and ammonia accumulation; strategies include the partial disruption of lactate dehydrogenase A (LDH-A) gene, or the overexpression of pyruvate carboxylase (PYC2), increasing the flux of glucose into TCA cycle (Kim and Lee 2007b), or the overexpression of urea cycle enzymes, such as carbamoyl phosphate synthetase I and ornithine transcarbamoylase (Chen et al. 2001; Kim and Lee 2007a; Park et al. 2000; Wilkens and Gerdtzen 2015).

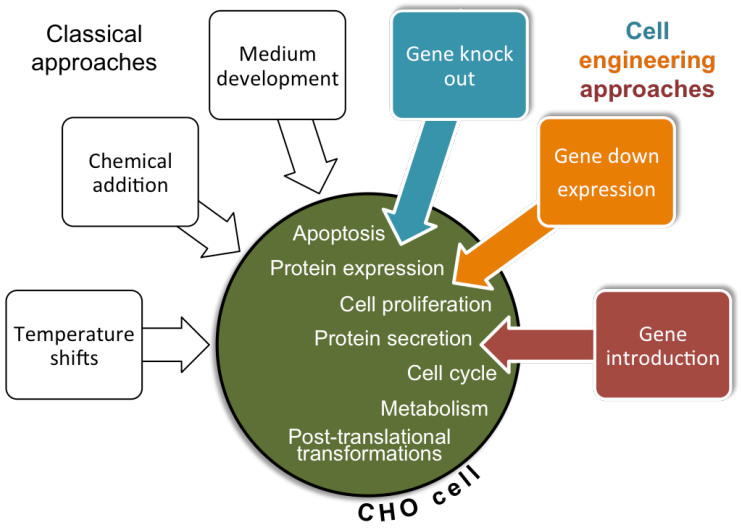

Figure 1.2 Classical and cell engineering approaches to improve the specific productivity of CHO cells. Inside the CHO cell representation are presented the common targets of cell engineering approaches (Fischer et al. 2015; Le et al. 2015).

Very recently, Wilkens and Gerdtzen (2015) compared different engineered CHO cell clones with overexpression of several metabolic genes, namely PYC2, MDH II (malate dehydrogenase II) and GLUT5 (fructose transporter), in terms of their effect on IgG production performance. Although previous studies had reported improved specific productivities when overexpressing these genes (Chong et al. 2010; Irani et al. 1999; Le et al. 2013), Wilkens study did not corroborate those studies. They propose that the modifications promote an unbalanced redox state which may have a negative impact on IgG assembly and, consequently, reducing its secretion.

Glycosylation pathway engineering has also received considerable attention because glycan structures on antibodies can have substantial impact on clearance rate and bioactivities. For instance, gene deletion technologies have been used to decrease or eliminate the fucose on antibodies to dramatically improve antibody-dependent cellular cytotoxicity (ADCC) (Malphettes et al. 2010). In particular, non-fucosylated antibodies present a substantially higher efficacy than their fucosylated counterparts, in most cases, due to a higher ADCC activity (Konno et al. 2012). However, these

approaches are often host cell dependent, as each host has its own specific post-translational modifications fingerprint.

1.4 Systems biotechnology

With the progress made in Omics technologies in last 10 years, it became possible to study the molecular traits that characterize a high-producer cell (reviewed by Carinhas et al. 2012). High-throughput experimental techniques and superior computer power have permitted obtaining great amounts of Omics data, allowing to gain in-depth knowledge of biological processes. Although we cannot integrate yet all levels of information, we can use parts of it to determine new targets for host improvement (Lee et al. 2005). The recent sequencing of CHO genome, combined with advances in technologies that allow a better characterization of the proteome and metabolome of cells under different environments, may now permit a comprehensive understanding of these industrially relevant cell lines (Datta et al. 2013; Xu et al. 2011). Figure 1.3 summarizes most of the state-of-the-art tools used in systems biology studies.

1.4.1 Transcriptome and proteome layers

Transcriptomics, the study of all RNA forms encoded by the genome, has been widely exploited for cell line and bioreactor process development in the last decades (Chen et al. 2016). DNA microarrays have revolutionized the quantitative analysis of gene expression as they allow covering a large number of genes simultaneously in a single assay. This genome-scale technology has been applied to i) investigate gene expression under culture conditions that enhance productivity, including temperature shifts, butyrate treatment, and high osmolality (Gatti et al. 2007; Kantardjieff et al. 2010), ii) to compare CHO cell lines expressing different levels of recombinat protein (Clarke et al. 2011; Doolan et al. 2010; Kang et al. 2014), or iii) at different culture stages. For instance, Wong and co-workers applied comparative transcriptomic analysis to find key factors regulating the apoptosis, which occurs at the later stages of batch and fed-batch cultures (Wong et al. 2006a; 2006b). Overexpressing the identified anti-apoptotic genes (Fadd and Faim), or knocking down the pro-apoptotic genes (Alg-2, and

Requiem), allowed to increase the yields of the recombinant protein up to 2.5-fold in CHO cells.

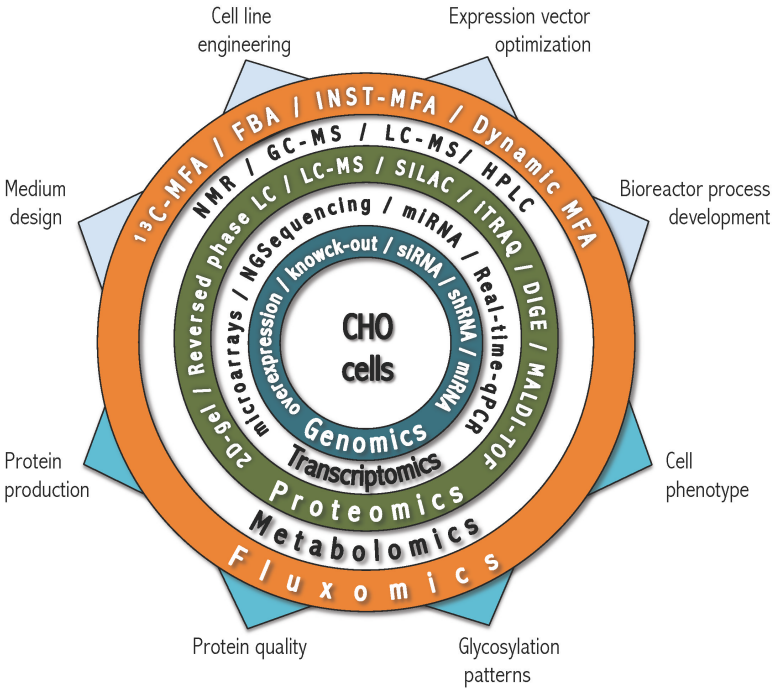

Figure 1.3 Diagram of systems biology and state-of-the-art technologies and methods used to improve the performance of CHO cells. Main goals for Omics approaches (upper arrows) and main insights (lower arrows) to be obtained or predicted (Chen et al. 2016; Kildegaard et al. 2013; Lewis et al. 2016).

MicroRNAs are a class of small non-coding RNAs that can regulate global gene expression at the post-transcriptional level by mRNA cleavage or translational repression, or both. The ability of microRNAs to bind multiple target genes and regulate their abundance has made them significantly interesting for CHO cell engineering (Barron et al. 2011). There are several studies focused on improving productivity, either through miRNA overexpression or knockdown (Fischer et al. 2015). Jadhav and co-workers managed to improve cell growth and enhance the specific protein productivity of CHO cells (3-fold) through the stable overexpression of miR-17 (Jadhav et al. 2014). The stable miR-30 overexpression in CHO cells allowed to improve

secreted alkaline phosphatase (SEAP) productivity or maximum cell density by 2-fold (Fischer et al. 2014). Kelly and co-workers successfully improved productivity of SEAP-producing CHO cells through miR-23 knock-down, without affecting cell growth (Kelly et al. 2015). Interestingly, the improved productive phenopype was associated with an enhanced mitochondrial function and TCA cycle activity.

Comparatively, proteomics has been less explored than the transcriptional analysis for cell culture engineering (Griffin et al. 2007). Proteomics has been applied to identify differentially expressed proteins that may have an impact in cell growth and death, metabolism and protein processing, including glycosylation (Baycin-Hizal et al. 2012). Since the transcriptome and the proteome might not be directly correlated, combined approaches are often chosen in order to deepen our understanding of cellular physiology (Baycin-Hizal et al. 2012). For instance, Doolan and co-workers combined microarray and proteomic expression profiling of CHO cells to identify genes and proteins involved in high cell growth rates and protein production (Doolan et al. 2010). 21 targets were identified and associated to high growth rate, from which 5 were validated by siRNA knockdown and considered feasible for further studies. More recently, multiple mAb-producing CHO cell lines were compared through a multiomics approach, including microarray-based transcriptomics and LC-MS/MS shotgun proteomics, in order to identify features associated to a high productivity (Kang et al. 2014). This approach allowed identifying several potential genes and proteins associated to productivity, cell size and proliferation.

1.4.2 Metabolome and Fluxome layers

Although metabolomics had been shadowed by genomics, transcriptomics and proteomics, it has reached a “golden era” potentiated by analytical techniques and computational power (Idle and Gonzalez 2007). The comprehensive quantification of the cellular metabolome (the collection of metabolites at any given time) can be carried out by state-of-the-art analytical approaches based on nuclear magnetic resonance (NMR) or mass spectrometry (MS) (Fig. 1.3).

Obtaining an accurate snapshot of cellular metabolite levels is dependent of several delicate steps, which address significant challenges inherent to physicochemical diversity, variety and rapid turnover of metabolites in mammalian cells. The sampling and arrest of metabolic activity (usually achieved by the use of a quenching solution at low temperatures) should be fast to prevent significant changes in metabolite concentrations due to ongoing metabolic activity. As opposed to extracellular metabolites that can be easily quantified through supernatant analysis, the accurate quantification of intracellular metabolite pools is dependent also of an extraction step. Furthermore, MS analysis is usually preceded by separation and ionization steps that allow reducing the complexity of a biological sample and the analysis of a smaller number of metabolites at different retention times (Alonso et al. 2015). Liquid and gas chromatography (LC and GC, respectively) are the most common separation techniques.

Additionally, after data acquisition through NMR or MS, spectral data must be processed through several sequential steps aimed at accurately identifying and quantifying the metabolites present in a culture sample, including baseline correction, peak detection or spectral alignment. Peak overlapping issues require deconvolution methods; several software are currently available to facilitate spectra integration, such as Chenomx NMR Suite or Agilent MassHunter.

Metabolomics tools have been used to support animal cell process development. For instance, Sellick et al. (2011b) developed a feeding approach based on the identification of limiting nutrients in a mAb-producing CHO cell culture by GC-MS analysis. By supplying the limiting nutrients, the biomass could be increased by 35 % and the antibody titre could be doubled (Sellick et al. 2011a). In another MS-based study, Chong et al. (2010) found a high accumulation rate of malate in the medium of CHO cells. Subsequent cell engineering to overexpress malate dehydrogenase II resulted in significant growth improvement.

On the other hand, it is the fluxome (collection of metabolic fluxes inside the cell) the actual target of considerable attention as it reflects the final output of the interactions between genome, transcriptome, proteome and metabolome layers; and it is closely related to the cells phenotype (Sauer 2006). As opposed to transcripts, proteins and metabolites, fluxes cannot be measured directly and they have to be inferred from data through model-based interpretation. Mathematical models became essential to quantify the cellular metabolism under different culture conditions, and generate the knowledge needed to optimize the performance of cell factories.

When metabolic steady-state can be assumed, metabolic flux analysis (MFA) became the preferential technique to obtain quantitative information about *in vivo* cellular metabolism (Wiechert 2001). Thus, MFA can provide the knowledge to allow a manipulation of metabolic fluxes, in order to obtain improved process yields and better quality attributes in biopharmaceuticals production (Sá et al. 2015).

Classical (or stoichiometric) MFA is based on the flux balancing of intracellular metabolites within a stoichiometric matrix, in which extracellular measurements such as nutrient uptake, by-product secretion and growth rate are used as constraints to determine intracellular fluxes (Antoniewicz 2015). Such stoichiometric flux analysis can provide a good snapshot of the fluxome state, allowing for instance a broad comparison of different culture conditions. However, it cannot resolve fluxes through cyclic pathways, reversible and parallel reactions; only the net fluxes can be calculated (Goudar et al. 2010).

Table 1.2 Compilation of recent studies performed on CHO cells using isotopic tracers (Ahn and Antoniewicz 2012; Lewis et al. 2016)

CHO cell lines	Tracers	Culture method	Techniques	Major Achievements	References; Year
CHO-K1	(U-^{13}C)glc;	Batch	INST-^{13}C -MFA	Central carbon metabolism flux mapped, highlighting metabolic reversibility and compartmentation	(Nicolae et al. 2014)
mAb-producing DHFR-CHO	(U-^{13}C)glc; (1,2-^{13}C)glc; (2-^{13}C)pyr; (U-^{13}C)gln	Fed-batch	^{13}C-MFA	Determination of changes in metabolic pathways and enzyme activities involved in cell growth regulation	(Dean and Reddy 2013)
mAb-producing DHFR-CHO	(1,2-^{13}C)glc; (U-^{13}C)glc; (1-^{13}C)glc	Fed-batch	^{13}C-MFA	Peak specific antibody production associated to highly oxidative metabolic state	(Templeton et al. 2013)
CHO-K1 (adherent)	(1,2-^{13}C)glc; (U-^{13}C)glc; (U-^{13}C)gln	Fed-batch	^{13}C-MFA	Significant rewiring of intracellular metabolism during shift from exponential to stationary phase	(Ahn and Antoniewicz 2013)
CHO-K1 (adherent)	(1,2-^{13}C)glc; (U-^{13}C)gln	Fed-batch	^{13}C-MFA; ^{13}C-NMFA	Intracellular metabolic fluxes in growth and non-growth phases	(Ahn and Antoniewicz 2011)
mAb-producing GS-CHO SF18	(U-^{13}C)glc	Fed-batch	^{13}C-MFA	Metabolic mapping for the late non-growth phase	(Sengupta et al. 2011)
Unknown	(U-^{13}C)glc; (1-^{13}C)glc	Perfusion	^{13}C-MFA	Determination of fluxes through PPP and anaplerotic conversion of pyruvate to oxaloacetate	(Goudar et al. 2010)

(mAb – monoclonal antibody; glc – glucose; pyr – pyruvate; gln – glutamine; INST – isotopically non-stationary; NMFA – non-stationary MFA; GS – glutamine synthetase; DHFR – dihydrofolate reductase)

Complementing extracellular data with isotopic labeling information in ^{13}C-MFA studies provides higher resolution, allowing to detect even the more subtle differences in flux phenotypes. An isotopic tracer is a molecule where a specific atom has been replaced with a different stable isotope, usually ^{13}C, ^{15}N or ^{2}H. When labeled versions of nutrients are added to cells, the label propagates through the network as a function of metabolic activity, producing labeling patterns in the backbone of metabolic intermediates over time. Mathematical models describing this propagation of the label are then used to calculate the *in vivo* fluxes from measured isotopic patterns and extracellular transport rates. The accumulation of a specific labeled metabolite allows to identify preferential pathways or their activity through time. Isotopic tracers became essential for providing insights on intracellular pathways, in particular on the presence

of parallel, reversible or cyclic pathways (Crown and Antoniewicz 2012; Quek et al. 2010). These approaches have been applied primarily to support metabolic engineering of simpler biological systems (Crown et al. 2015; Leighty and Antoniewicz 2012; Toya and Shimizu 2013), but are starting to be applied more and more to animal cell cultures as well. Table 1.2 shows a compilation of recent MFA studies done on CHO cells, using isotopic tracers.

A recent trend to resolve intracellular pathways has been the use of parallel labelling experiments. This technique has been addressed as COMPLETE-MFA – short for complementary parallel labelling experiments technique for metabolic flux analysis. This method results from fitting several data sets from several experiments into a single flux model (Antoniewicz et al. 2007). The main advantage is that it allows producing results with increased accuracy over ^{13}C-MFA (Antoniewicz 2015). This approach minimizes the issue of selecting the best single tracer that would allow a good screening of the whole network and with a good resolution (Crown and Antoniewicz 2012).

1.5 Thesis motivation and outline

Up to now, cell engineering has encompassed intuitive manipulations of enzyme activities, allowing slight improvements in yields and quality of therapeutic protein production. More efficient production requires deeper understanding of cellular metabolism and its regulation, which provides the building blocks and energy for cell growth and recombinant protein production.

This thesis aims at studying the central metabolism of producer cells in order to identify markers for posterior metabolic engineering and ultimately to improve the production of target proteins. We combined experimental and computational tools for quantitative dissection of the metabolome and fluxome of GS-CHO cell lines expressing a model monoclonal antibody. In chapter 2, the exometabolome of two IgG_4-producing GS-CHO cell clones cutured in control and butyrate-treated conditions was analysed

through ^{1}H-NMR spectroscopy, allowing a comprehensive characterization of medium composition, in particular the identification of i) the most consumed substrates, and ii) several metabolic by-products secreted over culture time besides the common lactate and ammonia. This data was then integrated into an extended metabolic network to estimate the *in vivo* fluxes in different productivity states using MFA, to identify metabolic features correlated with higher productivity. In chapter 3, we performed short-term parallel labelling experiments using ^{13}C and ^{15}N labeled versions of the three most consumed substrates (glucose, asparagine and serine), to explore with more detail the intracellular metabolism of GS-CHO cells in control and butyrate-treated cultures. The incorporation of ^{13}C/^{15}N from each substrate into intracellular metabolites, including amino acids and intermediates from glycolysis, pentose phosphate pathways and TCA cycle, was followed over time by GC-MS and LC-MS. In chapter 4, modulations of asparagine and serine availability in cell culture media were performed, in order to study their essentiality and effect on cell physiology, namely their inter-relationships in nitrogen and carbon metabolism, biosynthesis and the impact on culture performance. Furthermore, we used ^{13}C labeled pyruvate and GC-MS analysis to discern intracellular partitioning of this substrate in the presence or absence of asparagine or serine. Chapter 5 presents a global discussion of the results obtained.

Overall, this thesis provides an in-depth study of the metabolic network of GS-CHO cells that allowed identification of potential targets for minimizing overflow metabolism, reducing the diversion of resources to by-product accumulation, or minimising their impact on recombinant protein production. Also, it allowed the association of PPP and ME activities, important sources of NADPH, with a high productive phenotype in GS-CHO cells. These biological markers can represent an opportunity for future process and cell engineering efforts aiming towards the improvement of biopharmaceuticals production.

1.6 Author contribution

Tiago Duarte wrote this chapter.

1.7 References

Ahn WS, Antoniewicz MR. 2011. Metabolic flux analysis of CHO cells at growth and non-growth phases using isotopic tracers and mass spectrometry. Metab Eng 13(5):598-609.

Ahn WS, Antoniewicz MR. 2012. Towards dynamic metabolic flux analysis in CHO cell cultures. Biotechnol J 7(1):61-74.

Ahn WS, Antoniewicz MR. 2013. Parallel labeling experiments with [1,2-13C]glucose and [U-13C]glutamine provide new insights into CHO cell metabolism. Metab Eng 15:34-47.

Al-Fageeh MB, Marchant RJ, Carden MJ, Smales CM. 2006. The cold-shock response in cultured mammalian cells: harnessing the response for the improvement of recombinant protein production. Biotechnol Bioeng 93(5):829-35.

Allen MJ, Boyce JP, Trentalange MT, Treiber DL, Rasmussen B, Tillotson B, Davis R, Reddy P. 2008. Identification of novel small molecule enhancers of protein production by cultured mammalian cells. Biotechnol Bioeng 100(6):1193-204.

Alonso A, Marsal S, Julia A. 2015. Analytical methods in untargeted metabolomics: state of the art in 2015. Front Bioeng Biotechnol 3:23.

Antoniewicz MR. 2015. Methods and advances in metabolic flux analysis: a mini-review. J Ind Microbiol Biotechnol 42(3):317-25.

Antoniewicz MR, Kelleher JK, Stephanopoulos G. 2007. Elementary metabolite units (EMU): a novel framework for modeling isotopic distributions. Metab Eng 9(1):68-86.

Balcarcel RR, Stephanopoulos G. 2001. Rapamycin Reduces Hybridoma Cell Death and Enhances Monoclonal Antibody Production. Biotechnology & Bioengineering 76(1):10.

Barron N, Sanchez N, Kelly P, Clynes M. 2011. MicroRNAs: tiny targets for engineering CHO cell phenotypes? Biotechnol Lett 33(1):11-21.

Baycin-Hizal D, Tabb DL, Chaerkady R, Chen L, Lewis NE, Nagarajan H, Sarkaria V, Kumar A, Wolozny D, Colao J and others. 2012. Proteomic analysis of Chinese hamster ovary cells. J Proteome Res 11(11):5265-76.

Bruhlmann D, Jordan M, Hemberger J, Sauer M, Stettler M, Broly H. 2015. Tailoring recombinant protein quality by rational media design. Biotechnol Prog 31(3):615-29.

Butler M, Spearman M. 2014. The choice of mammalian cell host and possibilities for glycosylation engineering. Curr Opin Biotechnol 30:107-12.

Cacciatore JJ, Chasin LA, Leonard EF. 2010. Gene amplification and vector engineering to achieve rapid and high-level therapeutic protein production using the Dhfr-based CHO cell selection system. Biotechnol Adv 28(6):673-81.

Carinhas N, Oliveira R, Alves PM, Carrondo MJ, Teixeira AP. 2012. Systems biotechnology of animal cells: the road to prediction. Trends Biotechnol 30(7):377-85.

Chen C, Le H, Goudar CT. 2016. Integration of systems biology in cell line and process development for biopharmaceutical manufacturing. Biochemical Engineering Journal 107:11-17.

Chen K, Liu Q, Xie L, Sharp PA, Wang DIC. 2001. Engineering of a mammalian cell line for reduction of lactate formation and high monoclonal antibody production. Biotechnology & Bioengineering 72(1):7.

Chong WP, Reddy SG, Yusufi FN, Lee DY, Wong NS, Heng CK, Yap MG, Ho YS. 2010. Metabolomics-driven approach for the improvement of Chinese hamster ovary cell growth: overexpression of malate dehydrogenase II. J Biotechnol 147(2):116-21.

Clarke C, Doolan P, Barron N, Meleady P, O'Sullivan F, Gammell P, Melville M, Leonard M, Clynes M. 2011. Large scale microarray profiling and coexpression network analysis of CHO cells identifies transcriptional modules associated with growth and productivity. J Biotechnol 155(3):350-9.

Crown SB, Antoniewicz MR. 2012. Selection of tracers for 13C-metabolic flux analysis using elementary metabolite units (EMU) basis vector methodology. Metab Eng 14(2):150-61.
Crown SB, Long CP, Antoniewicz MR. 2015. Integrated 13C-metabolic flux analysis of 14 parallel labeling experiments in Escherichia coli. Metab Eng 28:151-8.
Datta P, Linhardt RJ, Sharfstein ST. 2013. An 'omics approach towards CHO cell engineering. Biotechnol Bioeng 110(5):1255-71.
Dean J, Reddy P. 2013. Metabolic analysis of antibody producing CHO cells in fed-batch production. Biotechnology & Bioengineering 110(6):13.
Doolan P, Meleady P, Barron N, Henry M, Gallagher R, Gammell P, Melville M, Sinacore M, McCarthy K, Leonard M and others. 2010. Microarray and proteomics expression profiling identifies several candidates, including the valosin-containing protein (VCP), involved in regulating high cellular growth rate in production CHO cell lines. Biotechnol Bioeng 106(1):42-56.
Durocher Y, Butler M. 2009. Expression systems for therapeutic glycoprotein production. Curr Opin Biotechnol 20(6):700-7.
Ecker DM, Jones SD, Levine HL. 2015. The therapeutic monoclonal antibody market. MAbs 7(1):9-14.
Fan L, Kadura I, Krebs LE, Hatfield CC, Shaw MM, Frye CC. 2012. Improving the efficiency of CHO cell line generation using glutamine synthetase gene knockout cells. Biotechnol Bioeng 109(4):1007-15.
Fan L, Kadura I, Krebs LE, Larson JL, Bowden DM, Frye CC. 2013. Development of a highly-efficient CHO cell line generation system with engineered SV40E promoter. J Biotechnol 168(4):652-8.
Figueroa B, Jr., Ailor E, Osborne D, Hardwick JM, Reff M, Betenbaugh MJ. 2007. Enhanced cell culture performance using inducible anti-apoptotic genes E1B-19K and Aven in the production of a monoclonal antibody with Chinese hamster ovary cells. Biotechnol Bioeng 97(4):877-92.
Fischer S, Buck T, Wagner A, Ehrhart C, Giancaterino J, Mang S, Schad M, Mathias S, Aschrafi A, Handrick R and others. 2014. A functional high-content miRNA screen identifies miR-30 family to boost recombinant protein production in CHO cells. Biotechnol J 9(10):1279-92.
Fischer S, Handrick R, Otte K. 2015. The art of CHO cell engineering: A comprehensive retrospect and future perspectives. Biotechnol Adv 33(8):1878-96.
Gatti ML, Wlaschin KF, Nissom PM, Yap M, Hu WS. 2007. Comparative transcriptional analysis of mouse hybridoma and recombinant Chinese hamster ovary cells undergoing butyrate treatment. J Biosci Bioeng 103(1):82-91.
Goudar C, Biener R, Boisart C, Heidemann R, Piret J, de Graaf A, Konstantinov K. 2010. Metabolic flux analysis of CHO cells in perfusion culture by metabolite balancing and 2D [13C, 1H] COSY NMR spectroscopy. Metab Eng 12(2):138-49.
Goulart HR, Arthuso Fdos S, Capone MV, Oliveira TL, Bartolini P, Soares CR. 2010. Enhancement of human prolactin synthesis by sodium butyrate addition to serum-free CHO cell culture. J Biomed Biotechnol 2010:405872.
Griffin TJ, Seth G, Xie H, Bandhakavi S, Hu WS. 2007. Advancing mammalian cell culture engineering using genome-scale technologies. Trends Biotechnol 25(9):401-8.
Hacker DL, De Jesus M, Wurm FM. 2009. 25 years of recombinant proteins from reactor-grown cells - where do we go from here? Biotechnol Adv 27(6):1023-7.
Idle JR, Gonzalez FJ. 2007. Metabolomics. Cell Metab 6(5):348-51.
Irani N, Wirth M, Heuvel J, Wagner R. 1999. Improvement of the primary metabolism of cell cultures by introducing a new cytoplasmic pyruvate carboxylase reaction. Biotechnology & Bioengineering 66(4):9.
Jadhav V, Hackl M, Klanert G, Hernandez Bort JA, Kunert R, Grillari J, Borth N. 2014. Stable overexpression of miR-17 enhances recombinant protein production of CHO cells. J Biotechnol 175:38-44.
Jayapal KP, Wlaschin KF, Hu WS. 2007. Recombinant Protein Therapeutics from CHO cells - 20 years and counting. CHO Consortium SBE Special Section:8.
Jiang Z, Sharfstein ST. 2008. Sodium butyrate stimulates monoclonal antibody over-expression in CHO cells by improving gene accessibility. Biotechnol Bioeng 100(1):189-94.
Kang S, Ren D, Xiao G, Daris K, Buck L, Enyenihi AA, Zubarev R, Bondarenko PV, Deshpande R. 2014. Cell line profiling to improve monoclonal antibody production. Biotechnology & Bioengineering 111(4):12.

Kantardjieff A, Jacob NM, Yee JC, Epstein E, Kok YJ, Philp R, Betenbaugh M, Hu WS. 2010. Transcriptome and proteome analysis of Chinese hamster ovary cells under low temperature and butyrate treatment. J Biotechnol 145(2):143-59.

Kelly PS, Breen L, Gallagher C, Kelly S, Henry M, Lao NT, Meleady P, O'Gorman D, Clynes M, Barron N. 2015. Re-programming CHO cell metabolism using miR-23 tips the balance towards a highly productive phenotype. Biotechnol J 10(7):1029-40.

Kildegaard HF, Baycin-Hizal D, Lewis NE, Betenbaugh MJ. 2013. The emerging CHO systems biology era: harnessing the 'omics revolution for biotechnology. Curr Opin Biotechnol 24(6):1102-7.

Kim EJ, Kim NS, Lee GM. 1998. Development of a serum-free medium for the production of humanized antibody from chinese hamster ovary cells using a statistical design. In Vitro Cell. Dev. Biol. 24:5.

Kim SH, Lee GM. 2007a. Down-regulation of lactate dehydrogenase-A by siRNAs for reduced lactic acid formation of Chinese hamster ovary cells producing thrombopoietin. Appl Microbiol Biotechnol 74(1):152-9.

Kim SH, Lee GM. 2007b. Functional expression of human pyruvate carboxylase for reduced lactic acid formation of Chinese hamster ovary cells (DG44). Appl Microbiol Biotechnol 76(3):659-65.

Kim SH, Lee GM. 2009. Development of serum-free medium supplemented with hydrolysates for the production of therapeutic antibodies in CHO cell cultures using design of experiments. Appl Microbiol Biotechnol 83(4):639-48.

Konno Y, Kobayashi Y, Takahashi K, Takahashi E, Sakae S, Wakitani M, Yamano K, Suzawa T, Yano K, Ohta T and others. 2012. Fucose content of monoclonal antibodies can be controlled by culture medium osmolality for high antibody-dependent cellular cytotoxicity. Cytotechnology 64(3):249-65.

Laken HA, Leonard MW. 2001. Understanding and modulating apoptosis in industrial cell culture. Current Opinion in Biotechnology 12:5.

Le H, Vishwanathan N, Jacob NM, Gadgil M, Hu WS. 2015. Cell line development for biomanufacturing processes: recent advances and an outlook. Biotechnol Lett 37(8):1553-64.

Le H, Vishwanathan N, Kantardjieff A, Doo I, Srienc M, Zheng X, Somia N, Hu WS. 2013. Dynamic gene expression for metabolic engineering of mammalian cells in culture. Metab Eng 20:212-20.

Lee GM, Kim EJ, Kim NS, Yoon SK, Yong HA, Song JY. 1999. Development of a serum-free medium for the production of erythropoietin by suspension culture of recombinant Chinese hamster ovary cells using a statistical design. Journal of Biotechnology 69:9.

Lee S-Y, Kwon Y-B, Cho J-M, Park K-H, Chang S-J, Kim D-I. 2012. Effect of process change from perfusion to fed-batch on product comparability for biosimilar monoclonal antibody. Process Biochemistry 47(9):1411-1418.

Lee SY, Lee DY, Kim TY. 2005. Systems biotechnology for strain improvement. Trends Biotechnol 23(7):349-58.

Leighty RW, Antoniewicz MR. 2012. Parallel labeling experiments with [U-13C]glucose validate E. coli metabolic network model for 13C metabolic flux analysis. Metab Eng 14(5):533-41.

Lewis AM, Abu-Absi NR, Borys MC, Li ZJ. 2016. The use of 'Omics technology to rationally improve industrial mammalian cell line performance. Biotechnol Bioeng 113(1):26-38.

Li F, Vijayasankaran N, Shen A, Kiss R, Amanullah A. 2014. Cell culture processes for monoclonal antibody production. mAbs 2(5):466-479.

Liu C, Chu I, Hwang S. 2001. Factorial designs combined with the steepest ascent method to optimize serum-free media for CHO cells. Enzyme and Microbial Technology 28:8.

Majors BS, Betenbaugh MJ, Chiang GG. 2007. Links between metabolism and apoptosis in mammalian cells: applications for anti-apoptosis engineering. Metab Eng 9(4):317-26.

Malphettes L, Freyvert Y, Chang J, Liu PQ, Chan E, Miller JC, Zhou Z, Nguyen T, Tsai C, Snowden AW and others. 2010. Highly efficient deletion of FUT8 in CHO cell lines using zinc-finger nucleases yields cells that produce completely nonfucosylated antibodies. Biotechnol Bioeng 106(5):774-83.

Mastrangelo AJ, Hardwick JM, Zou S, Betenbaugh MJ. 2000. Part II. Overexpression of bcl-2 Family members enhances survival of Mammalian cells in response to various culture insults. Biotechnology & Bioengineering 67(5):10.

Mead EJ, Chiverton LM, Spurgeon SK, Martin EB, Montague GA, Smales CM, von der Haar T. 2012. Experimental and in silico modelling analyses of the gene expression pathway for recombinant antibody and by-product production in NS0 cell lines. PLoS One 7(10):e47422.

Michiels JF, Barbau J, De Boel S, Dessy S, Agathos SN, Schneider YJ. 2011. Characterisation of beneficial and detrimental effects of a soy peptone, as an additive for CHO cell cultivation. Process Biochemistry 46(3):671-681.

Mimura Y, Lund J, Church S, Dong S, Li J, Goodall M, Jefferis R. 2000. Butyrate increases production of human chimeric IgG in CHO- K1 cells whilst maintaining function and glycoform profile. Journal of Immunological Methods 247:12.

Mimura Y, Lund J, Church S, Dong S, Li J, Goodall M, Jefferis R. 2001. Butyrate increases production of human chimeric IgG in CHO-K1 cells whilst maintaining function and glycoform profile. Journal of Immunological Methods 247:12.

Nicolae A, Wahrheit J, Bahnemann J, Zeng A-P, Heinzle E. 2014. Non-stationary 13C metabolic flux analysis of Chinese hamster ovary cells in batch culture using extracellular labeling highlights metabolic reversibility and compartmentation. BMC Syst Biol 8(50):15.

Noh SM, Sathyamurthy M, Lee GM. 2013. Development of recombinant Chinese hamster ovary cell lines for therapeutic protein production. Current Opinion in Chemical Engineering 2:8.

Palermo DP, DeGraaf ME, Marotti KR, Rehberg E, Post LE. 1991. Production of analytical quantities of recombinant proteins in Chinese hamster ovary cells using sodium butyrate to elevate gene expression. Journal of Biotechnology 19:13.

Park HS, Kim IH, Kim IY, Kim KH, Kim HJ. 2000. Expression of carbamoyl phosphate synthetase I and ornithine transcarbamoylase genes in Chinese hamster ovary dhfr-cells decreases accumulation of ammonium ion in culture media. Journal of Biotechnology 81:12.

Pasupuleti VK, Holmes C, Demain AL. 2008. Applications of Protein Hydrolysates in Biotechnology.1-9.

Puck TT, Cieciura SJ, Robinson A. 1958. Genetics of somatic mammalian cells. J Mol Med 108:945–955

Quek LE, Dietmair S, Kromer JO, Nielsen LK. 2010. Metabolic flux analysis in mammalian cell culture. Metab Eng 12(2):161-71.

Sá JV, Duarte TM, Carrondo MJT, Alves PM, Teixeira AP. 2015. Metabolic Flux Analysis: A Powerful Tool in Animal Cell Culture. 9:521-539.

Sauer U. 2006. Metabolic networks in motion: 13C-based flux analysis. Mol Syst Biol 2:62.

Sellick CA, Croxford AS, Maqsood AR, Stephens G, Westerhoff HV, Goodacre R, Dickson AJ. 2011a. Metabolite profiling of recombinant CHO cells: designing tailored feeding regimes that enhance recombinant antibody production. Biotechnol Bioeng 108(12):3025-31.

Sellick CA, Hansen R, Stephens GM, Goodacre R, Dickson AJ. 2011b. Metabolite extraction from suspension-cultured mammalian cells for global metabolite profiling. Nat Protoc 6(8):1241-9.

Selvarasu S, Ho YS, Chong WP, Wong NS, Yusufi FN, Lee YY, Yap MG, Lee DY. 2012. Combined in silico modeling and metabolomics analysis to characterize fed-batch CHO cell culture. Biotechnol Bioeng 109(6):1415-29.

Sengupta N, Rose ST, Morgan JA. 2011. Metabolic flux analysis of CHO cell metabolism in the late non-growth phase. Biotechnol Bioeng 108(1):82-92.

Sheikholeslami Z, Jolicoeur M, Henry O. 2013. Probing the metabolism of an inducible mammalian expression system using extracellular isotopomer analysis. J Biotechnol 164(4):469-78.

Tan JG, Lee YY, Wang T, Yap MG, Tan TW, Ng SK. 2015. Heat shock protein 27 overexpression in CHO cells modulates apoptosis pathways and delays activation of caspases to improve recombinant monoclonal antibody titre in fed-batch bioreactors. Biotechnol J 10(5):790-800.

Templeton N, Dean J, Reddy P, Young JD. 2013. Peak antibody production is associated with increased oxidative metabolism in an industrially relevant fed-batch CHO cell culture. Biotechnol Bioeng 110(7):2013-24.

Toya Y, Shimizu H. 2013. Flux analysis and metabolomics for systematic metabolic engineering of microorganisms. Biotechnol Adv 31(6):818-26.

Walsh G. 2014. Biopharmaceutical benchmarks 2014. Nature 32(10):11.

Wang Z, Park JH, Park HH, Tan W, Park TH. 2011. Enhancement of recombinant human EPO production and sialylation in chinese hamster ovary cells through Bombyx mori 30Kc19 gene expression. Biotechnol Bioeng 108(7):1634-42.

Wiechert W. 2001. 13C metabolic flux analysis. Metab Eng 3(3):195-206.

Wilkens CA, Gerdtzen ZP. 2015. Comparative Metabolic Analysis of CHO Cell Clones Obtained through Cell Engineering, for IgG Productivity, Growth and Cell Longevity. PLoS One 10(3):e0119053.

Wong DC, Wong KT, Lee YY, Morin PN, Heng CK, Yap MG. 2006a. Transcriptional profiling of apoptotic pathways in batch and fed-batch CHO cell cultures. Biotechnol Bioeng 94(2):373-82.

Wong DC, Wong KT, Nissom PM, Heng CK, Yap MG. 2006b. Targeting early apoptotic genes in batch and fed-batch CHO cell cultures. Biotechnol Bioeng 95(3):350-61.

Wurm F. 2013. CHO Quasispecies—Implications for Manufacturing Processes. Processes 1(3):296-311.

Wurm FM. 2004. Production of recombinant protein therapeutics in cultivated mammalian cells. Nat Biotechnol 22(11):1393-8.

Xu X, Nagarajan H, Lewis NE, Pan S, Cai Z, Liu X, Chen W, Xie M, Wang W, Hammond S and others. 2011. The genomic sequence of the Chinese hamster ovary (CHO)-K1 cell line. Nat Biotechnol 29(8):735-41.

Yee JC, de Leon Gatti M, Philp RJ, Yap M, Hu WS. 2008. Genomic and proteomic exploration of CHO and hybridoma cells under sodium butyrate treatment. Biotechnol Bioeng 99(5):1186-204.

Yoon SK, Hong JK, Choo SH, Song JY, Park HW, Lee GM. 2006. Adaptation of Chinese hamster ovary cells to low culture temperature: cell growth and recombinant protein production. J Biotechnol 122(4):463-72.

CHAPTER 2

Metabolic signatures of GS-CHO cell clones associated with butyrate treatment and culture phase transition

Adapted from:

Carinhas N*, Duarte TM*, Barreiro LC, Carrondo MJT, Alves PM, Teixeira AP, 2013, Metabolic signatures of GS-CHO cell clones associated with butyrate treatment and culture phase transition, Biotechnol. Bioeng. 110(12):3244-3257 *equal contributions

Abstract

Chinese hamster ovary (CHO) cells are preferred hosts for the production of recombinant biopharmaceuticals. Efforts to optimize these bioprocesses have largely relied on empirical experience and our knowledge of cellular behavior in culture is highly incomplete. More recently, comprehensive investigations of metabolic network operation have started to be used to uncover traits associated with optimal growth and recombinant protein production. In this work, we used ^{1}H-nuclear magnetic resonance (^{1}H-NMR) to analyze the supernatants of glutamine-synthetase (GS)-CHO cell clones expressing variable amounts of an IgG_4 under control and butyrate-treated conditions. Exometabolomic data was contextualized in a detailed network of 117 reactions and the cellular fluxomes estimated through metabolic flux analysis (MFA). This approach allowed comparing metabolic activity across different clones, growth phases and culture conditions, in particular the efficiency pertaining to carbon lost to glycerol and lactate accumulation and the characteristic nitrogen metabolism involving high asparagine and serine uptake rates. Importantly, this study shows that early butyrate treatment has a marked effect on sustaining high nutrient consumption along culture time, being its effect more pronounced during the stationary phase when extra energy generation and biosynthetic activity is fueled to increase IgG formation. Collectively, the information generated contributes to deepening our understanding of mammalian CHO cells metabolism in culture, facilitating future design of improved bioprocesses.

CONTENTS

2.1 Introduction

Mammalian cell lines are the preferred hosts for industrial production of complex protein therapeutics (Wurm, 2004). In particular, Chinese hamster ovary (CHO) cells are often used to express, among other products, monoclonal antibodies (mAbs) to treat cancer and immunological disorders. Although mammalian cell culture is

relatively mature, fundamental knowledge on how changes in the bioprocess contribute to differences in recombinant protein yields, glycosylation, aggregation and folding, potentially resulting in altered therapeutic activity, remains scarce. At the same time, there is increasing pressure to improve bioprocess performance to further reduce costs, calling for a renewed effort to account for the complexity of the cellular biological systems and its culture behavior.

Metabolic models play an important role in our understanding of biological production systems as they are closely connected with the growth and productive phenotypes. Metabolic flux analysis (MFA) is such a tool based on the principle of mass conservation within a stoichiometric network of cellular metabolism, allowing the estimation of intracellular fluxes under assumed metabolic steady state given measurable rates of nutrient consumption and byproduct accumulation (Stephanopoulos et al., 1998). This technique has been applied for over a decade to several CHO cell lines to identify bottlenecks in primary and secondary metabolic pathways and to gain insights about the balance between catabolic and anabolic processes (reviewed in Ahn and Antoniewicz, 2012). Central to these works has been the study of overflow metabolism that leads to by-product accumulation such as lactate, ammonia and alanine, which negatively impacts cell growth and recombinant product formation through resource waste and toxicity build-up. The information generated has guided the development of bioprocess strategies to minimize these limitations; for instance, Altamirano et al. (2000, 2004) have studied media design and fed-batch strategies involving the substitution of the main carbon (glucose) and nitrogen (glutamine) sources by the more slowly metabolized compounds galactose and glutamate, respectively. Also, genetic engineering efforts have targeted lower lactate production through enzymatic manipulation (Fogolín et al., 2004; Kim and Lee, 2007; Zhou et al., 2011). During the last few years, ^{13}C-MFA techniques using isotopic tracers have been useful to distinguish reversible and parallel reaction fluxes, in particular elucidating the diversion of glucose to the pentose phosphate pathway (PPP) and the activity of

pyruvate carboxylase (PC) at the bridge between glycolysis and the tricarboxylic acids (TCA) cycle (Ahn and Antoniewicz, 2011, 2013; Goudar et al., 2010; Sengupta et al., 2011; Templeton et al., 2013). However, despite the collective knowledge, we are still lacking a comprehensive understanding of how mammalian cell metabolism is regulated under variable bioprocess conditions, limiting rational optimization efforts (Ahn and Antoniewicz, 2012).

With the advent of systems biotechnology tools for generation and contextualization of "omic" cellular data, together with high-throughput culture technologies, the quantity and quality attributes of mammalian cell bioprocess performance are starting to be elucidated (Carinhas et al., 2012; Griffin et al., 2007). Noteworthy, the genome sequence of the CHO-K1 cell line has been recently published (Xu et al., 2011), opening the way for reliable genome-based omic analyses and large-scale metabolic network reconstruction. In parallel, advances in metabolomics tools have materialized in their application to mammalian cell cultures, significantly increasing in recent years to study CHO cells. Examples include the analysis of growth characteristics using different culture media (Dietmair et al., 2012), metabolic engineering of TCA cycle activity resulting in growth improvement (Chong et al., 2010), characterization of CHO cells with high mAb productivities (Chong et al., 2012), understanding the production-to-consumption lactate shift along culture time (Luo et al., 2011) and designing feeding strategies to improve metabolic efficiency and productivity (Ma et al., 2009; Sellick et al., 2011). Furthermore, the analysis of the exometabolome in the culture supernatant provides an indirect snapshot of the intracellular metabolism and is an important data input for metabolic models (Selvarasu et al., 2012).

In the present work, we apply ^{1}H-nuclear magnetic resonance (^{1}H-NMR) to analyze the exometabolome of glutamine synthetase (GS)-CHO cells along culture time, which is then used to identify an extended metabolic network through MFA. Two GS-CHO cell clones with different growth and production phenotypes are studied under control and butyrate-treated conditions. Comparatively to other mammalian expression systems,

GS-CHO cells are poorly characterized, and the metabolic comparison of different CHO producer clones is limited (Dean and Reddy, 2013; Chong et al., 2012). In addition, butyrate treatment has been investigated before on the transcriptomic and proteomic levels (Gatti et al., 2007; Kantardjieff et al., 2010; Yee et al., 2008), but not on the global exometabolome and fluxome levels. It is a histone deacetylase inhibitor with a pronounced effect on specific productivity of recombinant proteins in mammalian cell expression systems (Jiang and Sharfstein, 2008), being classically used both in fundamental research as well as for bioproduction. Of note, a recent breakthrough study has shown that lysine acetylation is a post-translational modification in most enzymes of the central metabolism (Zhao et al., 2010) and is able to increase or decrease the flux through the respective reactions up to twofold (Wang et al., 2010; Zhao et al., 2010). Thus, investigating the impact of butyrate treatment on the metabolism of producer cell lines can contribute to further enlighten its physiological effects.

2.2 Materials and Methods

2.2.1 Cells, culture conditions and sampling

CHO cell clones generated by stable transfection of the CHOK1SV cell line with a construct containing GS and the light and heavy chains of an IgG_4 mAb, were kindly provided by Lonza Biologics (UK). Cells were maintained in CDCHO chemically defined medium (Cat. No. 10743-029, Gibco, Life Technologies, Carlsbad, CA) supplemented with 25 μM methionine sulphoximine (Cat. No. M5379, Sigma-Aldrich, St. Louis, MO), in 125 mL shake flasks with 25 mL of culture volume and sub-cultured every 3–4 days with a seeding density of 0.4 x 10^6 cell/mL. All cultures were kept in a humidified incubator controlled at 37°C and 7% CO_2 with shaking at 130 rpm.

In this work, three sets of four cultures each were performed using two CHO cell clones (a lower and a higher producer, respectively LP and HP) with and without butyrate treatment (0.75 mM sodium butyrate (Cat. No. 8175000100, Merck, Germany) added

24 h after inoculation). Culture set I was performed using CDCHO media; culture set II used a custom CDCHO medium with slightly lower initial concentrations of glucose (30 mM compared to 40 mM in standard medium) and serine (5 mM compared to 6 mM); culture set III was performed as set II but with the addition at 72 h of 5 mM each of asparagine, aspartate and serine, and at 92 h of 10 mM glucose.

Samples were collected at intervals of 8–14 h. Cell number and viability were analysed under a light microscope using trypan blue dye and a hemocytometer. After counting cells, samples were clarified by centrifugation at 200 g during 10 min and the supernatant stored at −20 °C for later quantification of produced IgG and total protein, as well as exometabolome analysis.

2.2.2 Cell dry weight analysis

Cell dry weight was assessed with and without butyrate treatment at exponential and stationary growth. For each condition, duplicate cell pellets of at least 140 $x10^6$ cells were re-suspended in 1 mL PBS, transferred to eppendorf tubes and left drying in a 100 °C oven for up to 30 h. The tubes with dry pellets were weighed periodically until stabilization.

2.2.3 IgG quantification

Accumulation of IgG in the supernatant was monitored using sandwich ELISA assay. Briefly, Nunc Maxisorp 96-well plates (Cat. No. 437842, Thermo Scientific, USA) were coated with a goat anti-human IgG, Fcγ specific (Cat. No. 109-006-098, Jackson Immunoresearch Labs, USA) at a concentration of 2 µg/L in carbonate buffer. Blocking was performed with 0.5 % casein in carbonate buffer. Solutions with known concentrations of antibody were included on each plate for calibration. Bound antibody was detected using goat anti-human IgG (Fab specific)-peroxidase antibody (Cat. No. A0293, Sigma-Aldrich, USA). The complex was visualized with TMB substrate (Cat. No. 00-2023, Invitrogen, Life Technologies, USA) while 2.5 M sulphuric acid was used as stop solution. Colour development was measured at 450 nm.

2.2.4 Total protein quantification

The total protein content in supernatant samples along culture was quantified with the Coomassie Plus (Bradford) Protein Assay reagent (Cat. No. 23238, Pierce, Thermo Scientific, USA) using Bovine Gamma Globulin (Cat. No. 23212, Thermo Scientific, USA) as the protein reference standard. Briefly, 10 µL of each sample were mixed in a microplate with 300 µL of Coomassie Plus reagent for 30 s. The plate was incubated during 10 min at room temperature and the absorbance measured at 595 nm.

2.2.5 SDS-PAGE and western blot analysis

SDS–PAGE and Western blot analysis were performed in non-denaturating conditions in order to verify the quality of secreted IgG. Supernatant samples from HP and LP cultures were run on 1-mm NuPAGE Novex BisTris gels (Cat. No. NP0322BOX, Invitrogen, Life Technologies) using purified mAb as reference. Gels were either revealed with Instant blue (Cat. No. ISB1L, Expedeon, Harston, Cambridgeshire, UK) or electrically transferred to a nitrocellulose membrane (Cat. No. RPN203E, Amersham, GE HealthCare, Fairfield, CT). Immunochemical staining was carried out with goat antihuman IgG, Fcγ specific (see above) at 2 µg/L during 2 h at room temperature. The blot was developed using the ECL Prime Western Blotting Detection Reagent (Cat. No. RPN2232, Amersham, GE HealthCare) and exposed to X-ray light after 1 h incubation with ECL anti-mouse IgG, peroxidase-linked whole antibody from sheep (NA931, Amersham, GE Healthcare) at a 1:5.000 dilution at room temperature.

2.2.6 Exometabolome analysis

^{1}H-NMR was performed in a 500 MHz Avance spectrometer (Bruker, USA) equipped with a 5 mm QXI inversed probe. Spectra were acquired using a NOESY-based pulse sequence with water presaturation, performing 256 scans with 4 s acquisition time, 1 s relaxation delay and 100 ms mixing time at 25 °C. DSS-d_6 (613150, Isotec, USA) was used as internal standard for metabolite quantification in all samples. In order to maintain a constant pH between samples, these were mixed with phosphate buffer (pH

7.4) prepared in D_2O (151882, Aldrich, Canada) at a 2:1 ratio. Before spectra acquisition, the spectrometer was calibrated by determining the 90° pulse and the water chemical shift centre of each sample.

Each spectrum was phased, baseline corrected and integrated using the Chenomx NMR Suite 7.1 (Chenomx, Canada). Most metabolites are defined by several clusters at different chemical shifts, which in some cases may overlap or be affected by the damping effect caused by water suppression inducing an underestimation of their metabolites. Therefore, after automatic fitting of each metabolite, the best resolved and farthest peak from the water region was chosen for manual adjustment and metabolite quantification. This method allowed accurate quantification of 39 metabolites, with a limit below 180 μM and an average error of 3 %. Chemical shifts of clusters used for quantification, correction factors, errors and limits are available in Duarte et al. (2013).

Ammonia was quantified using an enzymatic kit (Cat. No. AK00091, NZYTech, Portugal), based on the measurement at 340 nm of the amount of $NADP^+$ formed through the action of glutamate dehydrogenase (GIDH).

2.2.7 Metabolic network

A network of central metabolic pathways of CHO cells was initially assembled from published models (Quek et al., 2010; Sengupta et al., 2011; Zamorano et al., 2010). Based on our ^{1}H-NMR exometabolomic analysis, it was further complemented with reactions taken from basic biochemistry textbooks to account for the metabolism of compounds not previously considered (see Results section), therefore filling the gaps in our comprehensive model. The extended network is composed of the main reactions of central metabolism of cultured animal cells, namely glycolysis, pentose phosphate pathway (PPP), TCA cycle, glutaminolysis, amino acids metabolism, by-product formation and extracellular transport fluxes. Following are some assumptions and simplifications made: subcellular compartmentalization was not considered; PPP is defined by growth requirements only, not reconnecting back to glycolysis; pyruvate

carboxylase (PC) activity is not considered since it cannot be discriminated from that of pyruvate dehydrogenase (PDH). The complete list of reactions is depicted in Figure 2.1.

In order to account for culture growth, cell biomass was considered to be composed of proteins, lipids, nucleic acids and glycogen, and was taken from the literature (Sheikh et al., 2005). The amino acid composition of CHO cellular proteins was recently analysed and used in this work (Selvarasu et al., 2012). Measured cellular dry weights were taken in account to determine coefficients for a lumped reaction of biomass formation. For the product formation reaction, an average IgG molecular weight of 153 KDa was considered (Lodish et al., 1995), the amino acid composition was taken from Lewis et al. (1993) and N-glycosylation pattern from Voet and Voet (1995). Details of both reactions can be found on the Appendix.

2.2.8 Metabolic flux analysis

The metabolic model developed considers 117 reactions (including extracellular transport fluxes and the specific growth rate of cells) and 83 balanced metabolites. From our experimental data, 45 rates were determined (35 exometabolites, specific productivity and growth rate, plus 8 intracellular fluxes assumed to be equal to the corresponding measured extracellular rates; see Appendix). The rank of the stoichiometric matrix is 82, resulting in an over determined, redundant system of 10 degrees of freedom (82-(117-45)). To solve this system, a weighted-least squares estimate for the flux distribution was calculated under the pseudo-steady state assumption (Stephanopoulos et al., 1998). In addition, adjusted flux measurements were used to calculate a consistency index, h, as defined in Wang and Stephanopoulos (1983). Comparison of h with the χ^2 test function allowed evaluating the consistency of experimental data with the network constraints imposed within a 95 % confidence level. These calculations were performed with FluxAnalyzer (Version 5.3) (Klamt et al., 2003).

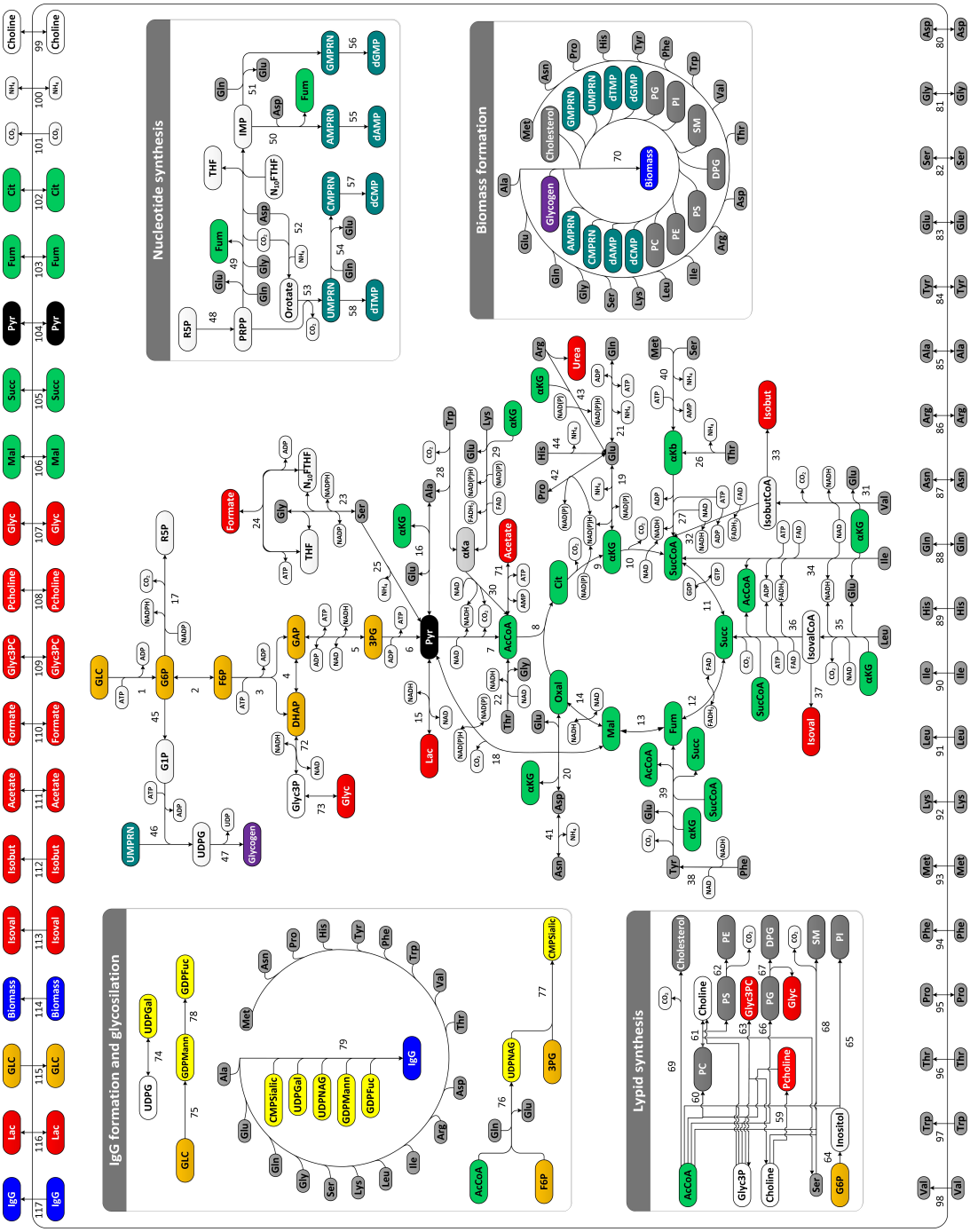

Figure 2.1 Network representation of metabolic reactions used for fluxome analysis.

2.3 Results and Discussion

2.3.1 Culture behaviour and exometabolomic trends of GS-CHO cells

Three culture sets were performed using LP and HP cell clones, with and without butyrate treatment as described in the Materials and Methods Section. Figure 2.2 shows typical growth and production profiles (corresponding to culture set I). The LP reaches higher cell densities in less time than the HP, which had a more prolonged stationary phase (Fig. 2.2A). It can be observed that the differences in growth profiles between clones are accompanied by a larger IgG production capacity in the HP (Fig. 2.2B), resulting in average specific productivities around 2.5-fold higher for the three culture sets (Fig. 2.2C). As expected, butyrate treatment negatively impacts growth in both clones, capping peak cell densities and inducing earlier entry into stationary phase, but sustains IgG_4 productivity, which increases on average by 1.5- and 3-fold on a per cell basis during the exponential and stationary growth phases, respectively. Interestingly, the concentration of butyrate in the supernatant does not change significantly over time in butyrate-treated cultures, while there is a small accumulation of butyrate in control cultures (Fig. 2.3). Several studies have shown that butyrate inhibits histone deacetylases activity and arrests cell proliferation, but its mode of action is still unknown.

While classical studies have analyzed only the main substrates and secretion products of CHO cells metabolism, exometabolome data provide an expanded view of metabolic trends during cell growth and mAb production. Besides glucose, the main carbon source, it was possible to measure the consumption of pyruvate, choline (Fig. 2.4A–C) and 19 amino acids (see Table 2.1). Asparagine was the highest consumed amino acid followed by serine and aspartate (Fig. 2.4D–F). Regarding by-product secretion, lactate, ammonia and alanine reached the highest concentrations in the supernatant (Fig. 2.5A–C), but other metabolites usually not reported in the literature were also significantly accumulated. This is the case of isovalerate and isobutyrate, which appeared as a result

of the breakdown of the branched chain amino acids leucine and valine, respectively (Fig. 2.5D and E).

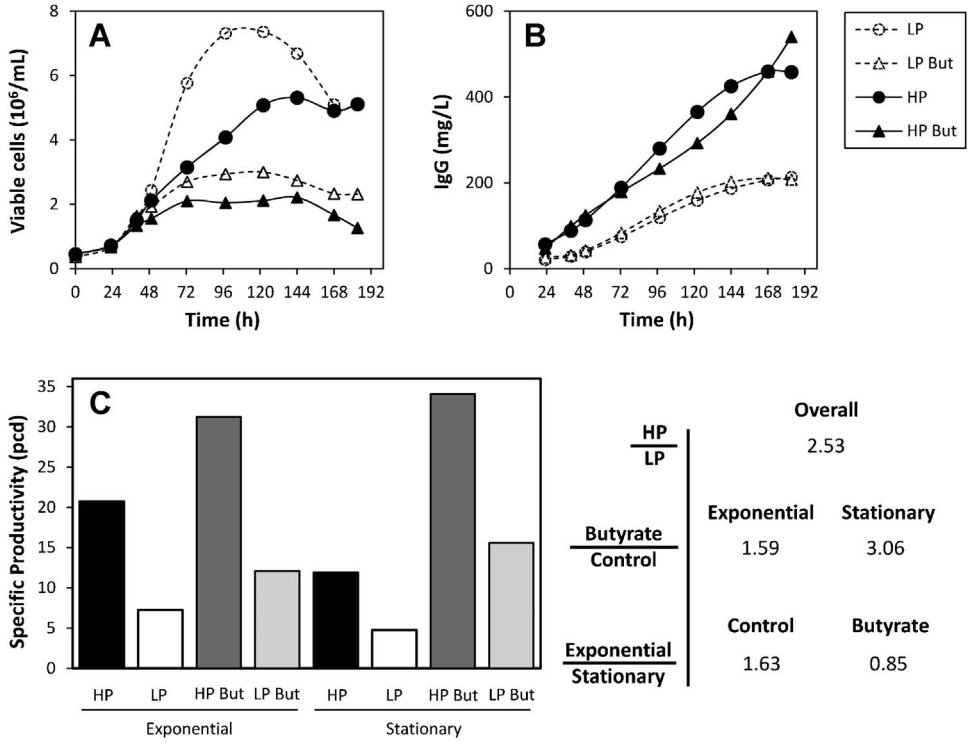

Figure 2.2 Cell growth and IgG production under control and butyrate-treated (But) conditions of HP and LP clones. Viable cell concentrations (A) and IgG concentration profiles (B) along time for culture set I. C: Specific IgG productivities and indicated ratios determined as the average from culture sets I, II, and III. Depending on the culture, metabolic phases were divided as follows: exponential from 24 to 72/96 h, stationary from 72/96 to 144/168 h. The HP/LP specific productivity ratio pools together both phases of control and butyrate treated cultures since no significant differences in this ratio could be observed between them. Likewise, the calculation of the remaining ratios pools together both clones.

Glycerol accumulated over culture time, branching from glycolysis at the dihydroxyacetone-phosphate (DHAP) node involving NADH oxidation (Fig. 2.5F), whereas acetate (from acetyl-CoA) starts to build up after the onset of the stationary phase (Fig. 2.5G). The profile of formate correlates well with that of glycine (Fig. 2.5H and I), both metabolites coming from the catabolism of serine, which is the main donor for 1C units metabolism (Narkewicz et al., 1996). TCA cycle intermediates such as citrate, fumarate, malate and succinate are also secreted to the supernatant (Fig. 2.5J–

M) as previously reported (Chong et al., 2010; Dietmair et al., 2012; Ma et al., 2009). Finally, metabolites from lipid metabolism, phosphocholine and glycerol-3-phosphocholine, both choline by-products, were detected in increasing amounts after the initial 72 h of culture (Fig. 2.5N and O). Overall, most carbon and nitrogen sources were consumed at higher rates during the exponential phase than during the stationary phase (Table 2.1). Only modest differences could be observed between clones, displaying qualitatively similar metabolite profiles and generally close specific metabolic rates. On the other hand, these were significantly affected by butyrate treatment, largely due to the negative effect on cell growth, resulting in substantially higher metabolic rates during the stationary phase (Table 2.1).

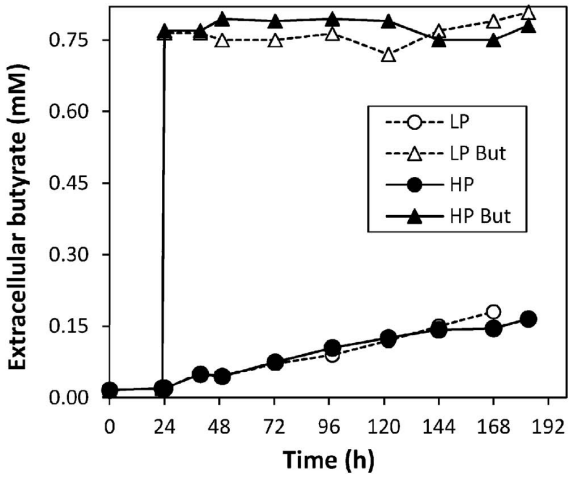

Figure 2.3 Extracellular butyrate concentration profiles under control and treated (But) conditions for culture set I. Sodium butyrate was added 24h after inoculation at a concentration of 0.75 mM.

The transition from exponential to stationary phase coincided with asparagine depletion in culture sets I (Fig. 2.4D) and II (data not shown), after which follows the exhaustion of aspartate (Fig. 2.4F) and, later, glucose (Fig. 2.4A), when viability starts decreasing. The addition of asparagine, aspartate, serine and glucose to culture set III led to a small increment in maximum cell density in the HP and prolongation of the stationary phase in both clones, but was not accompanied by any significant differences

in final mAb titers (data not shown). A shift from lactate production to consumption (between 48 and 72 h) occurred before cells had reached their maximum density and any of the analyzed nutrients was depleted (Fig. 2.5A). This metabolic switch has been reported to occur upon depletion of glucose (Martínez et al., 2013) or during later growth and stationary phases of CHO (Dean and Reddy, 2013; Ma et al., 2009) as well as NS0 cells (Khoo and Al-Rubeai, 2009; Ma et al., 2009; Mulukutla et al., 2012), and is related with decreased glucose consumption and balancing of the $NADH/NAD^+$ ratio (Mulukutla et al., 2010, 2012). Interestingly, our results confirm a previous observation by Ma et al. (2009) that the sum of the specific glucose and lactate metabolic rates is approximately constant across exponential and stationary phases; the only exception was the case of butyrate-treated HP cultures, owing to a much larger average lactate production rate during exponential growth. A switch from alanine secretion to consumption in control cultures was also observed concurrently with aspartate exhaustion, closely following asparagine depletion (Figs. 2.4D, F and 2.5C). This phenomenon is consistent across all cultures and is delayed in culture set III where both amino acids are supplemented at 72 h. On average, this resulted in a slightly negative specific alanine rate for the LP (consumption), which remained slightly positive for the HP (Table 2.1). In contrast, butyrate treatment kept alanine secretion high during the entire culture time as aspartate depletion does not occur before viability starts to decrease. To our knowledge, these modulations in alanine metabolism have not been reported before.

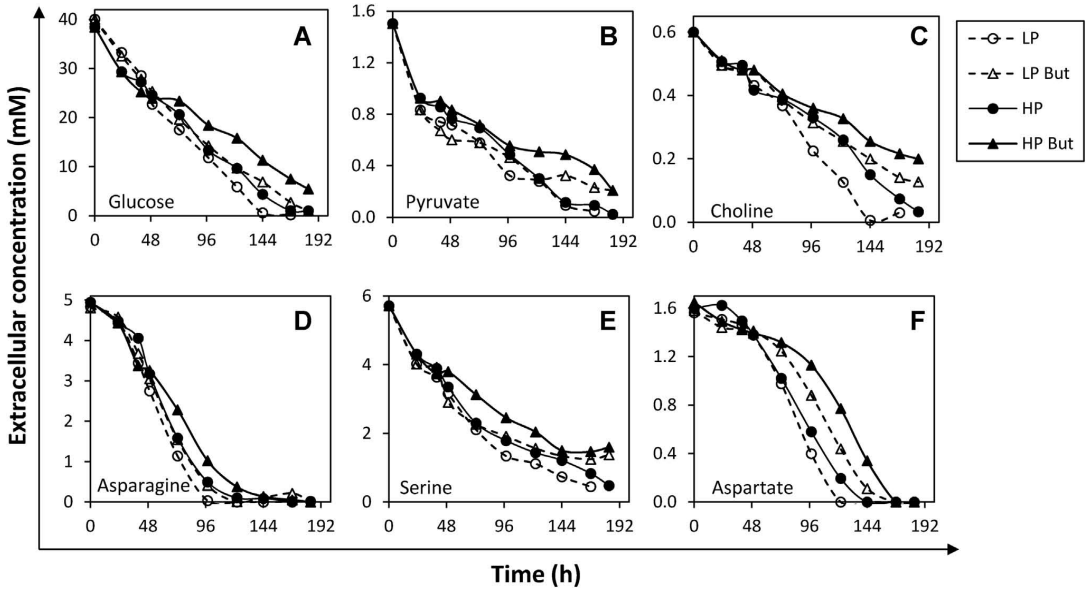

Figure 2.4 Extracellular concentration profiles of main substrate metabolites quantified in the exometabolome of culture set I, including control and butyrate-treated (But) cultures of HP and LP clones.

2.3.2 Metabolic flux analysis of GS-CHO cell cultures

Metabolic fluxomes were estimated based on exometabolomic data during exponential and stationary growth phases (Fig. 2.2). Rates of metabolite consumption and production (Table 2.1), together with specific growth and IgG_4 production rates, were used as constraints for MFA. Importantly, metabolic requirements for biomass synthesis were adjusted to the measured cell dry weights measured: on average 271 pg/cell for control and butyrate-treated cultures during exponential growth and a higher value of 368 pg/cell for butyrate-treated cultures during stationary phase. Importantly, comparisons of specific metabolic fluxes, in particular specific productivity, are not qualitatively altered when adjusting with the measured cell dry weights.

To our knowledge, this model contains the largest number of metabolic reactions in studies of CHO cells not involving the definition of an objective function for flux balancing (see review in Ahn and Antoniewicz, 2012). As a future endeavor, the time

profiles of exometabolomic data could further be used to establish a kinetic model combined to MFA allowing capturing the dynamics of metabolic behavior (Niklas et al., 2011; Nolan and Lee, 2011). The quality of the metabolic model and conclusions derived thereof requires that no faulty assumptions in the biochemistry or gross measurement errors are present. To evaluate this, the consistency index h was calculated and compared with the χ^2 value at a 95% confidence interval for each metabolic phase (see Materials and Methods Section). Furthermore, carbon (C) and nitrogen (N) balances were calculated based on the transport flux data and MFA estimated CO_2 production rates. A preliminary analysis showed that acceptable N balance results could only be obtained when considering the measurement of total extracellular protein content instead of ELISA-based IgG quantification. Further analysis through SDS–PAGE and Western blotting revealed that total protein was composed mostly of IgG_4, a portion of which was not correctly assembled into a quaternary structure (data not shown). Total protein measurements were hence used in all MFA calculations considering the IgG_4 composition detailed in Appendix 1. Importantly, these measurements yielded similar ratios of specific productivity between culture phases and between control and butyrate-treated cultures; only the ratio between HP and LP was smaller (around 1.5) when compared to that calculated based on ELISA results (around 2.5 as stated before). This may suggest the larger portion of productivity difference between clones is associated with correct antibody chain assembly.

On average, the C balance closes at 93% and the N balance at 86%, whereas for 19 out of 24 scenarios the h value is lower than the χ^2 threshold (Table 2.2). These results indicate that the network is well posed and that no gross measurement errors are being propagated in the estimated fluxes. Also, it suggests that our assessment of the exometabolome is reasonably comprehensive. The five phases where acceptable consistencies were not achieved included control and butyrate-treated cultures during either exponential or stationary growth, not revealing biases in the complete set of

conditions. An additional phase with h value bellow the threshold had significantly low C and N balances (78% and 64%, respectively). These six metabolic phases were likely due to experimental variability.

Table 2.1 Average specific metabolic secretion and consumption rates for HP and LP cultures under control and butyrate-treated conditions.

	HP		**HP But**		**LP**		**LP But**	
	Exp.	**Sta.**	**Exp.**	**Sta.**	**Exp.**	**Sta.**	**Exp.**	**Sta.**
Aspartate	-6.82	-2.49	-3.70	-8.70	-5.37	-2.70	-4.76	-5.63
Glycine	1.89	2.18	4.19	1.96	1.99	3.09	2.42	2.81
Serine	-11.67	-2.64	-11.02	-10.60	-9.69	-2.91	-13.35	-5.04
Glutamate	-3.36	-1.64	-6.01	-2.80	-3.59	-0.87	-3.63	-1.72
Tyrosine	-1.43	-0.47	-1.65	-1.57	-1.21	-0.39	-1.56	-0.90
Alanine	6.43	2.69	12.59	16.71	4.28	-0.47	8.22	8.50
Arginine	-2.99	-1.31	-3.92	-2.08	-3.13	-0.38	-4.71	-0.74
Asparagine	-20.25	-2.09	-25.35	-16.44	-16.09	-2.34	-24.64	-9.05
Glutamine	0.75	-0.33	2.21	0.24	0.09	0.13	0.85	0.38
Histidine	-1.75	-0.18	-0.88	-1.22	-1.01	-0.26	-1.62	-0.46
isoleucine	-3.20	-1.25	-3.43	-3.29	-3.34	-1.12	-3.54	-2.58
Leucine	-5.47	-2.26	-6.12	-5.47	-5.29	-2.02	-6.51	-4.56
Lysine	-3.41	-1.34	-5.68	-3.45	-4.16	-0.77	-4.30	-3.13
Methionine	-1.30	-0.21	-1.23	-1.10	-1.33	-0.19	-1.76	-0.70
Phenylalanine	-1.76	-0.44	-2.15	-1.41	-1.35	-0.33	-1.96	-1.00
Proline	-3.15	-1.14	-2.59	-2.39	-3.69	-0.80	-5.72	-1.22
Threonine	-4.15	-1.41	-10.18	-2.56	-1.48	-0.80	-4.42	-1.15
Tryptophan	-0.86	-0.45	-0.97	-0.92	-0.87	-0.24	-0.94	-0.51
Valine	-4.09	-1.15	-4.16	-3.72	-3.34	-1.15	-4.68	-2.20
Choline	-0.84	-0.41	-1.06	-0.88	-0.88	-0.44	-1.09	-0.64
Ammonia	11.86	4.55	14.69	3.89	6.01	5.05	12.49	4.52
Citrate	0.60	0.46	1.32	1.08	0.53	0.47	0.75	0.92
Fumarate	0.05	0.02	0.04	0.07	0.03	0.02	0.03	0.06
Pyruvate	-2.92	-0.92	-3.35	-1.79	-2.32	-0.78	-2.76	-1.04
Succinate	0.11	0.04	0.07	0.11	0.08	0.05	0.07	0.10
Malate	0.45	0.24	0.30	1.03	0.32	0.18	0.54	0.62
Glycerol	4.10	5.14	4.70	9.59	4.17	4.64	4.03	8.12
Phosphocoline	0.09	0.08	0.11	0.21	0.08	0.11	0.14	0.23
Glycero-3-phosphocholine	0.19	0.22	0.24	0.25	0.18	0.27	0.10	0.26
Formate	3.41	1.84	5.75	3.20	3.15	1.93	3.90	3.23
Acetate	0.02	2.08	0.10	0.75	0.02	1.35	-0.23	1.18
Isobutyrate	0.46	0.46	0.57	0.96	0.53	0.59	0.47	0.95
Isovalerate	1.28	1.56	1.60	2.29	1.38	1.95	1.32	2.63
Glucose	-73.46	-27.87	-77.80	-72.84	-83.92	-22.28	-106.65	-55.07
Lactate	36.75	-12.16	71.24	-14.57	36.42	-15.74	33.24	-14.30

Average rates were calculated from the three culture sets performed, and are expressed in nmol/10^6cells/h. Culture phases were divided as follows: exponential from 24 h to 72/96 h, stationary from 72/96 h to 144/168 h, depending on the culture. A negative sign indicates consumption.

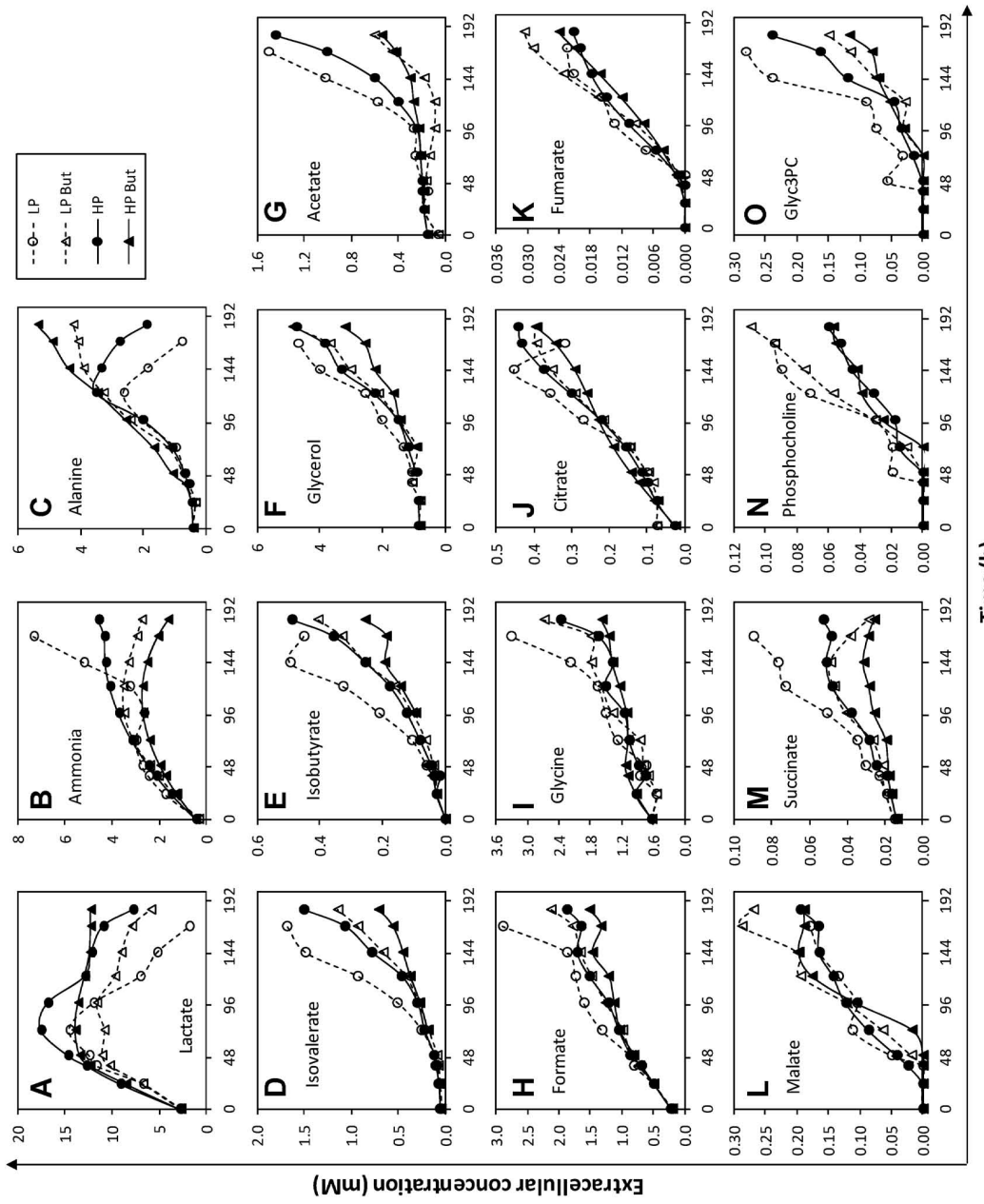

Figure 2.5 Extracellular concentration profiles of main secreted metabolites quantified in the exometabolome of culture set I, including control and butyrate-treated (But) cultures of HP and LP clones. Glyc3PC, glycerol-3-phosphocholine.

Table 2.2 Overview of metabolic phases studied. Carbon (C) and nitrogen (N) balances calculated from transport flux data and MFA estimated CO_2 production rates. To evaluate metabolic consistency, the cut-off χ^2 value at 95% confidence level for 10 degrees of freedom is 18.307. *Outlier with low C and N balance.

Clone	Condition	Growth phase	Culture set	Metabolic balance	Model consistency (h)
LP	Control	Exp.	I	C = 1.00; N = 0.97	0.25
			II	C = 0.93; N = 0.97	3.15
			III	C = 0.97; N = 0.94	0.48
		Sta.	I	C = 0.97; N = 0.87	1.42
			II	C = 0.78*; N = 0.64*	1.58
			III	C = 0.89; N = 0.84	> 18.307
	Butyrate	Exp.	I	C = 0.88; N = 0.71	> 18.307
			II	C = 0.84; N = 0.90	5.37
			III	C = 0.93; N = 0.78	7.75
		Sta.	I	C = 0.96; N = 0.71	6.27
			II	C = 0.84; N = 0.90	1.88
			III	C = 0.92; N = 0.87	11.10
HP	Control	Exp.	I	C = 0.90; N = 0.75	> 18.307
			II	C = 0.99; N = 0.98	0.37
			III	C = 0.97; N = 0.95	0.65
		Sta.	I	C = 0.95; N = 0.84	4.91
			II	C = 0.90; N = 0.84	2.92
			III	C = 0.98; N = 0.77	6.21
	Butyrate	Exp.	I	C = 0.98; N = 0.95	13.75
			II	C = 0.95; N = 0.92	2.70
			III	C = 0.90; N = 0.82	7.18
		Sta.	I	C = 0.93; N = 0.72	> 18.307
			II	C = 0.96; N = 0.94	5.22
			III	C = 0.93; N = 0.84	> 18.307

2.3.2.1 Metabolism overview under control conditions

In mammalian cells, an important determinant for glucose carbon loss to by-product formation is the balancing of the redox state between cytosol and mitochondria (Mulukutla et al., 2010). NADH produced in glycolysis must be regenerated to NAD^+ by transferring of reduced equivalents to mitochondria via the malate–aspartate and the glycerol-3-phosphate shuttle systems. During exponential growth, excess NADH produced that cannot be effectively transferred leads to high rates of lactate accumulation. Overall, the GS-CHO cell clones analyzed under standard culture

conditions displayed higher metabolic efficiency at the glycolysis–TCA cycle bridge than previously reported for other CHO/mammalian cell lines (Ahn and Antoniewicz, 2011, 2012). As an average for both clones, 26% of the pyruvate formed was channeled to lactate formation (Fig. 2.6). In addition, a smaller 5% diversion of carbon from glycolysis to glycerol accumulation during the exponential phase could be observed. Overall, the metabolic efficiency pertaining to these two key regulatory steps involving oxido-reductase reactions was 69% (100%-26%-5%), while the net percentage of pyruvate being fuelled to the TCA cycle was 67%. An increased diversion of glucose to glycerol production was observed during the stationary phase (24%).

This contrasts with the metabolic shift from lactate production to consumption (24% of pyruvate formed), which resulted in an increase to 100% (100%-24%+24%) in the efficiency of carbon flow associated with the same two metabolic nodes, and an increment to 92% in the percentage of pyruvate channeled to AcCoA formation. This divergent behavior suggests that increased glycerol accumulation fulfills other homeostatic roles such as regulation of cellular osmolarity; for instance, Sellick et al. (2011) detected accumulation of glycerol and sorbitol in a GS-CHO batch bioreactor. The modulations described above were accompanied by a general downtrend of metabolic flow into the stationary growth phase, as a result of lower nutrient consumption rates due to smaller growth requirements. Smaller sources of intracellular pyruvate were the activity of malic enzyme (ME), proportionately higher during exponential compared to stationary growth, as well as contributions from serine breakdown and pyruvate taken up from the medium (see also Fig. 2.4B). At the same time, carboxylates such as citrate, fumarate, malate and succinate were secreted (see Fig. 2.5J–M), representing approximately the same proportion to TCA cycle flux in both phases, possibly indicating it is operating close to maximum enzymatic capacity throughout culture time (Chong et al., 2010). It is important to note that the results presented herein are limited by the unavailability of labeling data and thus cannot discern pathways such as the flux through PC at the glycolysis–TCA cycle bridge (parallel to PDH) and the recycling of pentose–phosphates back to glycolysis (PPP

being determined by growth requirements alone). For instance, Sengupta et al. (2011) have analyzed metabolic efficiency at the glycolysis–TCA cycle bridge as well as the diversion of glucose to the PPP during the late non-growth phase of GS-CHO cells using ^{13}C-MFA. Their results are in accordance with those reported here with respect to a higher percentage of pyruvate being channeled to AcCoA formation in comparison to the growth phase, mainly associated with reduced or no lactate accumulation in Sengupta et al. (2011), or even consumption as observed herein. However, the assessment of glucose diversion to the PPP in Sengupta et al. (2011) largely exceeds the estimations shown in Figure 6, which are only driven by limited growth requirements; in the mentioned study, 37% or more of the glucose consumed is diverted to PPP. Other estimates using ^{13}C-MFA by Ahn and Antoniewicz (2011, 2013) in a CHO-k1 cell line show that, during the exponential phase, PPP activity in excess of nucleotide requirements for growth is insignificant (in agreement with the results presented here using simply metabolite balancing), while 21–31% of glucose was channeled through this pathway during the early non-growth phase. Even more recently, Templeton et al. (2013) have reported ^{13}C-MFA results in a DHFR-deficient CHO cell line under industrially relevant fed-batch culture, observing that the proportion of PPP activity and glycolytic recycling, almost negligible during early exponential growth, increases to absorb all incoming glucose during late exponential and stationary growth phases. These studies also estimated significant anaplerotic fluxes through PC during the exponential phase, although generally limited to a fraction of the PDH flux, further decreasing or being negligible during later phases. The increase of PPP activity along culture has been suggested to counteract the excessive reactive oxygen species formation associated with a higher oxidative metabolism and/or assist remodeling the lipid membranes of vesicles for recombinant protein secretion, thus requiring production of a significant NADPH surplus (Ahn and Antoniewicz, 2012; Sengupta et al., 2011; Templeton et al., 2013). In contrast, a lower activity during earlier growth can be in part related to a more glycolytic, and less oxidative, metabolism, and in part to higher ME activities leading to NADPH regeneration (as confirmed in this study).

Finally, as it relates to the overall metabolic picture, Goudar et al. (2010) have evaluated the sensitivity of the metabolic flux distribution in a perfusion culture of CHO cells to different values of PC and PPP fluxes, showing that omission of isotope tracer information does not significantly impact estimations of most fluxes in the network.

With regard to nitrogen metabolism, most of consumed asparagine was intracellularly deaminated to aspartate generating ammonia (Fig. 2.6). In turn, around 63% of the aspartate formed was transaminated to yield oxaloacetate during exponential growth, decreasing to 49% in the stationary phase. Alanine was also produced for nitrogen detoxification during exponential growth, corresponding to 6% of pyruvate usage, but decreased to less than 1% during the stationary phase. As mentioned before, this average value for both clones includes a small production rate for the HP and a small consumption rate for the LP, which is, however, not meaningful reflecting the slight delay of aspartate exhaustion in the HP culture (Fig. 2.4F). Serine was the precursor for 1C units metabolism, leading to glycine and formate accumulation (Fig. 2.5H and I). Glutamine was not available in the culture medium and was synthesized intracellularly through GS activity in amounts approximately needed to meet the growth and productivity requirements.

On average, 25% of the essential amino acids consumed were not fueled to biomass or IgG production during exponential growth, instead generating TCA cycle intermediates. This contribution further increased to 35% during the stationary phase, showing that essential amino acids play an important role in regulating central carbon metabolism, particularly sustaining energy production throughout the culture. At the αKG node, most of its formation and consumption was due to TCA cycle activity via isocitrate dehydrogenase and αKG dehydrogenase, respectively (Fig. 2.6). The contribution of amino acids metabolism via GLDH and transamination reactions is collectively limited to less than 20% in either direction and for both exponential and stationary phases. This is markedly different from what is reported in mammalian cell lines that take up glutamine from the medium and display high glutaminolysis rates. For instance,

Martínez et al. (2013) estimated that 92% of the αKG pool is originated from GLDH during exponential growth in CHOXL99 cells, while we observed on average only a 3% contribution from this flux. In the outflow direction, 12% of the αKG pool was used by aspartate aminotransferase to produce glutamate and oxaloacetate.

2.3.2.2 LP versus HP

In general, metabolic flow during both culture phases was similar between clones. The overall efficiency of the glycolysis–TCA cycle bridge increased from the exponential to the stationary phase with only small differences at the glycerol and lactate production checkpoints between clones. Interestingly, the contribution of ME activity was substantially higher in the HP, around fourfold and twofold for exponential and stationary growth, respectively (for simplicity, these differences are not represented in Fig. 2.6). This is in agreement with the recent observation that higher producer CHO cells tend to have elevated levels of metabolites involved in redox state regulation, facilitating the generation of energy and activated sugars for mAb expression (Chong et al., 2012). One way to achieve this is through the combined anaplerotic and cataplerotic activities of PC and ME, effectively creating a separate cycle overlapping the TCA cycle supporting NADPH regeneration (Templeton et al., 2013).

These results show that clonal differences associated with productivity can be too subtle to investigate by metabolite balancing of central metabolism alone, even aided by a comprehensive exometabolome mapping. This is in contrast with the results obtained by Dean and Reddy (2013), which compared DHFR-CHO cell clones and concluded that the ability to channel glucose-derived carbon to mitochondria fueling TCA cycle activity was a distinguishing feature of robust cell performance. However, an important difference to this work is that one of the clones used in the mentioned study had markedly superior growth and mAb accumulation profiles, as well as a distinct lactate phenotype, when compared to the other. As described above, in the comparison carried out here both clones were able to fuel the TCA cycle with above average

efficiencies even after accounting for carbon lost to glycerol production at the DHAP node. This indicates that regulatory mechanisms independent of central carbon flow influence recombinant protein production, namely transcriptional regulation and the cellular redox state, and that an in-depth analysis combining multiple levels of cellular information (gene expression, post-translational and metabolic) is required to unveil functional connections between operation of production pathways and central metabolism (Carinhas et al., 2012).

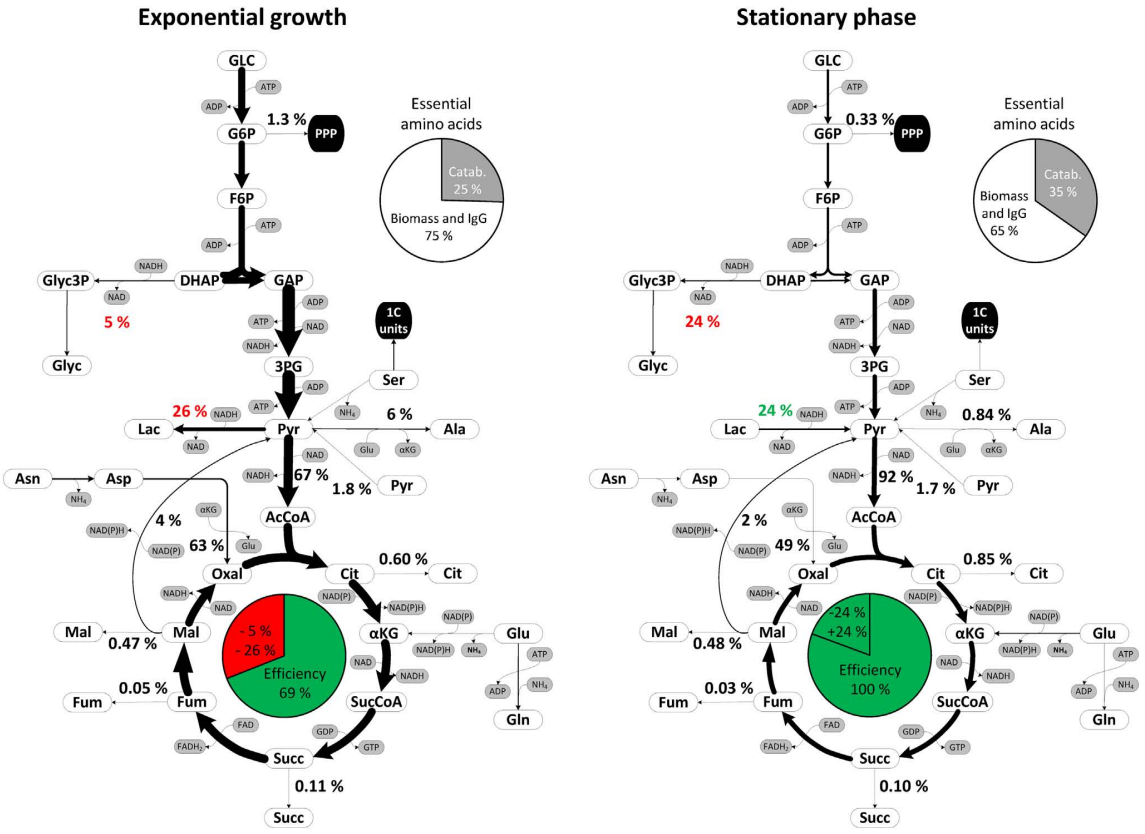

Figure 2.6 Metabolic flux distributions during exponential growth and stationary phase. Arrow thickness represents the average net flux in each reaction for all cultures (sets I, II, and III) performed with both clones. For simplicity, flux percentages are shown at only some branch points. Metabolic efficiency is represented in pie charts as the percentage of carbon flow to TCA cycle that is not lost to glycerol or lactate formation; carbon diversion to other metabolites is not considered for this calculation (see text).

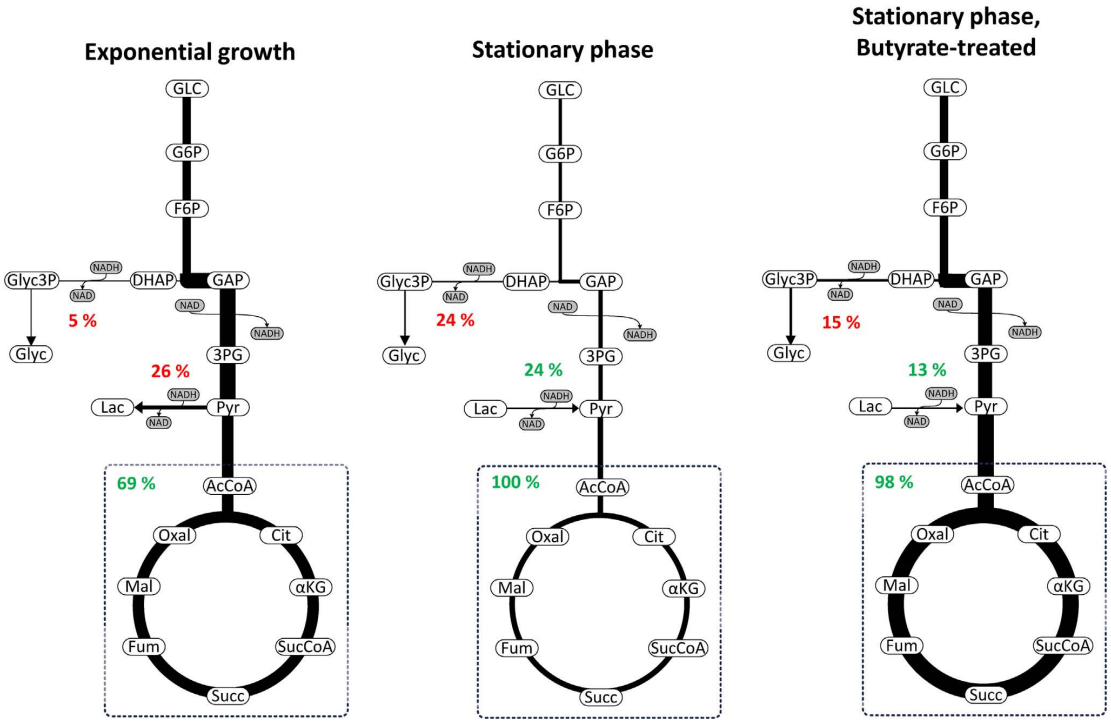

Figure 2.7 Main modulations in central carbon metabolism associated with culture phase transition and butyrate treatment. Arrow thickness reflects the relative flow from glucose entering the glycolytic pathway accounting for carbon lost only at the glycerol and lactate branch points; the contribution from other reactions is not represented. Average values for all cultures (sets I, II and III) performed with both clones were used.

2.3.2.3 Effect of butyrate treatment

A striking effect of butyrate treatment on sustaining overall metabolic activity during the stationary phase was observed, instead of the steep decline seen in control cultures, including the main carbon flows through glycolysis and TCA cycle as well as amino acids metabolism (Table 2.1; Fig. 2.7). This observation coincides with the sustained IgG-specific productivities observed in the transition to the stationary phase, typically decreasing by over a third under control conditions (Fig. 2.2C). These results are in accordance with a previous study focusing on the effect of butyrate treatment on intracellular nucleotide and nucleoside concentrations and ratios in CHO cells

expressing recombinant tissue plasminogen activator (McMurray-Beaulieu et al., 2009). Noteworthy, the authors have shown that addition of Na-butyrate at mid exponential growth phase (48 h) resulted in a sustained energetic state during later culture stages, which coincided with sustained high specific t-PA productivity. As mentioned above, this "delayed" effect on metabolic activity was evident in our cultures, since addition at 24 h had the greatest impact during stationary phase. In terms of flux partitioning, a substantially lower contribution of lactate consumption during the stationary phase could be observed at the pyruvate node, decreasing by nearly half (from 24% to 13%) when compared to the average control (Fig. 2.7). The proportion of alanine production also significantly increased on average for both clones due to aspartate availability in all three culture sets, maintaining levels comparable to exponential growth (data not shown). Despite these alterations, the effect of butyrate treatment on the combined metabolic efficiency at the glycerol and lactate nodes was small, increasing from the exponential phase to roughly 100% during the stationary phase. Likewise, the net percentage of pyruvate being directed to AcCoA formation was comparable to that of control cultures, increasing from 56% during exponential to 88% during stationary growth (data not shown). Contextualization of these observations with other "omic" analyses in the literature is difficult due to lack of a sufficient coverage of metabolic genes. Gatti et al. (2007) were first to report a transcriptomic analysis of CHO cultures as a response to butyrate treatment, but the study coverage was limited by the lack of a CHO genomic sequence and low sensitivity when performing cross species hybridization with hybridoma sequences. Furthermore, the authors compared cells before and 27 h after treatment, thus confounding the treatment effect with culture growth. Besides known effects of sodium butyrate pertaining to chromatin destabilization, modulations of apoptotic and cell-cycle genes, among others, the data revealed differential expression of some enzymatic transcripts from glycolysis and lipid metabolism, in particular the downregulation of lactate dehydrogenase, but were insufficient to discern a consistent metabolic pattern. Interestingly, a general down-regulation of the translational machinery was also observed, obscuring the reason for

increased specific recombinant protein production. This phenomenon bears resemblance to that of increased specific productivity following treatment of hybridoma cell cultures with the mTOR inhibitor rapamycin, having been proposed that the negative impact on growth may free protein translation capacity to recombinant mRNAs or exert its effect through modulation of metabolic efficiency (Balcarcel and Stephanopoulos, 2001). Following on Gatti et al. (2007), Yee et al. (2008) compared CHO and hybridoma cell responses to butyrate treatment using species-specific DNA microarrays with an increase number of probes and complemented by 2D-gel protein electrophoresis. They were able to shed light into the effect on increased specific productivity, discerning a consistent trend of increased protein processing and secretion capacity. This observation has been more recently corroborated by Kantardjieff et al. (2010), who found elevated secretory capacity under butyrate treatment and low temperature (33°C) conditions in a combined transcriptomic and proteomic study. Clearly, butyrate treatment has a generalized effect on cellular physiology; further studies integrating a comprehensive metabolic fluxome analysis with quantitative surveys of enzyme expression and activity are important to unravel its global effect on metabolic behavior in culture.

2.4 Conclusions

This work evaluated metabolic flux distributions of GS-CHO cell clones based on exometabolome profiling. Supernatant metabolites were quantified along culture time through ^{1}H-NMR under control and butyrate-treated conditions, allowing the identification of a comprehensive network of 117 intracellular or transport reactions and its validation with experimental data of 24 metabolic phases. Estimated fluxomes reveal higher metabolic efficiency than other CHO cell lines and a differentiated nitrogen metabolism, characterized by high asparagine utilization (instead of glutamine) which is the major nitrogen source for the cell and at the same time is used for energy generation. Moreover, serine was consumed at high rates and fuels 1C units metabolism, leading to glycine and formate accumulation. The most distinctive

observation in the transition from the exponential to the stationary phase was a substantial decrease in metabolite transport rates associated with a general depression in metabolic activity. However, as previously reported, metabolic efficiency significantly increases, mainly due to a shift from lactate production to consumption. While metabolic differences between the two cell clones studied were only modest, butyrate treatment had a marked effect on sustaining high nutrient consumption along culture time, increasing energy generation and biosynthetic activity during stationary phase, when the effect on increased specific productivity was also higher. These results further clarify the behavior of CHO cells in culture under different growth and production conditions.

2.5 Acknowledgements

This work was supported by project grants FP7/HEALTH.2011.1.1-1/279039, PTDC/EBB-EBI/102750/2008 and PTDC/BBB-BSS/0518/2012. Nuno Carinhas acknowledges Fundação para a Ciência e a Tecnologia (FCT) for his post-doctoral fellowship grant (SFRH/BPD/80514/2011). Tiago Duarte acknowledges FCT for his Ph.D. grant (SFRH/BD/81553/2011). FCT is also acknowledged for supporting the National NMR Network (REDE/1517/RMN/2005).

2.6 Author contribution

Tiago Duarte participated in the experimental design, performed the experiments, analyzed the data and participated in the writing of the chapter.

2.7 References

Ahn WS, Antoniewicz MR. 2011. Metabolic flux analysis of CHO cells at growth and non-growth phases using isotopic tracers and mass spectrometry. Metab Eng 13:598-609.

Ahn WS, Antoniewicz MR. 2012. Towards dynamic metabolic flux analysis in CHO cell culture. Biotechnol J 7:61-74.

Ahn WS, Antoniewicz MR. 2013. Parallel labeling experiments with [1,2-^{13}C] glucose and [U-^{13}C]glutamine provide new insights into CHO cell metabolism. Metab Eng 15:34-47.

Altamirano C, Paredes C, Cairó JJ, Gòdia F. 2000. Improvement of CHO cell culture medium formulation: simultaneous substitution of glucose and glutamine. Biotechnol Prog 16:69-75.

Altamirano C, Paredes C, Illanes A, Cairó JJ, Gòdia F. 2004. Strategies for fed-batch cultivation of t-PA producing CHO cells: substitution of glucose and glutamine and rational design of culture medium. J Biotechnol 110:171-179.

Balcarcel RR, Stephanopoulos G. 2001. Rapamycin reduces hybridoma cell death and enhances monoclonal antibody production. Biotechnol Bioeng 76:1-10.

Carinhas N, Oliveira R, Alves PM, Carrondo MJT, Teixeira AP. 2012. Systems biotechnology of animal cells: the road to prediction. Trends Biotechnol 30:377-385.

Chong WPK, Reddy SG, Yusufi FNK, Lee D-Y, Wong NSC, Heng CK, Yap MGS, Ho YS. 2010. Metabolomics-driven approach for the improvement of Chinese hamster ovary cell growth: Overexpression of malate dehydrogenase II. J Biotechnol 147:116-121.

Chong WPK, Thng SH, Hiu AP, Lee DY, Chan ECY, Ho YS. 2012. LC-MS-based metabolic characterization of monoclonal antibody-producing chinese hamster ovary cells. Biotechnol Bioeng 109:3103-3111.

Dean J, Reddy P. 2013. Metabolic analysis of antibody producing CHO cells in fed batch production. Biotechnol Bioeng 110:1735–1747.

Dietmair S, Hodson MP, Quek LE, Timmins NE, Chrysanthopoulos P, Jacob SS, Gray P, Nielsen LK. 2012. Metabolite profiling of CHO cells with different growth characteristics. Biotechnol Bioeng 109:1404-1414.

Duarte TM, Carinhas N, Silva AC, Alves PM, Teixeira AP. 2013. ^{1}H-NMR protocol for exometabolome analysis of cultured mammalian cells. Animal Cell Biotechnology - Methods and Protocols, 3rd Edition, Springer, Part III:237-247.

Fogolín MB, Wagner R, Etcheverrigaray M, Kratje R. 2004. Impact of temperature reduction and expression of yeast pyruvate carboxylase on hGM-CSF-producing CHO cells. J Biotechnol 109:179-191.

Gatti MDL, Wlaschin KF, Nissom PM, Yap M, Hu W-S. 2007. Comparative transcriptional analysis of mouse hybridoma and recombinant Chinese hamster ovary cells undergoing butyrate treatment. J Biosci Bioeng 103:82-91.

Goudar C, Biener R, Boisart C, Heidemann R, Piret J, Graaf A, Konstantinov K. 2010. Metabolic flux analysis of CHO cells in perfusión cultura by metabolite balancing and 2D [^{13}C, ^{1}H] COSY NMR spectroscopy. Metab Eng 12:138-149.

Griffin TJ, Seth G, Xie H, Bandhakavi S, Hu W-S. 2007. Advancing mammalian cell culture engineering using genome-scale technologies. Trends Biotechnol 25:401-408.

Jiang Z, Sharfstein ST. 2008. Sodium butyrate stimulates monoclonal antibody over-expression in CHO Cells by improving gene accessibility. Biotechnol Bioeng 100:189-194.

Kantardjieff A, Jacob NM, Yee JC, Epstein E, Kok Y-J, Philp R, Betenbaugh M, Hu W-S. 2010. Transcriptome and proteome analysis of Chinese hamster ovary cells under low temperature and butyrate treatment. J Biotechnol 145:143–159.

Khoo SHG, Al-Rubeai M. 2009. Metabolic characterization of a hyper-productive state in an antibody producing NSO myeloma cell line. Metab Eng 11:199-211.

Kim SH, Lee GM. 2007. Down-regulation of lactate dehydrogenase-A by siRNAs for reduced lactic acid formation of Chinese hamster ovary cells producing thrombopoietin. Appl Microbiol Biotechnol 74:152-159.

Klamt S, Stelling J, Ginkel M, Gilles ED. 2003. FluxAnalyzer: exploring structure, pathways, and flux distributions in metabolic networks on interactive flux maps. Bioinformatics 19:2.

Lewis AP, Lemon SM, Barber KA, Murphy P, Parry NR, Peakman TC, Sims MJ, Worden J, Crowe JS. 1993. Rescue, expression, and analysis of a neutralizing human anti-hepatitis A virus monoclonal antibody. J Immunol 151:2829-2838.

Lodish H, Baltimore D, Berk A, Zipursky SL, Matsudaira P, Darnell J. 1995. Molecular cell biology. New York: Scientific American Books, Inc. 89 p.

Luo J, Vijayasankaran N, Austsen J, Santuary R, Hudson T, Amanullah A, Li F. 2011. Comparative metabolite analysis to understand lactate metabolism shift in Chinese hamster ovary cell culture process. Biotechnol Bioeng 109:146-156.

Ma N, Ellet J, Okediadi C, Hermes P, McCormick E, Casnocha S. 2009. A single nutrient feed supports both chemically defined NSO and CHO fed-batch processes: improved productivity and lactate metabolism. Biotechnol Prog 25:1353-1363.

Martínez VS, Dietmair S, Quek L-E, Hodson MP, Gray P, Nielsen LK. 2013. Flux balance analysis of CHO cells before and after a metabolic switch from lactate production to consumption. Biotechnol Bioeng 110:660-666.

McMurray-Beaulieu V, Hisiger S, Durand C, Perrier M, Jolicoeur M. 2009. Na-butyrate sustains energetic states of metabolism and t-PA productivity of CHO cells. J Biosci Bioeng 108:160-167.

Mulukutla BC, Gramer M, Hu WS. 2012. On metabolic shift to lactate consumption in fed-batch culture of mammalian cells. Metab Eng 14:138-149.

Mulukutla BC, Khan S, Lange A, Hu WS. 2010. Glucose metabolism in mammalian cell culture: new insights for tweaking vintage pathways. Trends Biotechnol 28:476-484.

Narkewicz MR, Sauls SD, Tjoa SS, Teng C, Fennessey PV. 1996. Evidence for intracellular partitioning of serine and glycine metabolism in Chinese hamster ovary cells. Biochem J 313:991–96.

Niklas J, Schräder E, Sandig V, Noll T, Heinzle E. 2011. Quantitative characterization of metabolism and metabolic shifts during growth of the new human cell line AGE1.HN using time resolved metabolic flux analysis. Bioprocess Biosyst Eng 34:533–545.

Nolan RP, Lee K. 2011. Dynamic model of CHO cell metabolism.Metab Eng 13:108–124.

Quek L-E, Dietmair S, Krömer JO, Nielsen LK. 2010. Metabolic flux analysis in mammalian cell culture. Metab Eng 12:161-171.

Sellick CA, Croxford AS, Maqsood AR, Stephens G, Westerhoff HV, Goodacre R, Dickson AJ. 2011. Metabolite profiling of recombinant CHO cells: designing feeding regimens that enhance recombinant antibody production. Biotechnol Bioeng 108:3025–3031

Selvarasu S, Ho YS, Chong WPk, Wong NSC, Yusufi FNK, Lee YY, Yap MGS, Lee D-Y. 2012. Combined in silico modeling and metabolomics analysis to characterize fed-batch CHO cell culture. Biotechnol Bioeng 109:1415-1428.

Sengupta N, Rose ST, Morgan JA. 2011. Metabolic flux analysis of CHO cell metabolism in the late non-growth phase. Biotechnol Bioeng 108:82-92.

Sheikh K, Förster J, Nielsen LK. 2005. Modeling hybridoma cell metabolism using a generic genome-scale metabolic model of *Mus musculus*. Biotechnol Prog 21:112-121.

Stephanopoulos G, Aristidou AA, Nielsen J. 1998. Metabolic engineering. Principles and Methodologies. San Diego: Academic Press. p 333-341.

Templeton N, Dean J, Reddy P, Young JD. 2013. Peak antibody production is associated with increased oxidative metabolism in an industrially relevant fed-batch CHO cell culture. Biotechnol Bioeng (in press).

Voet D, Voet JG. 1995. Biochemistry. New York: John Wiley & Sons. p 271-272.

Wang NS, Stephanopoulos G. 1983. Application of macroscopic balances to the identification of gross measurement errors. Biotechnol Bioeng 25:2177-2208.

Wang Q, Zhang Y, Yang C, Xiong H, Lin Y, Yao J, Li H, Xie L, Zhao W, Yao Y, Ning ZB, Zeng R, Xiong Y, Guan KL, Zhao S, Zhao GP. 2010. Acetylation of metabolic enzymes coordinates carbon source utilization and metabolic flux. Science 327:1004-1007.

Wurm FM. 2004. Production of recombinant protein therapeutics in cultivated mammalian cells. Nat Biotechnol 22:1393-1398.

Xu X, Nagarajan H, Lewis NE, Pan S, Cai Z, Liu X, Chen W, Xie M, Wang W, Hammond S, Andersen MR, Neff N, Passarelli B, Koh W, Fan HC, Wang J, Gui Y, Lee KH, Betenbaugh MJ, Quake SR, Famili I, Palsson BO, Wang J. 2011. The genomic sequence of the chinese hamster ovary (CHO)-K1 cell line. Nat Biotechnol 29:735-741.

Yee JC, Gatti ML, Philp RJ, Yap M, Hu W-S. 2008. Genomic and proteomic exploration of CHO and Hybridoma cells under sodium butyrate treatment. Biotechnol Bioeng 99:1186–1204.

Zamorano F, Wouwer AV, Bastin G. 2010. A detailed metabolic flux analysis of an underdetermined network of CHO cells. J Biotechnol 150:497-508.

Zhao S, Xu W, Jiang W, Yu W, Yan L, Zhang T, Yao J, Zhou L, Zeng Y, Li H, Li Y, Shi J, An W, Hancock SM, He F, Qin L, Chin J, Yang P, Chen X, Lei Q, Xiong Y, Guan K-L. 2010. Regulation of cellular metabolism by protein lysine acetylation. Science 327:1000-1004.

Zhou M, Crawford Y, Ng D, Tung J, Pynn AFJ, Meier A, Yuk IH, Vijayasankaran N, Leach K, Joly J, Snedecor B, Shen A. 2011. Decreasing lactate level and increasing antibody production in Chinese Hamster Ovary cells (CHO) by reducing the expression of lactate dehydrogenase and pyruvate dehydrogenase kynases. J Biotechnol 153:27-34.

CHAPTER 3

Exploring GS-CHO cells metabolism under control and butyrate-treated conditions through parallel ^{13}C-labeling experiments

Adapted from:

Duarte TM, Seifar RM, Wahl AS, Alves PM, Teixeira AP, Exploring GS-CHO cells metabolism under control and butyrate-treated conditions through parallel ^{13}C-labeling experiments (manuscript in preparation)

Abstract

Identifying host cell metabolic wphenotypes that support high recombinant protein production is a major goal in biotechnology. Incubation with stable ^{13}C and ^{15}N isotope labeled nutrients is a powerful strategy to map the flow of carbon and nitrogen through intracellular metabolic pathways, providing insights into relative pathway activities and nutrient contributions. In this study, we applied state-of-the-art ^{13}C metabolomics based on GC/LC-MS to analyse the central metabolism of GS-CHO cells, under control and butyrate-treated conditions. This was achieved through short-term parallel labeling experiments using [1,2-^{13}C]glucose, [U-^{13}C^{15}N]asparagine and [U-^{13}C^{15}N]serine, during the mid-exponential growth phase. Analysis of ^{13}C positional enrichment of glycolytic and pentose phosphate pathway (PPP) intermediates suggests that about 30% of glucose is diverted to the PPP and recycled back to glycolysis. Furthermore, the mass isotopomer distributions (MID) of (G6P) glucose-6-phosphate and (6PG) 6-phosphogluconate suggest a partially cyclic operation of the PPP, possibly to generate more NADPH for biosynthesis. Another important source of NADPH was the flux through the malic enzyme reaction, as suggested by the labeling of [^{13}C]asparagine-derived pyruvate. Noteworthy, asparagine was essential for TCA cycle intermediates replenishment, as well as for glutamine synthesis in GS-CHO cells, growing in a glutamine-free culture media. Asparagine and serine were confirmed to be the most important nitrogen sources in these cells, with ^{15}N from both highly present in many non-essential amino acids. Finally, butyrate treatment increased significantly most measured intracellular pools. Furthermore, the ^{13}C incorporation data suggests butyrate enhances the malic enzyme activity, associated to increased NADPH production. Overall, our results represent important insights into the metabolism of a widely employed mAb-producing CHO cell host. The identified metabolic traits can be explored to enhance cellular performance.

CONTENTS

3.1 Introduction

Chinese hamster ovary cells are widely used in industrial processes for the production of recombinant proteins due to their robust growth and ability to perform post-translational modifications (Wurm 2004). Several culture strategies have been applied to improve CHO cells capabilities for protein production, such as temperature shift, media optimization and chemical approaches (Carinhas et al. 2013; Yoon et al. 2006; Yu et al. 2011). More recently, the development of systems biotechnology tools significantly has allowed enriching our knowledge about cellular physiology. The fields of genomics, transcriptomics and proteomics provide valuable information on the physiological state of a cell; whereas the metabolome and fluxome integrate the information from these omic layers into functional phenotypic snapshots. In this sense, the study of metabolic phenotypes of CHO cells in culture is essential for productivity improvement through bioprocess development and cell engineering (Ahn and Antoniewicz 2012). However, despite the extensive research on CHO cells, there is still a lack of comprehensive knowledge on the metabolism of these cells in cell culture.

^{13}C-based metabolic analysis has allowed obtaining the most comprehensive information to characterize cellular metabolic states, through NMR or mass spectrometry (MS) (Crown and Antoniewicz 2012; Metallo et al. 2012; Yang et al. 2006). The combination of the mass isotopomer analysis of metabolites derived from ^{13}C-labeled substrates with classical metabolomics can have a synergistic effect on the discovery of apparently unrelated pathways (Yang et al. 2006). So far, very few ^{13}C-based metabolic analysis studies have been performed to study the performance of CHO cells in culture. In the last years, CHO cells behavior were studied elucidating pathways such as PPP and glycolysis, which could only be estimated using isotopic tracers (Goudar et al. 2010; Sengupta et al. 2011). Recently, the intracellular fluxes of CHO cells in batch culture were mapped, based on solely the labeling patterns of extracellular metabolites resulting from a [U-^{13}C]-glucose feed, highlighting metabolic reversibility and compartmentation (Nicolae et al. 2014). Moreover, there have been

even fewer studies on the metabolism of GS-CHO cells, a proprietary cell line derived from CHO K1 which uses a selection system that couples the expression of glutamine synthetase (GS) gene with a protein of interest (Lonza Biologics, UK). This selection system also grants GS-CHO cells the ability to grow in a glutamine-free culture medium, minimizing the accumulation of ammonia, and making GS-CHO cells one of the most used industrially (Wurm 2013).

In this work, we report a comprehensive metabolic investigation of a mAb-producing GS-CHO cell line, with and without butyrate treatment, through mass isotopomer distribution (MID) analysis of intracellular metabolites from ^{13}C-labeled substrates combined with exometabolome profiling trough ^{1}H-NMR. Three isotopic tracers were used, [1,2-^{13}C]-glucose, [U-$^{13}C^{15}N$]-asparagine and [U-$^{13}C^{15}N$]-serine, in order to explore the preferred pathways of each substrate and evaluate the effect of butyrate treatment on central metabolism. Butyrate is a histone deacetylase inhibitor with the ability to change chromatin structure, and has been empirically applied in the industry to improve specific productivity of recombinant proteins in mammalian cells (Crowell et al. 2008; Jiang and Sharfstein 2008). We have shown recently that butyrate treatment has a significant effect on sustaining the overall metabolic activity of GS-CHO cells (Carinhas et al. 2013). Additionally, it was observed that most enzymes of central metabolism are acetylated, as a result of post-translational modifications (Zhao et al. 2010), which are able to modulate enzyme activity and increase or decrease reactions fluxes up to twofold (Wang et al. 2011; Zhao et al. 2010). Further evidence of butyrate's effect on central metabolism is provided herein. The work will be presented in two parts: firstly, the detailed description of total isotopomer yields and MID analysis from parallel labeling experiments under control conditions; and secondly the integration of MID analysis of intracellular metabolites with exometabolome dynamics under butyrate treatment.

3.2 Materials and Methods

3.2.1 Cell culture conditions

A CHO cell clone generated by stable transfection of the CHOK1SV cell line with a construct containing GS and the light and heavy chains of an IgG_4 mAb was provided by Lonza Biologics. Cells were maintained in CDCHO chemically defined medium (Cat. No. 10743-029, Gibco, Life Technologies, Carlsbad, CA) supplemented with 25 μM methionine sulphoximine (MSX; Cat. No. M5379, Sigma-Aldrich, St. Louis, MO), in 125 mL shake flasks with 25 mL culture volume and sub-cultured every 3–4 days with a seeding density of 0.4 x 10^6 cell/mL. All cultures were kept in a humidified incubator controlled at 37 °C and 7 % CO_2 with orbital shaking at 130 rpm.

In this work, eight shake flask cultures were performed, four with 0.75 mM sodium butyrate (Cat. No. 8175000100, Merck, Germany) added 24 h after inoculation) and the remaining four without butyrate addition (control). For all eight cultures, a custom made CDCHO media without glucose, serine and asparagine, was supplemented with 20 mM glucose, 3.5 mM asparagine, 2.5 mM serine and 25 μM MSX.

3.2.2 Labeling experiments

Before adding the isotopic tracers at 48 h, the bulk of cultured cells either in control or butyrate-treated shake flasks, were each divided in four shake flasks – four controls and four butyrate-treated cell cultures. Addition of isotopic tracers was done so that each pair of shake flasks, one control and one with butyrate, had 20 mM [1,2-^{13}C]glucose (CIL, MA, USA), two other had 4 mM [U-^{13}C/^{15}N]asparagine (CIL, MA, USA) and two other had 4 mM [U-^{13}C/^{15}N]serine (CIL, MA, USA) (Fig. 3.1A). Remaining concentrations of unlabeled substrates (glucose, asparagine and serine) were also added to the feed, matching the concentration of the labeled substrates. These six shake flasks were used for mass isotopologue distribution (MID) analysis throughout 24 h after adding the labels. The two remaining shake flasks had no [^{13}C] label and were used for ^{1}H-NMR analysis of the supernatants and quantification of intracellular

metabolite pools.

3.2.3 Sampling

Cell number and viability were analyzed under a light microscope using trypan blue dye and a hemocytometer, for all cultures. After counting cells, samples were clarified by centrifugation at 200 g during 10 min and the supernatant stored at -20 °C for later quantification of produced IgG_4 and total protein, as well as exometabolome analysis (Fig. 3.1A).

During labeling experiment, samples from cultures with [^{13}C] labels were collected at time points 0, 3 and 10 min, 1 h, 3 h, 8 h and 24 h, for MID analysis; and from the cultures without isotopic tracers, samples were collected from time points 0 h, 8 h and 24 h, for ^{1}H-NMR and absolute quantification of intracellular metabolites (Fig. 3.1A).

3.2.4 Quenching and extraction of intracellular metabolites

Quenching was performed by rapidly adding four parts of ice-cold 0.9% (w/v) NaCl solution followed by two cycles of 1 min centrifugation at 1,000 x g and 4 °C. An internal standard was added to the samples from the unlabeled cultures only, for quantification of intracellular metabolites, previous to extraction. Intracellular metabolites were then extracted in ice-cold 50% (v/v) acetonitrile, with brief vortexing, incubation for 10 min in ice and snap freezing in liquid nitrogen. After thawing on ice, samples were centrifuged for 10 min at 15,000 x g and 4 °C. The supernatants (cell extracts) were dried by vacuum centrifugation overnight and stored at -20 °C until derivatization.

3.2.5 IgG quantification

Accumulation of IgG in the supernatant was monitored using a sandwich ELISA assay. Briefly, Nunc Maxisorp 96-well plates (Cat. No. 437842, Thermo Scientific, Waltham, MA) were coated with a goat anti-human IgG, Fcγ specific (Cat. No. 109-006-098, Jackson Immunoresearch Labs, West Grove, PA) at a concentration of 2 μg/L in carbonate buffer. Blocking was performed with 0.5% casein in carbonate buffer. Solutions with known concentrations of antibody were included on each plate for

calibration. Bound antibody was detected using goat anti-human IgG (Fab specific)—peroxidase antibody (Cat. No. A0293, Sigma-Aldrich). The complex was visualized with TMB substrate (Cat. No. 00-2023, Invitrogen, Life Technologies, Carlsbad, CA) while 2.5 M sulfuric acid was used as stop solution. Color development was measured at 450 nm.

3.2.6 Total protein quantification

The total protein content in supernatant samples collected along culture was quantified with the Coomassie Plus (Bradford) Protein Assay reagent (Cat. No. 23238, Pierce, Thermo Scientific, Waltham, MA) using Bovine Gamma Globulin (Cat. No. 23212, Thermo Scientific) as the protein reference standard. Briefly, 10 μL of each sample were mixed in a microplate with 300 μL of Coomassie Plus reagent for 30 s. The plate was incubated during 10 min at room temperature and the absorbance measured at 595 nm.

3.2.7 Exometabolome analysis

^{1}H-NMR analysis of supernatant samples from unlabeled cultures was performed on a 500MHz Avance spectrometer (Bruker, Billerica, MA) equipped with a 5-mm QXI inversed probe. Spectra were acquired using a NOESY-based pulse sequence with water presaturation, performing 256 scans with 4 s acquisition time, 1 s relaxation delay and 100 ms mixing time at 25 °C. DSS-d_6 (Cat. No. 613150, Isotec, Sigma-Aldrich, St. Louis, MO) was used as internal standard for metabolite quantification in all samples. In order to maintain a constant pH between samples, these were mixed with phosphate buffer (pH 7.4) prepared in D_2O (Cat. No. 151882, Sigma-Aldrich, St. Louis, MO) at a 2:1 ratio. Before spectra acquisition, the spectrometer was calibrated by determining the 90° pulse and the water chemical shift centre of each sample. Each spectrum was phased; baseline corrected and integrated using the Chenomx NMR Suite 7.1 (Chenomx, Inc., Edmonton, Alberta, Canada). Chemical shifts of clusters used for quantification, correction factors, errors, and limits are available in Duarte et al. (2014b).

Ammonia was quantified in supernatant samples from all cultures using an enzymatic kit (Cat. No. AK00091, NZYTech, Lisboa, Portugal) based on the measurement at 340

nm of the amount of $NADP^+$ formed through the activity of glutamate dehydrogenase (GLDH).

The amino acids content in cell supernatant samples from all cultures (time points 0 h, 8 h and 24 h) were also quantified by HPLC on a Hewlett Packard 1100 system (Agilent Technologies, Palo Alto, CA). Prior to derivatization, sample proteins were precipitated by adding an equal volume of acetonitrile and removed by centrifugation at 12,400 g for 15 min, at room temperature. Following derivatization with o-phthaldialdehyde, samples were separated on a Zorbax SB-C18 (4.6 mm, 150 mm, 3.5 lm) column from Agilent using a phosphate buffer (50 mM, pH 5.9) and a solution of methanol and tetrahydrofurane (98.75%/1.25%) as eluents. An internal standard (g-aminobutyric acid) was added to ensure consistent measurements between runs. The separated amino acids were detected by fluorescence and quantified by comparison with a standard curve of known amino acids concentrations.

Total glucose and lactate concentrations in the culture supernatants from the same time points, were also determined with automated enzymatic assays (YSI 7100 Multiparameter Bioanalytical System; Dayton, OH, USA).

3.2.8 Derivatization of intracellular metabolites

Amino acids, lactate and TCA cycle intermediates were firstly transformed to their methyloximes derivatives with 20 µL of O-methoxyamine hydrochloride (MOX solution; Sigma Aldrich, DE) in a pyridine (Sigma Aldrich, DE) solution (10 mg/mL) for 2 h at 40 °C. In a second step, these methyloximes reacted with 40 µL of MBDSTFA at room temperature for 1h, followed by heating at 60 °C for 1 h, to obtain the *tert*-butyldimethylsilyl derivatives. Glycolytic and PPP intermediates were firstly incubated for 50 min at 70 °C with MOX solution; and, secondly, derivatized using MSTFA-TMCS for 50 min at 70 °C.

3.2.9 GC-MS analysis

Amino acids, lactate and TCA cycle intermediates

GC–MS analysis was performed on a QP2010 mass spectrometer (Shimadzu, Japan) in the EI mode (70 eV). The ionic source temperature was 250 °C, the same as the interface that connects to the column. GC was performed on a HP-5MS column (30 m length, 0.25 mm internal diameter, composed of dimethylpolysiloxane with 5% phenyl groups, 0.25 μm film thickness; Agilent Technologies, Inc) in split or splitless mode depending on the peak intensities, with helium as carrier gas at an inlet pressure of 600 kPa. Injections were carried out automatically with an AOC-5000 Plus autosampler (Shimadzu, Japan) using an injection volume of 1 μL and injector temperature set at 250 °C (Chaves das Neves and Vasconcelos 1987). Mass spectra were analyzed using the GC-MS Solution software version 2.50 SU1 (Shimadzu, Japan). Metabolite identification was confirmed by comparison with standard solutions prepared in the same conditions in water and/or by spiking experiments - through the supplementation of the pure compounds, at different concentrations, in cell culture medium. Mass isotopomer distributions were obtained by integration of ion chromatograms and corrected for natural isotope abundances. For each metabolite, all ions were measured (M, corresponding to the naturally labeled metabolite; Mn, where n is the number of labeled carbons or nitrogens).

Glycolytic and PPP intermediates

Mass isotopomer distributions (MID) of glycolytic intermediates (GAP, DHAP, 3PG, 2PG, Pyr), and PPP intermediates (E4P, R5P, Ru5P, X5P, S7P) were determined through a GC-MS-based analysis, performed on a GC-EI-MS (GC: 7890A, MS: 5975C Agilent Technologies, Santa Clara, CA, USA) with PTV injection system (Cooled Injection System CIS4, Gerstel GmbH, Mülheim an der Ruhr, Germany), equipped with a Zebron ZB-50 column (30 mÅ~250 μm, 0.25 μm film thickness; Phenomenex, Torrance, CA, USA). Injection temperature was set at 300 °C and the injection volume was 1 μl. The system was operated in split-less mode or in split mode for metabolites in high concentration

(additional parameters can be found in Wahl et al. 2014). MS settings include transfer line at 250 °C, source temperature 230 °C and quadrupole temperature at 150 °C.

3.2.10 LC-MS/MS analysis

The glycolytic intermediates G6P, F6P, 6PG, PEP, and FBP and succinate were analysed through anion exchange chromatography and electrospray ionization with tandem mass spectrometric detection using a HPLC system Alliance HT pump 2795 system (Waters, USA) combined with an MS Quattro LC™ triple quadrupole (Waters, UK). This system is equipped with a 515 HPLC pump (Waters, USA), a 2-position-Ten port stainless steel LabPro Selector valve (Rheodyne, USA), a two way LabPro Solvent select (Rheodyne, USA) and an ASRS® 300 with 4 mm self-regenerating suppressor (Dionex, USA). An LC IonPac AS11 (Dionex, Sunnyvale, USA) column with 4 mm inner diameter column to 250 mm in length was used in combination with a A XTerra® MS C18 column with 3 mm inner diameter and 20 mm length (Waters, Ireland). Further details can be found in (van Dam et al. 2002).

3.2.11 Quantification of intracellular total metabolite pools

Quantification of intracellular metabolites was made through MS methods as described above, using a ^{13}C-extract as reference, in a ratio usually of 1:5 volumes of ^{13}C-extract to sample volume. This ratio may vary slightly accordingly to the metabolite concentration in the sample. Further details can be found in Wahl et al (2014).

3.3 Results and discussion

3.3.1 Cell growth and antibody production

GS-CHO cells were cultured under control and butyrate-treated conditions (Fig. 3.1A). Butyrate was added 24 h after inoculation, when viable cell concentration was $1x10^6$ cell/ml, immediately impacting cell growth (Fig. 3.1B): maximum cell density was limited to $1.3x10^6$ cells/ml, in comparison to the $3.2x10^6$ cells/ml reached in control conditions after 72 h. At the end of this period, similar antibody titres were reached in both culture conditions (Fig. 3.1C), with butyrate-treated cultures showing a 1.4-fold

increase in specific productivity in comparison to the control (Fig. 3.1D), as observed previously during the exponential growth phase (Carinhas et al. 2013).

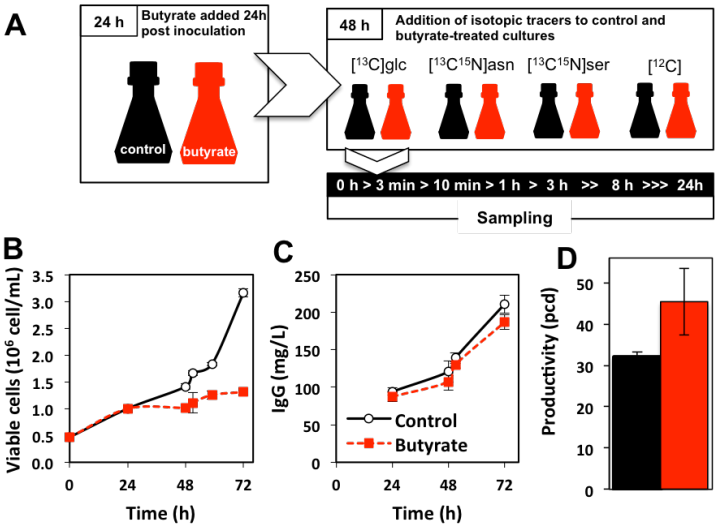

Figure 3.1 (A) Timeline of experimental setup. Viable cell (B) and antibody concentration (IgG_4) (C) profiles, and specific productivity (D) in control and butyrate-treated cultures. Values represent the averages of 4 replicates, accompanied by the respective error bars.

3.3.2 ^{13}C-labeling dynamics of GS-CHO cells under control conditions

Three isotopic tracers were used to investigate the intracellular metabolism of GS-CHO cells in further detail, added 48 h after inoculation (Fig. 3.1A). [1,2-^{13}C]glucose was used since it has been established as the best tracer for the analysis of overall cellular metabolism of mammalian cells (Antoniewicz et al. 2007; Metallo et al. 2009). [U-^{13}C^{15}N]asparagine and [U-^{13}C^{15}N]serine were also selected to explore their fate in central carbon metabolism as these are the two most consumed amino acids in GS-CHO cells (Duarte et al. 2014a).

3.3.2.1 Mass isotopomer distribution of intracellular metabolites from [1,2-^{13}C]glucose

The fate of glucose carbons 1 and 2 on energetic metabolism are detailed on Figure 3.2, through the label enrichment profiles of downstream metabolites. The composition of

glucose in the culture medium was 58 % [1,2-^{13}C]glucose and 42 % natural glucose. We analysed the distribution of mass isotopomers in intermediates of glycolysis, PPP and TCA cycle, as well as in some amino acids. Most metabolites did not reach an isotopic steady state 24 h after the isotopic tracer was added to culture media.

Figure 3.2A shows the MIDs of upper glycolysis and PPP throughout the labeling experiment. After cellular uptake, each molecule of glucose is phosphorylated to glucose-6-phosphate (G6P), which in turn can be converted to fructose-6-phosphate (F6P) down the glycolytic pathway, or used to generate pentose phosphates, where the first ^{13}C atom is lost as CO_2 (6-phosphogluconate dehydrogenase (6PGDH) catalysed reaction). When the need for reducing power (NADPH) exceeds the need for pentose precursors (R5P) for nucleotide synthesis, the PPP-derived F6P and G3P are transformed into pyruvate through glycolysis. Therefore, the ratio of M1/M2 isotopomers of glycolytic metabolites (G6P, F6P, FBP, DHAP, 3PG, PEP and pyruvate) give an idea on the flux partitioning of glucose through glycolysis and the non-oxidative branch of PPP, which was around 70 and 30 %, respectively. These results significantly differ from other studies, where non-oxidative PPP has been described inactive or insignificant during early exponential phase of both non-producing (Ahn and Antoniewicz 2011) and producing CHO cell lines (Templeton et al. 2013).

Interestingly, the high abundance of M1 G6P (14%) and M1 6PG (20%), 24 h after label was added, which are metabolites upstream to the reaction where the loss of $^{13}CO_2$ occurs (6PGDH enzyme), suggests that oxidative PPP is operating in cyclic mode, with considerable conversion of F6P into G6P. This feature has been described for the late exponential phase of CHO cell cultures, when the glucose-6-phosphate dehydrogenase (G6PDH) flux was determined to be greater than the hexokinase (HK) flux (Templeton et al. 2013). The recycling of G6P from PPP-derived F6P may represent an energetic advantage, since the redox energy of glucose can be conserved as NADPH at the expense of only one carbon per G6P (Bouzier-Sore and Bolanos 2015). As S7P results

from the condensation of PPP intermediates X5P and R5P, which may be both labeled, abundant heavier isotopomers were observed for this metabolite (e.g 15% M3).

Fig. 3.2B shows the MID profiles of the metabolites from lower glycolysis and pyruvate branch. 24 h post-label addition, the glucose-derived carbon in pyruvate, lactate and alanine were approximately 71, 77 and 52%, respectively. Stoichiometry was taken in consideration since each molecule of glucose is converted into two pyruvate molecules, one labeled and one unlabeled. The fact that lactate is more enriched than its precursor pyruvate suggests different pyruvate compartmentation pools (Amaral et al. 2011; Duarte et al. 2014a).

Although the lactate production to glucose consumption ratio was $Y_{Lac/Glc}$ 1.14, from the labeling patterns only 77% of the lactate pool was derived from glucose, i.e. about 44% of the glucose consumed was secreted as lactate. The remaining glucose entering the cells can be either channelled to the TCA cycle or diverted to biosynthesis. Fig. 3.2C shows the MIDs of TCA cycle metabolites citrate, αKG and malate, which were essentially also M1 and M2 isotopomers. At 24 h post-label addition approximately 85% of citrate had glucose-derived carbon, but only 73% of αKG and 43% of malate was derived from glucose, suggesting other carbon sources entering the TCA cycle downstream to the citrate node. Dean and Reddy (2013) have previously discussed the importance of certain amino acids for the replenishment of TCA metabolites, which led to the formation of lipogenic palmitate, in CHO cells. Interestingly, a small percentage of ^{13}C incorporation in serine and glycine indicates that glucose was also a source of one carbon units (data not shown). While serine was composed of M1 and M2 isotopomers (about 1.3% each at 24 h), only M1 glycine (0.9%) was observed due to loss of one labeled carbon during conversion of serine to glycine. Finally, we could not detect measurable label incorporation into asparagine from the glucose tracer (data not shown), which suggests inactivity of asparagine synthetase.

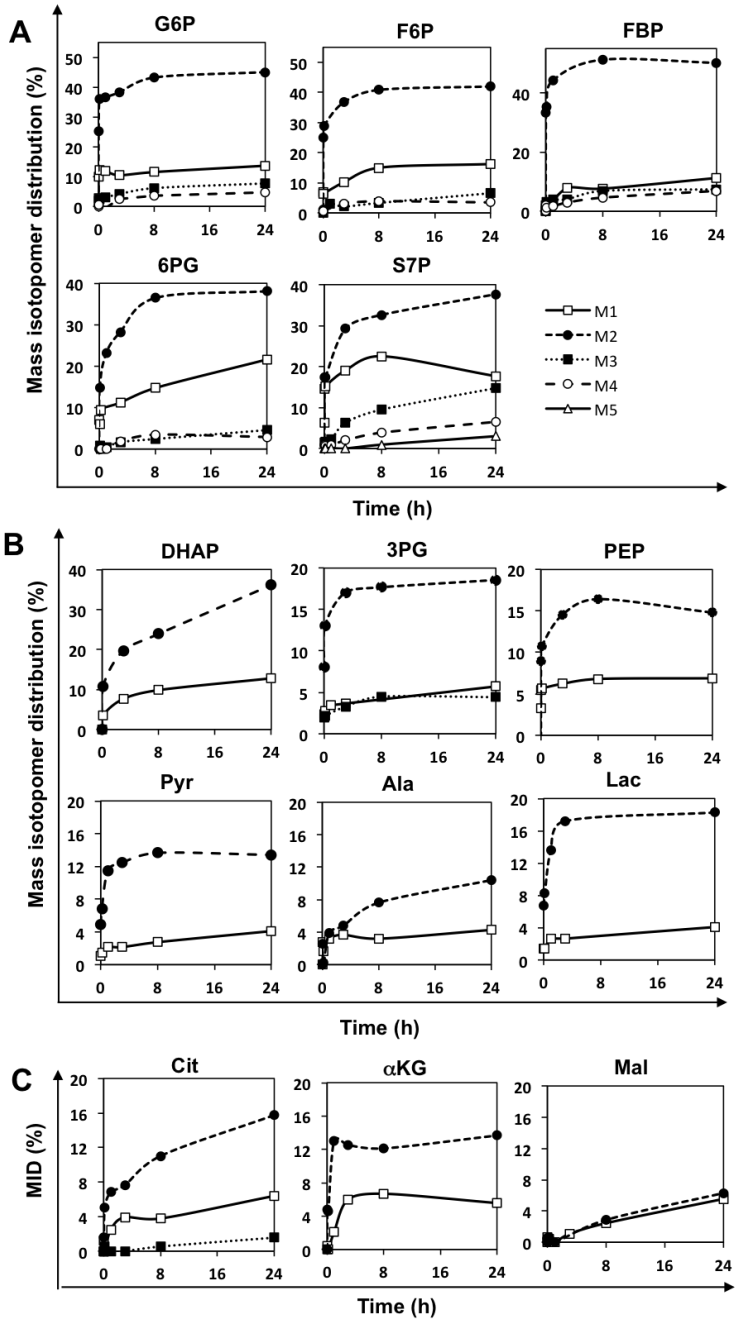

Figure 3.2 - Mass isotopomer distribution profiles for [1,2-^{13}C]-glucose experiment, during 24 h after isotopic tracer feed. (A) Upper glycolysis and PPP (B) Lower glycolysis and pyruvate branch (C) TCA cycle intermediates and related amino acids. Initial labeled-glucose in cell culture was 58%.

3.3.2.2 Mass isotopomer distribution of intracellular metabolites from [U-^{13}C^{15}N]-asparagine

Figure 3.3 shows the distribution of most prevalent isotopomers in a simplified model of GS-CHO cell metabolism after fully labeled asparagine was administered to cell culture. The experimentally measured ^{13}C enrichment in intracellular metabolites can be followed in Figure 3.4.

At the beginning of the labeling experiment, 63% of extracellular asparagine was fully labeled (M6) and intracellular asparagine reached an isotopic steady state after 3 h at approximately 59% (Fig. 3.4A). Asparagine can be deaminated to aspartate through a transamination reaction, with the loss of one amide labeled nitrogen as ammonia (Fig. 3.3). Surprisingly, aspartate was only 5% M5, showing a major prevalence of M1 label (26%), followed by M4 at 11% (Fig. 3.4A). M1 isotopomer was also the most abundant among other measured amino acids, namely glutamate (27%), glutamine (31%) and alanine (19%), which suggests that it corresponds to the amine group.

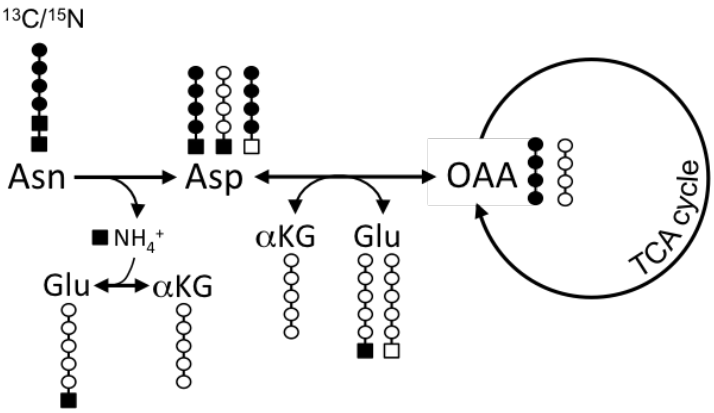

Figure 3.3 Simplified model for GS-CHO cell metabolism in cultures with fully labeled [U-^{13}C/^{15}N]-asparagine, in control condition. Representation of the two most prevalent mass isotopomers, in intracellular metabolites, detected 24 h after isotopic tracer feed. Circles and squares represent carbon and nitrogen atoms, respectively; in full, if labeled; or empty, without label.

These results are in agreement with Huang and colleagues' work, who studied the nitrogen metabolism of asparagine and glutamate, as glutamine replacers, in Vero cells

cultured in a glutamine-free medium (Huang et al. 2007). They reported that the amine nitrogen of asparagine was essentially metabolized to the amine group of aspartate, glutamate and glutamine; while the amide group of asparagine would be used as ammonia source for glutamine synthesis, where it would appear also in the amide group (Huang et al. 2007). These results also suggest the preferential pathway for isotope enrichment to be through the reversible transamination of aspartate and αKG to oxaloacetate and glutamate, as discussed previously.

Importantly, these results are indicative of the contribution of asparagine to glutamine synthesis, in GS-CHO cells growing in a glutamine-free media. Also, alanine M1 was up to 25% in the culture supernatant (data not shown), which confirms the contribution of asparagine as nitrogen source to fuel alanine production (Dean and Reddy 2013; Duarte et al. 2014a).

Noteworthy, pyruvate mass isotopomers M3 (11%) and M1 (3%) were observed (Fig. 3.4B). One possible explanation for the isotopomer distribution of pyruvate is the oxidative decarboxylation of malate into pyruvate through the activity of malic enzymes (ME) (Wahrheit et al. 2014). The [^{13}C] label on pyruvate could have not come from any other source, considering PEP and other glycolytic intermediates presented no [^{13}C] enrichment (data not shown). Malic enzymes are required for maintaining NADPH cellular levels as well as having a regulatory role in TCA flux matching cellular demand for energy and biosynthetic precursors (Jiang et al. 2013). Therefore, these results could also confirm that a cycle involving malic enzymes and PC may take a key role during exponential growth phase in replenishing NADPH (Dean and Reddy 2013; Templeton et al. 2013). The MID profiles of glycolytic intermediates did not show significant labeling from [U-^{13}C]asparagine, even after 24 h, suggesting that the gluconeogenesis pathway was negligible in these cells.

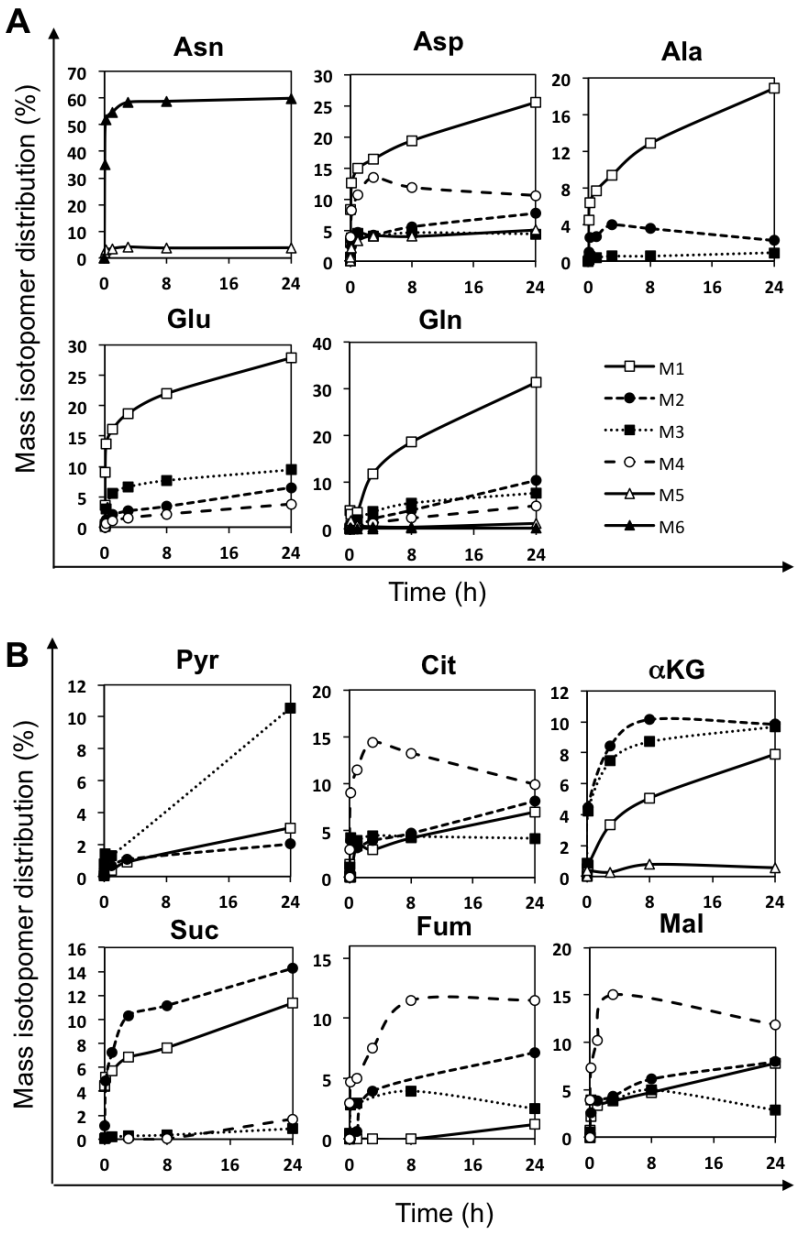

Figure 3.4 Mass isotopomer distribution profiles for [U-^{13}C/^{15}N]asparagine experiment, during 24 h after isotopic tracer feed. Initial fully labeled asparagine in cell culture was 63%. (A) Amino acids (B) Pyruvate and TCA cycle intermediates.

The total asparagine-derived carbon at 24 h post-label addition in the TCA cycle was 50% for citrate, and 53% for fumarate and malate. The utilization of asparagine to

replenish TCA cycle intermediates has been shown important, particularly during the exponential phase (Dean and Reddy 2013). Interestingly, the 11% M4 approximately both in fumarate and malate is consistent with the M4 enrichment observed on aspartate (also 11%), indicating the reversibility between these metabolites (Fig. 3.4B). Succinate, on the other hand, was only 2% M4 suggesting that succinate dehydrogenase has limited reverse activity. The TCA cycle operating in the forward direction produces succinate M2 (14% 24 h post label addition) from [U-^{13}C]asparagine because two of the labeled carbons of asparagine-derived citrate are lost as CO_2 before generating succinate. In agreement, M2 is then the second most abundant isotopomer of fumarate and malate (about 7%).

3.3.2.3 ^{13}C-labeling dynamics of metabolites derived from [U-^{13}C^{15}N]-serine

Serine is the second most consumed amino acid by these GS-CHO cells, following asparagine, thus it becomes important to evaluate its fate in central metabolism. It is an important precursor of one-carbon units in nucleotide synthesis.

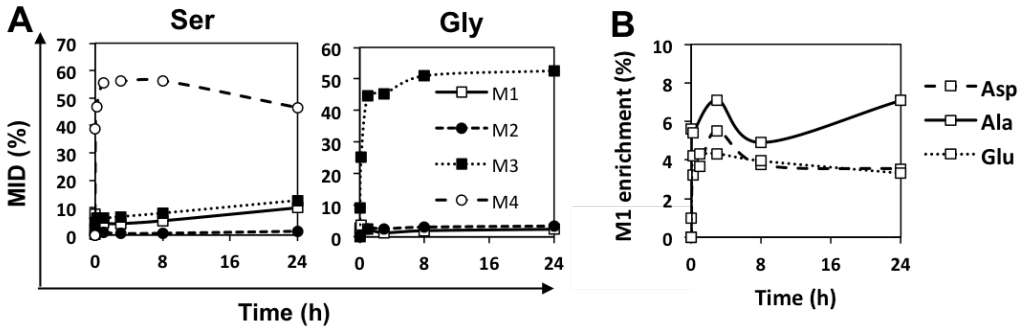

Figure 3.5 Mass isotopomer distribution profiles for [U-^{13}C/^{15}N]serine experiment, during 24h after isotopic tracer feed.

Serine M4 isotopomer was measured at 69% in cell culture media, immediately after tracer feed to cell culture (Fig. 3.5), but the intracellular pool reached a maximum M4 of 56%, after 1 h from the labeling experiment. There was considerable ^{13}C incorporation into glycine, which showed a maximum enrichment on M3 isotopomer at 51% by 8 h post-label addition. Interestingly, intracellular alanine M1 was 8% 24 h post-label addition. As the carbon backbone of alanine derives from pyruvate, which is very little

labeled, the M1 of alanine should correspond to ^{15}N enrichment, as previously discussed for the asparagine-derived alanine. Furthermore, the M1 isotopomer of glutamate (3%), glutamine (3%) and aspartate (4%) suggests serine is also an important nitrogen donor in GS-CHO cells, although contributing much less to the ^{15}N enrichment than asparagine. Low label values on most glycolytic and TCA cycle metabolites suggest the low utilization of serine as catabolic substrate.

3.3.3 Impact of butyrate on metabolome and ^{13}C label distribution

Sodium butyrate is a histone deacetylase inhibitor that has been widely adopted in industry to improve the production of recombinant proteins (McMurray-Beaulieu et al. 2009). Although its effect on metabolism is poorly known, it was demonstrated to have a significant impact on sustaining high nutrient consumption along culture time, especially during stationary phase, when IgG formation is more pronounced (Carinhas et al. 2013). In this study, our aim was to investigate in more detail CHO cell metabolism in the presence of sodium butyrate, recurring to the use of labeled isotopic tracers. Our hypothesis is that while butyrate causes cell growth arrest (Fig. 3.1B), it induces a metabolic adaptation with a re-channelling of resources towards recombinant protein production.

In butyrate-treated conditions glucose consumption was 1.5-fold higher, and the lactate production to glucose consumption ratio decreased to the same extent, when compared to control cultures, suggesting a higher metabolic efficiency (Carinhas et al. 2013; McMurray-Beaulieu et al. 2009). Glutamine, alanine, glycine and ammonia were secreted to the media at rates over 2-fold higher under butyrate-treated condition. By turn, glycerol secretion was reduced to half in butyrate treated cultures.

Interestingly, the intracellular concentration pools of most metabolites measured in butyrate-treated cultures were 2.5-fold higher (in average) when compared to control cultures (Fig. 3.6). These results correlate with the observed increase in cell size (Carinhas et al. 2013). Noteworthy, glutamine intracellular pool was approximately 4-

fold higher in cells under butyrate treatment. This may be due to higher glutamine synthetase abundance, which is being expressed from the same locus of the IgG_4 heavy and light chains, correlating with an increased specific protein production rate. It is known that the human cytomegalovirus promoter (P_{CMV}) driving expression of the genes of interest has high susceptibility to methylation (Kim et al. 2011), and its epigenetic silencing has recently been shown to occur also via histone methylation (Meilinger et al. 2009). Therefore, butyrate seems to prevent methylation, at the same time that it sustains acetylation, keeping this region of the chromatin in an open state. These two epigenetic mechanisms, demethylation and histone (or non-histone proteins) acetylation, have been associated to gene expression up-regulation in several mammalian cell lines (Camolotto et al. 2013; Gu et al. 2013; Ma and Schultz 2008; Paredes et al. 2013).

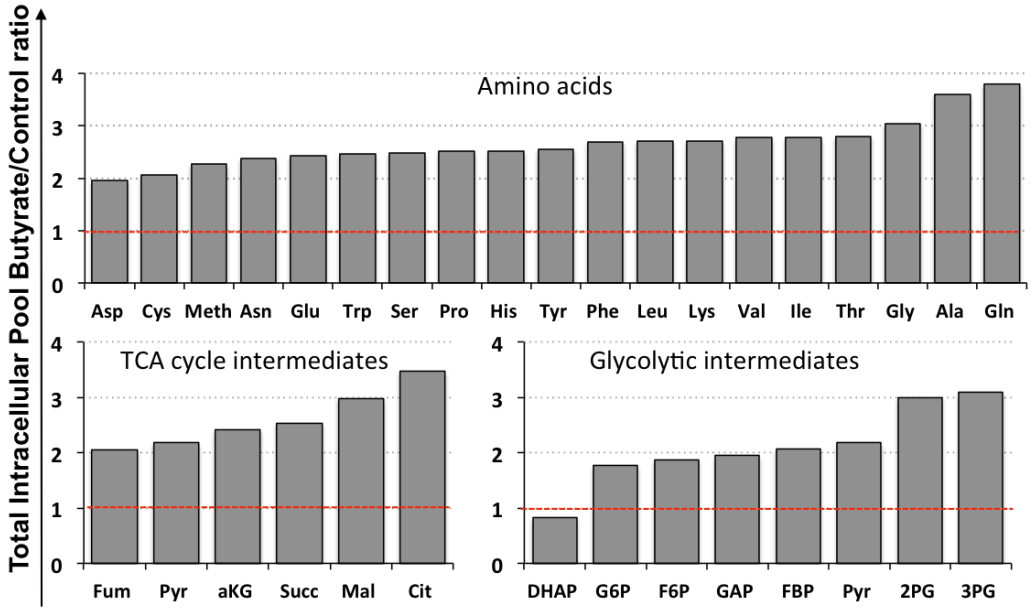

Figure 3.6 Total intracellular metabolite pools ratio butyrate/control for amino acids, TCA cycle and glycolytic intermediates.

The two glycolytic intermediates 2PG and 3PG have pools 3-fold higher in butyrate-treated cultures. Citrate is another metabolite which has its abundance significantly augmented in butyrate-treated cultures (about 3.5-fold). These changes should be further investigated to disclose possible relations with high-production phenotypes.

^{13}C enrichment analysis

Overall, the labeling dynamics from control and butyrate-treated cell cultures were similar (Fig. 3.7), indicating that essentially the same metabolic routes are operating after butyrate addition, although quantitative flux differences should exist because of the differences observed in the uptake/secretion rates.

The mass isotopomer enrichment values collected after 24 h of incubation with [1,2-^{13}C]glucose for control and butyrate-treated conditions are compiled on Fig. 3.7A. PEP M1 (8%) was 50% higher in the butyrate-treated condition when compared to the control, while for pyruvate (6%) and F6P (20%) the [M1] increased 42% and 10%, respectively. However, the [M1]/[M2] ratios of these metabolites were not significantly different between conditions, and therefore indicative of a similar relation between glycolysis and PPP.

Some differences are also observed in asparagine labeled cultures (Fig. 3.7B). For instance, butyrate treatment led to increases on pyruvate M3 by 40% which suggests that butyrate may induce an increase of the malate-pyruvate cycle activity with concomitant increase of PC activity, as mentioned previously for the control condition. Malic enzymes, which catalyze the oxidative decarboxylation of malate to generate pyruvate and NADPH, would this way supply mitochondrial pyruvate pool, compensating any insufficient pyruvate transport capacity from the cytosol (Wahrheit et al. 2014). An increase in NADPH production could act as a counter measure to excessive reactive oxygen species, or as cofactor in lipid and nucleic acid synthesis, being the main reductive power source (Ahn and Antoniewicz 2012; Sengupta et al. 2011; Templeton et al. 2013). Additionally, a surplus of NADPH could fuel folate cycle

and the regeneration of glutathione, important for the maintenance of the ratio between NADPH and $NADP^+$, through its ability to reduce reactive oxygen species (Locasale 2013; Sengupta et al. 2011). Butyrate had no significant impact on the [^{13}C]-label enrichment of metabolites derived from [U-^{13}C/^{15}N]-serine (data not shown). Integration of labeling and extracellular metabolic rate data from the three parallel cultures with labeled glucose, asparagine and serine into a metabolic network model is required to gain further insights on the impact of butyrate into the cell fluxome.

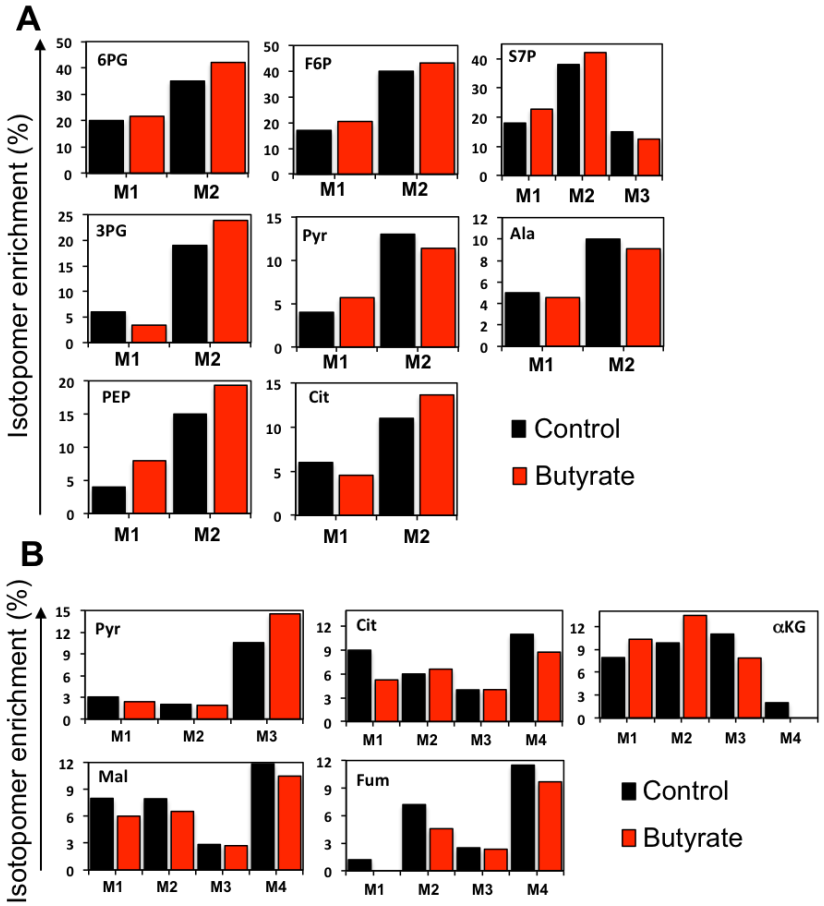

Figure 3.7(A) MID of intracellular metabolites derived from [1,2-^{13}C]glucose, under control (black) and butyrate-treated (red) conditions, after 24 h. (B) MID of intracellular metabolites derived from [U-^{13}C/^{15}N]asparagine, under control (black) and butyrate-treated (red) conditions, after 24 h. Butyrate-treated results were normalized for comparison with control condition.

3.4 Conclusions

Over the recent past, increased efforts on analytical and computational fronts have allowed more comprehensive and detailed analysis of flux distributions in cultured cells that can guide the design of cell and process engineering strategies to meet the requirements of improved production titers. Recent publications have addressed the metabolism of producer and non-producer CHO cell lines using different labeled substrates. In this work, we used a range of methods to characterize the metabolism of GS-CHO cells during exponential growth and butyrate treatment. The CHO cell clone used in this study produces a recombinant mAb at relatively high rates during the exponential phase (30 pg/cell/day), while butyrate enhanced specific productivity by 1.4-fold (approx. 45 pg/cell/day). One of the most distinct features of this high producer clone when comparing to published data from non-producer or lower producer cell lines growing exponentially is the high flux through PPP suggested by the ^{13}C labeling patterns of glycolytic and PPP intermediates in both culture conditions.

Furthermore, MID analysis of asparagine-derived pyruvate suggests high activity of the malic enzyme in control conditions, and importantly, it seems to be enhanced in cells under butyrate treatment. Therefore, a high flux through pathways in which NADPH is generated seems to be necessary to support mAb synthesis. Asparagine and serine were highlighted as important nitrogen sources, namely for glutamine and alanine synthesis.

Aside from a general upregulation of cellular carbon metabolism upon butyrate addition, we have identified specific altered metabolite pools which could be explored as targets in future optimization of production processes of recombinant proteins in these cells.

Overall, this work contributes to unfold important insights into GS-CHO cells metabolism. Ongoing is the contextualization of the data from the parallel labeling

cultures into a metabolic network model for detailed mapping of cellular fluxomes in each scenario. ^{13}C stable isotope labeling, when combined with metabolic flux analysis (MFA), allows the greatest quantitative interrogation of cellular metabolic activity (Wiechert 2001). Although being considerably more demanding, both experimentally and computationally, this approach allows discerning several parallel and reversible pathways not observable by simple material balancing (Chapter 2), enabling a clearer overview of metabolic network operation and diagnosing of phenotypic alterations.

3.5 Acknowledgements

This work was supported by project grants FP7/HEALTH.2011.1.1-1/279039 and PTDC/BBB-BSS/0518/2012. Tiago Duarte acknowledges Fundação para a Ciência e a Tecnologia for his Ph.D. grant (SFRH/BD/81553/2011). FCT is also acknowledged for supporting the National NMR Network (REDE/1517/RMN/2005).

3.6 Author contribution

Tiago Duarte participated in the experimental design, performed the experiments, analyzed the data and participated in the writing of the chapter.

3.7 References

Ahn WS, Antoniewicz MR. 2012. Towards dynamic metabolic flux analysis in CHO cell cultures. Biotechnol J 7(1):61-74.

Amaral AI, Teixeira AP, Sonnewald U, Alves PM. 2011. Estimation of intracellular fluxes in cerebellar neurons after hypoglycemia: importance of the pyruvate recycling pathway and glutamine oxidation. J Neurosci Res 89(5):700-10.

Antoniewicz MR, Kelleher JK, Stephanopoulos G. 2007. Elementary metabolite units (EMU): a novel framework for modeling isotopic distributions. Metab Eng 9(1):68-86.

Bouzier-Sore AK, Bolanos JP. 2015. Uncertainties in pentose-phosphate pathway flux assessment underestimate its contribution to neuronal glucose consumption: relevance for neurodegeneration and aging. Front Aging Neurosci 7:89.

Camolotto SA, Racca AC, Ridano ME, Genti-Raimondi S, Panzetta-Dutari GM. 2013. PSG gene expression is up-regulated by lysine acetylation involving histone and nonhistone proteins. PLoS One 8(2):e55992.

Carinhas N, Duarte TM, Barreiro LC, Carrondo MJ, Alves PM, Teixeira AP. 2013. Metabolic signatures of GS-CHO cell clones associated with butyrate treatment and culture phase transition. Biotechnol Bioeng 110(12):3244-57.

Chaves das Neves HJ, Vasconcelos AMP. 1987. Capillary gas cromatography of amino acids, including asparagine and glutamine: sensitive gas chromatographic-mass spectrometric and selected ion

monitoring gas chromatographic-mass spectrometric detection of the N,O(S)-tert.-Butyldimethylsilyl derivatives. Journal of Chromatography 392:10.

Crowell CK, Qin Q, Grampp GE, Radcliffe RA, Rogers GN, Scheinman RI. 2008. Sodium butyrate alters erythropoietin glycosylation via multiple mechanisms. Biotechnol Bioeng 99(1):201-13.

Crown SB, Antoniewicz MR. 2012. Selection of tracers for 13C-metabolic flux analysis using elementary metabolite units (EMU) basis vector methodology. Metab Eng 14(2):150-61.

Dean J, Reddy P. 2013. Metabolic analysis of antibody producing CHO cells in fed-batch production. Biotechnology & Bioengineering 110(6):13.

Duarte TM, Carinhas N, Barreiro LC, Carrondo MJ, Alves PM, Teixeira AP. 2014a. Metabolic responses of CHO cells to limitation of key amino acids. Biotechnol Bioeng 111(10):2095-106.

Duarte TM, Carinhas N, Silva AC, Alves PM, Teixeira AP. 2014b. 1H-NMR Protocol for Exometabolome Analysis of Cultured Mammalian Cells. In: Portner R, editor. Animal Cell Biotechnology: Methods and Protocols: Springer.

Goudar C, Biener R, Boisart C, Heidemann R, Piret J, de Graaf A, Konstantinov K. 2010. Metabolic flux analysis of CHO cells in perfusion culture by metabolite balancing and 2D [13C, 1H] COSY NMR spectroscopy. Metab Eng 12(2):138-49.

Gu X, Sun J, Li S, Wu X, Li L. 2013. Oxidative stress induces DNA demethylation and histone acetylation in SH-SY5Y cells: potential epigenetic mechanisms in gene transcription in Abeta production. Neurobiol Aging 34(4):1069-79.

Huang H, Yu Y, Yi X, Zhang Y. 2007. Nitrogen metabolism of asparagine and glutamate in Vero cells studied by (1)H/ (15)N NMR spectroscopy. Appl Microbiol Biotechnol 77(2):427-36.

Jiang P, Du W, Mancuso A, Wellen KE, Yang X. 2013. Reciprocal regulation of p53 and malic enzymes modulates metabolism and senescence. Nature 493(7434):689-93.

Jiang Z, Sharfstein ST. 2008. Sodium butyrate stimulates monoclonal antibody over-expression in CHO cells by improving gene accessibility. Biotechnol Bioeng 100(1):189-94.

Kim M, O'Callaghan PM, Droms KA, James DC. 2011. A mechanistic understanding of production instability in CHO cell lines expressing recombinant monoclonal antibodies. Biotechnol Bioeng 108(10):2434-46.

Locasale JW. 2013. Serine, glycine and one-carbon units: cancer metabolism in full circle. Nat Rev Cancer 13(8):572-83.

Ma P, Schultz RM. 2008. Histone deacetylase 1 (HDAC1) regulates histone acetylation, development, and gene expression in preimplantation mouse embryos. Dev Biol 319(1):110-20.

McMurray-Beaulieu V, Hisiger S, Durand C, Perrier M, Jolicoeur M. 2009. Na-butyrate sustains energetic states of metabolism and t-PA productivity of CHO cells. J Biosci Bioeng 108(2):160-7.

Meilinger D, Fellinger K, Bultmann S, Rothbauer U, Bonapace IM, Klinkert WE, Spada F, Leonhardt H. 2009. Np95 interacts with de novo DNA methyltransferases, Dnmt3a and Dnmt3b, and mediates epigenetic silencing of the viral CMV promoter in embryonic stem cells. EMBO Rep 10(11):1259-64.

Metallo CM, Gameiro PA, Bell EL, Mattaini KR, Yang J, Hiller K, Jewell CM, Johnson ZR, Irvine DJ, Guarente L and others. 2012. Reductive glutamine metabolism by IDH1 mediates lipogenesis under hypoxia. Nature 481(7381):380-4.

Metallo CM, Walther JL, Stephanopoulos G. 2009. Evaluation of 13C isotopic tracers for metabolic flux analysis in mammalian cells. J Biotechnol 144(3):167-74.

Nicolae A, Wahrheit J, Bahnemann J, Zeng A-P, Heinzle E. 2014. Non-stationary 13C metabolic flux analysis of Chinese hamster ovary cells in batch culture using extracellular labeling highlights metabolic reversibility and compartmentation. BMC Syst Biol 8(50):15.

Paredes V, Park JS, Jeong Y, Yoon J, Baek K. 2013. Unstable expression of recombinant antibody during long-term culture of CHO cells is accompanied by histone H3 hypoacetylation. Biotechnol Lett 35(7):987-93.

Sengupta N, Rose ST, Morgan JA. 2011. Metabolic flux analysis of CHO cell metabolism in the late non-growth phase. Biotechnol Bioeng 108(1):82-92.

Templeton N, Dean J, Reddy P, Young JD. 2013. Peak antibody production is associated with increased oxidative metabolism in an industrially relevant fed-batch CHO cell culture. Biotechnol Bioeng 110(7):2013-24.

van Dam JCE, M. R. Frank, J. , Lange HC, van Dedem GWK, Heijnen SJ. 2002. analysis of glycolytic intermediates in saccharomyces cerevisiae using anion exchange chromatography and electrospray ionization with tandem mass spectrometric detection. Analytica Chimica Acta 460:10.

Wahl SA, Seifar RM, Ten Pierick A, Ras C, van Dam JC, Heijnen JJ, van Gulik WM. 2014. Quantitative metabolomics using ID-MS. Methods Mol Biol 1191:91-105.

Wahrheit J, Niklas J, Heinzle E. 2014. Metabolic control at the cytosol-mitochondria interface in different growth phases of CHO cells. Metab Eng 23:9-21.

Wang Z, Park JH, Park HH, Tan W, Park TH. 2011. Enhancement of recombinant human EPO production and sialylation in chinese hamster ovary cells through Bombyx mori 30Kc19 gene expression. Biotechnol Bioeng 108(7):1634-42.

Wiechert W. 2001. 13C metabolic flux analysis. Metab Eng 3(3):195-206.

Wurm F. 2013. CHO Quasispecies—Implications for Manufacturing Processes. Processes 1(3):296-311.

Wurm FM. 2004. Production of recombinant protein therapeutics in cultivated mammalian cells. Nat Biotechnol 22(11):1393-8.

Yang L, Kasumov T, Yu L, Jobbins KA, David F, Previs SF, Kelleher JK, Brunengraber H. 2006. Metabolomic assays of the concentration and mass isotopomer distribution of gluconeogenic and citric acid cycle intermediates. Metabolomics 2(2):85-94.

Yoon SK, Hong JK, Choo SH, Song JY, Park HW, Lee GM. 2006. Adaptation of Chinese hamster ovary cells to low culture temperature: cell growth and recombinant protein production. J Biotechnol 122(4):463-72.

Yu M, Hu Z, Pacis E, Vijayasankaran N, Shen A, Li F. 2011. Understanding the intracellular effect of enhanced nutrient feeding toward high titer antibody production process. Biotechnol Bioeng 108(5):1078-88.

Zhao S, Xu W, Jiang W, Yu W, Lin Y, Zhang T, Yao J, Zhou L, Zeng Y, Li H and others. 2010. Regulation of cellular metabolism by protein lysine acetylation. Science 327(5968):1000-4.

CHAPTER 4

Metabolic responses of CHO cells to limitation of key amino acids

Adapted from:

Duarte, TM*, Carinhas, N*, Barreiro, LC, Carrondo, MJT, Alves, PM, Teixeira, AP, 2014, Metabolic responses of CHO cells to limitation of key amino acids. Biotechnol. Bioeng 111(10):2095–2106

*equal contributions

Abstract

Chinese hamster ovary (CHO) cells are the predominant host for production of therapeutic glycoproteins. In particular, the glutamine-synthetase (GS) expression system has been widely used in the biopharmaceutical industry for efficient selection of high-yielding clones. However, much remains unclear on how metabolic wiring affects culture performance. For instance, asparagine and serine have been observed to be the largest nitrogen sources taken up by GS-CHO cells, but their roles in biosynthesis and energy generation are poorly understood. In this work, a comprehensive profiling of extracellular metabolites coupled with an analysis of intracellular label distributions after 1-^{13}C-pyruvate supplementation were used to trace metabolic rearrangements in different scenarios of asparagine and serine availability. The absence of asparagine in the medium caused growth arrest, and was associated with a dramatic increase in pyruvate uptake, a higher ratio of pyruvate carboxylation to dehydrogenation and an inability for *de novo* asparagine synthesis. The release of ammonia and amino acids such as aspartate, glutamate and alanine were deeply impacted. This confirms asparagine to be essential for these GS-CHO cells as the main source of intracellular nitrogen as well as having an important anaplerotic role in TCA cycle activity. In turn, serine unavailability also negatively affected culture growth while triggering its *de novo* synthesis, confirmed by label incorporation coming from pyruvate, and reduced glycine and formate secretion congruent with its role as a precursor in the metabolism of one-carbon units. Overall, these results unfold important insights into GS-CHO cells metabolism that lay a clearer basis for fine-tuning bioprocess optimization.

CONTENTS

4.1 Introduction

Chinese hamster ovary (CHO) cells are preferred mammalian hosts for industrial production of therapeutic glycoproteins such as monoclonal antibodies (mAbs) used to treat cancer and immunological disorders (Walsh, 2010). Earlier rational efforts towards bioprocess optimization allowed the identification of conditions supporting

better cell growth and recombinant protein production (Butler, 2005; Wurm, 2004). However, fundamental knowledge on the metabolic behavior of cells in culture and its impact on product yield and critical quality attributes (folding, glycosylation, aggregation) have not been yet systematized (Carinhas et al., 2012).

Like other mammalian cell lines, CHO cells fuel carbon and nitrogen metabolism by taking up high quantities of glucose and glutamine from the medium, while releasing lactate and ammonia as by-products (Neermann and Wagner, 1996). Glutamine plays an important role not only as a nitrogen source but also as an anaplerotic metabolite fueling biosynthesis and energy generation (Csibi et al., 2013). The dependency of mammalian cell lines on exogenous glutamine has been explored as a means to generate the glutamine synthetase (GS) expression system for recombinant protein production. This system is based on transfecting cells with a plasmid expressing both GS and the protein-of-interest to enable selection of cells in glutamine-free media (Bebbington et al., 1990; Cockett et al., 1990). CHO cell lines, in particular, express sufficient endogenous GS to survive without external glutamine; in this case, the specific GS inhibitor methionine sulfoximine (MSX) is used to inhibit endogenous GS activity such that only transfectants with additional recombinant GS activity, and hence recombinant protein expression, can survive (Birch and Racher, 2006). This system has enjoyed popularity in large-scale monoclonal antibody production, offering a fast technology to establish stable, high-producing cells with the added bonus of reducing ammonia accumulation and avoiding its deleterious effects on culture performance (Yang and Butler, 2000; Cruz et al., 2000).

In comparison to cells with a highly active glutaminolysis pathway, amino acids metabolism in GS-CHO cells is poorly known. GS-catalyzed formation of glutamine occurs with glutamate being phosphorylated before reacting with ammonia to form glutamine. GS-CHO cells survive without exogenous glutamine in the medium by using glutamate and other amino acids such as asparagine (Zhang et al., 2006). From previous work with GS-CHO cell clones, we have observed that serine is the second

most consumed amino acid next to asparagine (Carinhas et al., 2013). Besides being used in proliferating cells for the synthesis of proteins, glycine, cysteine, nucleotides and lipids, serine is the major source of one-carbon units for methylation reactions (Ye et al., 2012). Importantly, the formation of serine-derived formate has been observed in a variety of CHO cell lines and has the potential to inhibit culture growth (Ihrig et al., 1995). Thus, the central roles of asparagine and serine in GS-CHO cells deserve further investigation on their essentiality, inter-regulation with the metabolism of other amino acids as well as the bridge to glucose and carbon metabolism.

In this work, the availability of asparagine and serine was modulated in two ways: i) by culturing cells in the absence of each amino acid, and ii) by culturing cells in the presence of a low concentration of either amino acid. The consumption of metabolic substrates, secretion of by-products and culture performance indicators (cell density and monoclonal antibody titer) were followed in the different scenarios. ^{1}H-NMR spectroscopy was used to simultaneously quantify a large number of metabolites in culture supernatant (Duarte et al., 2014). Furthermore, we exploited carbon-labeling experiments using 1-^{13}C-pyruvate and GC-MS analysis to discern intracellular partitioning in the presence or absence of asparagine or serine.

4.2 Materials and Methods

4.2.1 Cell culture

Two CHO cell clones, generated by stable transfection of the CHOK1SV cell line with a construct containing GS and the light and heavy chains of an IgG_4 mAb (kindly provided by Lonza Biologics (UK)), were used in this work. CDCHO chemically defined medium (Cat. No. 10743-029, Gibco, Life Technologies, USA), customized without asparagine, serine and glucose, was supplemented with 5 mM asparagine, 5 mM serine, 50 mM glucose and 25 μM MSX. Cells were maintained in 125 ml shake flasks with 25 ml of culture volume and sub-cultured every 3–4 days with a seeding density of 0.45×10^{6}

cells/ml. All cultures were kept in a humidified incubator controlled at 37°C and 7 % CO_2 with shaking at 130 rpm.

4.2.2 Asparagine and serine manipulation

Cells were cultured in medium initially supplemented with i) 1 mM asparagine (5 mM serine) and daily feeding of 1 mM asparagine, or ii) 1 mM serine (5 mM asparagine) followed by daily feeding of 0.5 mM serine, or iii) without asparagine (5 mM serine), or iv) without serine (5 mM asparagine). Samples were collected at intervals of 8–14 h. Cell density and viability were determined by the trypan blue dye exclusion assay. After cell counting, samples were clarified by centrifugation at 200 x g during 10 min and the supernatant stored at −20°C for later quantification of produced IgG_4 and exometabolome analysis.

4.2.3 Cultures with 1-^{13}C-pyruvate supplementation

1-^{13}C-labeled pyruvate (CLM-1082-0.25, Cambridge Isotope Laboratories, UK) was added in cultures without asparagine or without serine; duplicate cultures were performed for each scenario, paralleled by two independent sets of duplicate controls (with 5 mM each of serine and asparagine). Shake flasks were seeded at 0.5×10^6 cells/mL following inoculum centrifugation (200 x g, 10 min), all other conditions being kept as described above. 1-^{13}C-pyruvate was added to all cultures 1 h after inoculation such that 50 % labeling is reached after dilution of pyruvate present in the medium.

4.2.4 Exometabolome analysis

^{1}H-NMR spectra acquisition of culture supernatants was performed in a 500 MHz Avance spectrometer (Bruker, USA) equipped with a 5 mm QXI inversed probe. Spectra were acquired using a NOESY-based pulse sequence with water presaturation, performing 256 scans with 4 s acquisition time, 1 s relaxation delay and 100 ms mixing time at 25 °C. Deuterated 3-(trimethylsilyl)-1-propanesulfonic acid sodium salt, 2,2-Dimethyl-2-silapentane-5-sulfonate-d_6 sodium salt (DSS-d_6) was used as internal standard for metabolite quantification in all samples. In order to maintain a constant pH between samples, these were mixed with phosphate buffer (pH 7.4) prepared in

D_2O at a 2:1 ratio. The spectrometer was firstly calibrated by determining the 90° pulse and the water chemical shift centre of each sample. Each spectrum was phased, baseline corrected and integrated using the Chenomx NMR Suite 7.1 (Chenomx Inc., Canada). The assignment of metabolites was made by comparison with software and public databases or spiking experiments with pure compounds. Details on peak cluster integration and chemical shifts used for quantification can be found in Duarte et al. (2014).

Ammonia was quantified using an enzymatic kit (Cat. No. AK00091, NZYTech, Portugal) based on the measurement at 340 nm of the amount of $NADP^+$ formed through the action of glutamate dehydrogenase (GIDH).

4.2.5 IgG quantification

Accumulation of IgG in the supernatant was monitored using a sandwich ELISA assay. Briefly, Nunc Maxisorp 96-well plates (Cat. No. 437842, Thermo Scientific, USA) were coated with a goat anti-human IgG, Fcγ-specific (Cat. No. 109-006-098, Jackson Immunoresearch Labs, USA) at a concentration of 2 μg/L in carbonate buffer. Blocking was performed with 0.5 % casein in carbonate buffer. Bound antibody was detected with goat anti-human IgG (Fab-specific)-peroxidase antibody (Cat. No. A0293, Sigma-Aldrich, USA) and TMB substrate (Cat. No. 00-2023, Invitrogen, Life Technologies, USA). 2.5 M sulphuric acid was used as stop solution and color development was measured at 450 nm.

4.2.6 Sampling and extraction of intracellular metabolites

Samples for the determination of mass isotopomers of intracellular metabolites were collected immediately before 1-^{13}C-pyruvate supplementation as well as 2, 15 and 60 min afterwards. Quenching was performed by rapidly adding 4 parts of ice-cold 0.9 % (v/v) NaCl solution followed by two cycles of 1 min centrifugation at 1000 x g and 4 °C. Intracellular metabolites were extracted in ice-cold 50 % acetonitrile/water, with brief vortexing and snap freezing in liquid nitrogen. After thawing on ice, samples were

centrifuged for 10 min at 15 000 x g and 4 °C. The supernatants (cell extracts) were dried by vacuum centrifugation overnight and stored at 4 °C until derivatization.

4.2.7 Derivatization of intracellular metabolites

Two derivatization methods were adopted for two sets of metabolites (Hofmann et al.2008). Briefly, amino acids and lactate were derivatized to their *tert*-butyldimethylsilyl derivatives with 10 µL of N-*tert*-butyldimethylsilyl-N-methyltrifluoroacetamide (MBDSTFA; Aldrich, DE) and 30 µL of dimethylformamide (DMF; Sigma Aldrich, DE) at 75 °C for 30 min. Tricarboxylic acids were firstly derivatized to their methyloximes with 20 µL of O-methylhydroxylamine hydrochloride (Sigma Aldrich, DE) in a pyridine (Sigma Aldrich, DE) solution (10 mg/mL) for 2 h at 40 °C. In a second step, these methyloximes were reacted with 40 µL of MBDSTFA at room temperature for 1h, followed by heating at 60 °C for 1 h, to obtain the *tert*-butyldimethylsilyl derivatives.

4.2.8 GC-MS analysis

GC–MS analysis was performed on a QP2010 mass spectrometer (Shimadzu, Japan) in the EI mode (70 eV). The ionic source temperature was 250 °C, the same as the interface that connects to the column. GC was performed on a HP-5MS column (30 m length, 0.25 mm internal diameter, composed of dimethylpolysiloxane with 5 % phenyl groups, 0.25 µm film thickness; Agilent Technologies, Inc) in 1:10 split mode, with helium as carrier gas at an inlet pressure of 600 kPa. Injections were carried out automatically with an AOC-5000 Plus autosampler (Shimadzu, Japan) using an injection volume of 1 µL and injector temperature set at 250 °C (additional details can be found in Chaves das Neves and Vasconcelos (1987)). Mass spectra were analyzed using the GC-MS Solution software version 2.50 SU1 (Shimadzu, Japan). Metabolite identification was confirmed by comparison with standard solutions prepared in the same conditions in water and/or by spiking experiments - through the supplementation of the pure compounds, at different concentrations, in cell culture medium. Mass isotopomer distributions were obtained by integration of ion chromatograms and corrected for

natural isotope abundances. For each metabolite, all ions were measured (M; M1; Mn, where n is the number of labeled carbons). The percentages of the M1 isotopomers are presented in the results.

4.3 Results and Discussion

The main metabolic rearrangements undertaken by two mAb-producing GS-CHO cell clones were investigated in different scenarios of asparagine and serine availability, namely i) in the absence of one or the other amino acid in culture medium and ii) in the presence of a low concentration of either amino acid throughout culture (starting with 1 mM in each case with daily feeding of 1 mM Asn or 0.5 mM of Ser, respectively). The main results consistently observed for the two cell clones are presented and discussed below.

4.3.1 Modulating asparagine availability

4.3.1.1 Early asparagine exhaustion

Residual asparagine from the cell inoculum (0.1 mM) lasted less than 48 h in culture, allowing cells to grow to around 1×10^6 cells/mL and remaining at approximately the same concentration during 144 h of culture (Fig. 4.1). Comparing to the exponential phase of the control, asparagine uptake was expectedly decreased while ammonia and alanine were not produced, both displaying negligible consumption rates (Figs. 4.2 and 4.3). Interestingly, serine and aspartate consumption rates more than doubled to compensate decreased asparagine uptake, with concomitant increased production of formate and glycine (Figs. 4.2 and 4.3). Although glucose consumption rate was not substantially affected, an increase of around 2-fold in lactate production was observed. This is associated with the fact that, in the control culture, but not in the culture without asparagine, lactate production is shifted to consumption before the end of the exponential phase. Glycerol production also increased, further diminishing the overall carbon flow efficiency pertaining to these two metabolic nodes (Carinhas et al., 2013). Of more relevance, a large increment in pyruvate uptake (over 10-fold) in relation to

the control took place, leaving the compound practically exhausted after the initial 48 h of culture (Figs. 4.2 and 4.3). This likely indicates an anaplerotic role of this metabolite in replenishing TCA cycle intermediates to compensate for asparagine limitation; the consumption of pyruvate as an anaplerotic substitute of glutamine has been observed in studies of adaptation of mammalian cells to non-ammoniagenic medium (Hassell and Butler, 1990; Genzel et al., 2005).

The halt in growth upon asparagine depletion indicates its essentiality for GS-CHO cells (Fig. 4.1). Following this, a pronounced metabolic adaptation occurred in an environment characterized by high nutrient levels resembling those of an exponentially growing culture. For instance, glutamate and aspartate were still available and taken up by the cells, in opposition to being virtually depleted during the stationary phase of the control culture (Fig. 4.2). Linked to the consumption of these amino acids was the production of both ammonia and alanine, contrasting with a net ammonia consumption and also a minor alanine production rate during the stationary phase of the control (Figs. 4.2 and 4.3). While serine consumption drastically decreased in the transition to the stationary phase of the control, it only modestly decreased after growth halt in the culture with residual initial asparagine; consistently, higher secretion rates of glycine and formate were observed in the later scenario. Interestingly, glucose and choline consumption were over 3 and 5-fold higher than in the control during the respective non-growth phases (Table SI). Related with higher choline uptake, its by-products phosphocholine and glycerol-3-phosphocholine were accumulated at higher rates.

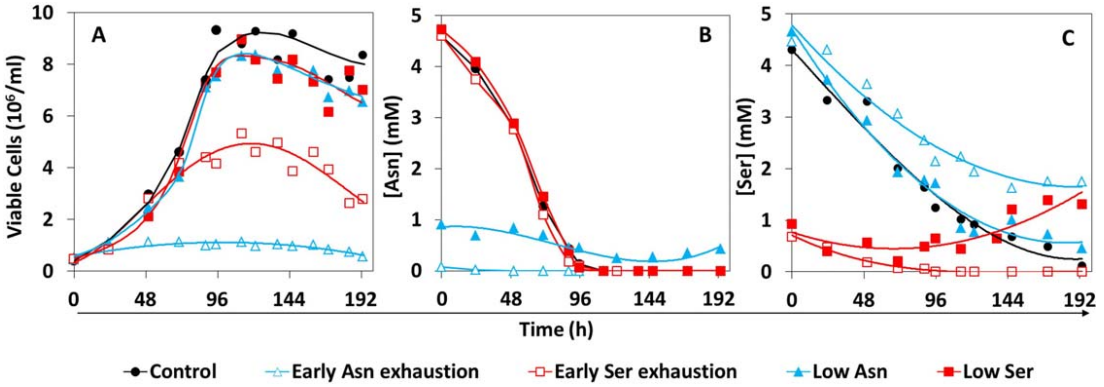

Figure 4.1 Cell growth (A), asparagine (B) and serine (C) profiles of control and modulated cultures. Early asparagine or serine exhaustion correspond to the culture starting with residual asparagine or serine concentration. Low Asn or Low Ser correspond to the cultures starting with 1 mM asparagine or serine, respectively, followed by daily feeding of the same amino acid. Data from clone I is shown.

The TCA cycle intermediates fumarate and malate, which typically start accumulating in the supernatant at the end of the exponential phase, failed to do so throughout the entire duration of the culture without asparagine (Figs. 4.2 and 4.3, Table SI). This indicates the cataplerotic assimilation of asparagine is related to the buildup of these carboxylates, however likely not as their direct carbon source since asparagine is depleted during the stationary phase of the control culture when most of the fumarate and malate secretion occurs. This is markedly different from the cases of citrate and succinate (Fig. 4.2 and Table SI), which start accumulating at the culture onset, displaying similar or slightly higher rates when compared to the control during the respective growth phases.

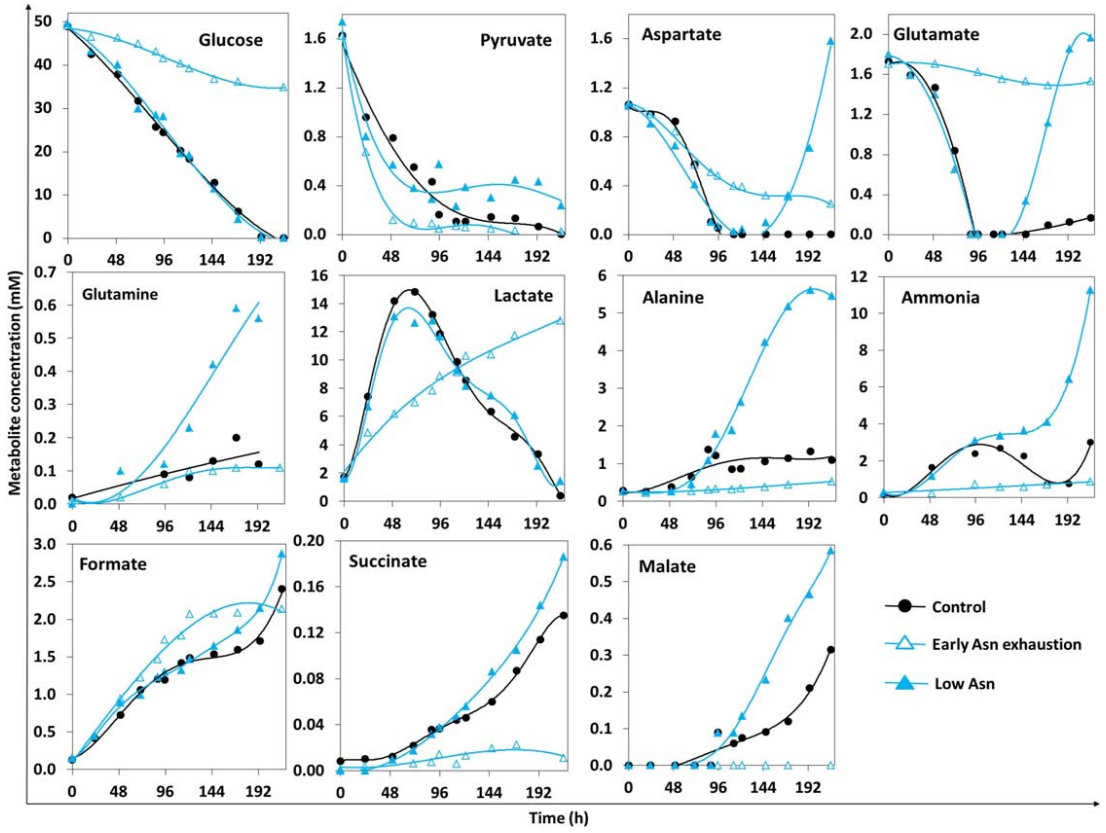

Figure 4.2 Time profile of selected nutrients and by-products in the supernatant of control and asparagine modulated cultures. Data from clone I is shown.

4.3.1.2 Cultures with low asparagine concentration

Substantial differences were not observed between the exponential growth phases of cultures with low (start at 1 mM and daily feeding of 1 mM) and control (start at 5 mM) asparagine concentrations, including growth, productivity (data not shown) and metabolic behavior. However, the stationary phase of the culture maintained at low asparagine concentration is characterized by the availability of this amino acid (Fig. 4.1), which is taken up at approximately the same rate as during exponential growth (Fig. 4.3), whereas in the control the onset of the stationary phase coincides with asparagine depletion. As the growth profiles of both cultures practically match, we can

conclude that asparagine exhaustion is not the sole cause for the onset of the stationary phase.

Correlated with asparagine availability throughout culture time was an interesting modulation in nitrogen metabolism: not only alanine and ammonia continued to be secreted; there was also a shift from aspartate and glutamate consumption to production, while glutamine secretion also increased significantly (see profiles in Fig. 4.2). Furthermore, reinforcing the mentioned relationship between asparagine, malate and fumarate, both carboxylates accumulated at higher rates with respect to the control during the stationary phase (more substantially malate). Of note, some of these rates were further increased in a different culture starting with a 3-fold higher asparagine concentration (data not shown). These results suggest that feeding schemes of asparagine should be tightly tuned to minimize by-product formation while assuring biosynthetic needs.

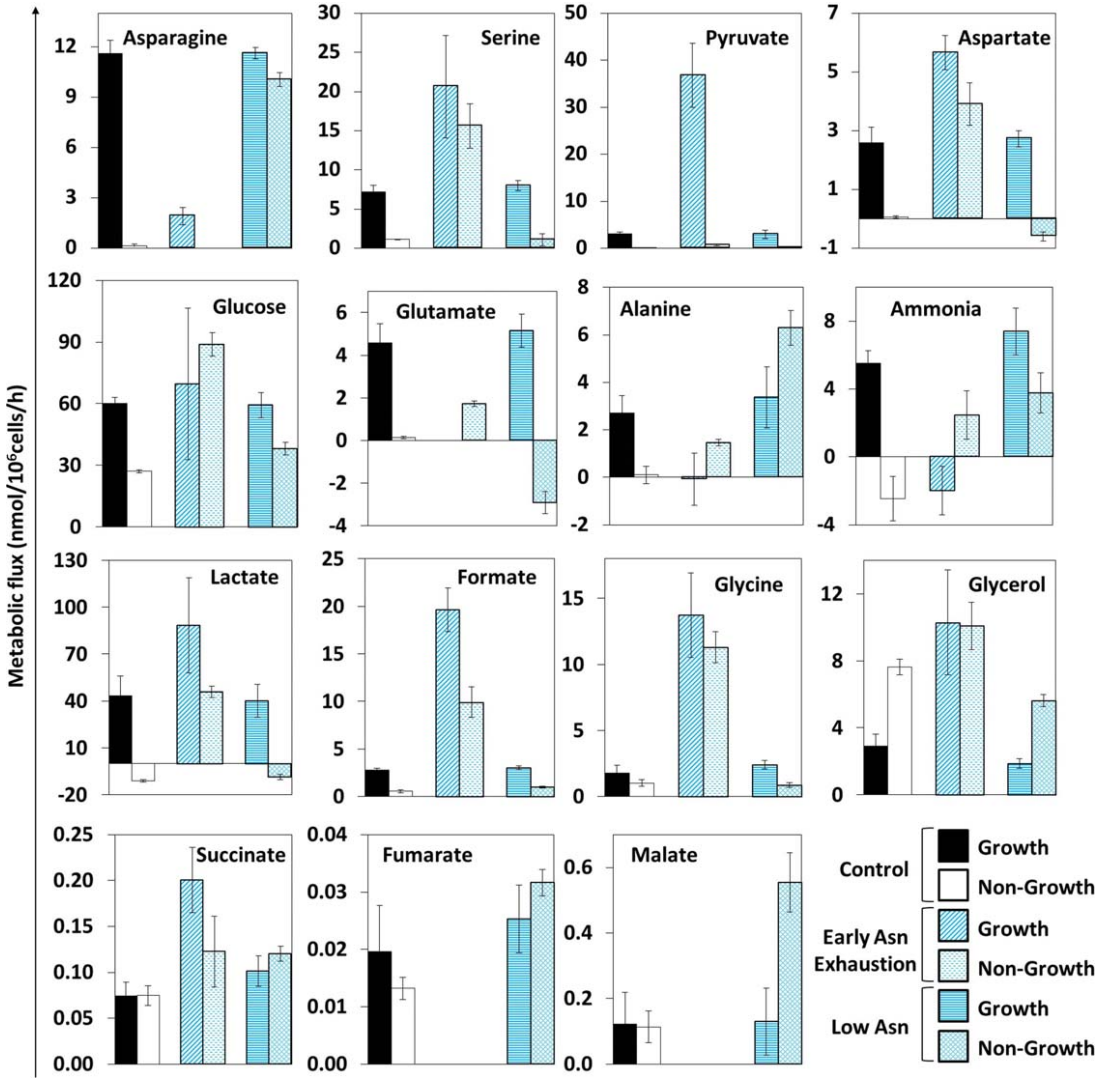

Figure 4.3 Overview of uptake/secretion rates in control and asparagine modulated cultures, represented in units of nmol/10^6cells/h. For asparagine, serine, pyruvate, aspartate, glucose and glutamate, a positive/negative value indicates consumption/secretion, respectively. For alanine, ammonia, lactate, formate, glycine, glycerol, succinate, fumarate and malate, a positive or negative value indicates secretion or consumption, respectively. The growth and non-growth phases of "Control" and "Low Asn" cultures are from 0h to 96h and from 96h to 168h, respectively, whereas for "Early Asn Exhaustion" culture, the transition between phases is at 48h. Error bars are standard deviations from two independent cultures of clone I.

4.3.2 Modulating serine availability

4.3.2.1 Early serine exhaustion

Residual serine (0.7 mM) lasted less than 72 h in culture, during which cells grew to a maximum cell density of 4×10^6 cells/mL, corresponding to half the maximum density attained in the control at around 96 h of culture (Fig. 4.1). The serine uptake rate was 40 % lower than in control conditions, prompting significant alterations in related metabolic fluxes. While the production rate of formate decreased to the same extent, glycine was consumed instead of secreted. Additionally, the asparagine consumption rate almost doubled, and alanine and ammonia secretion increased consistently (Figs. 4.4 and 4.5). Like in the limited asparagine culture, an increase around 2-fold in lactate production was observed, while pyruvate uptake doubled compared to the control (Fig. 4.5). In terms of TCA cycle intermediates, we could observe that fumarate accumulation started earlier, likely linked with increased asparagine uptake, corroborating previous observations in the culture where this amino acid was early exhausted (Fig. 4.4).

As in the early asparagine exhaustion scenario, the halt in growth upon serine depletion suggests its essentiality for GS-CHO cells (Fig. 4.1), although asparagine was also almost depleted around the same time. The ensuing metabolic state was characterized by pronounced alterations relatively to the control stationary phase. Again, linked to the consumption of aspartate and glutamate was the net production of both ammonia and alanine. Interestingly, alanine production is halted at around 120 h, coinciding with the depletion of glutamate and aspartate, whereas ammonia is produced throughout (Figs. 4.4 and 4.5). While glucose consumption remained similar to control cultures, the typical lactate production to consumption shift did not occur in serine-depleted cultures. With regard to TCA cycle intermediates, succinate secretion was halted after serine depletion, displaying a low consumption rate whilst maintaining a high production rate in the control. This interesting observation parallels the effect of asparagine availability on malate and fumarate secretion.

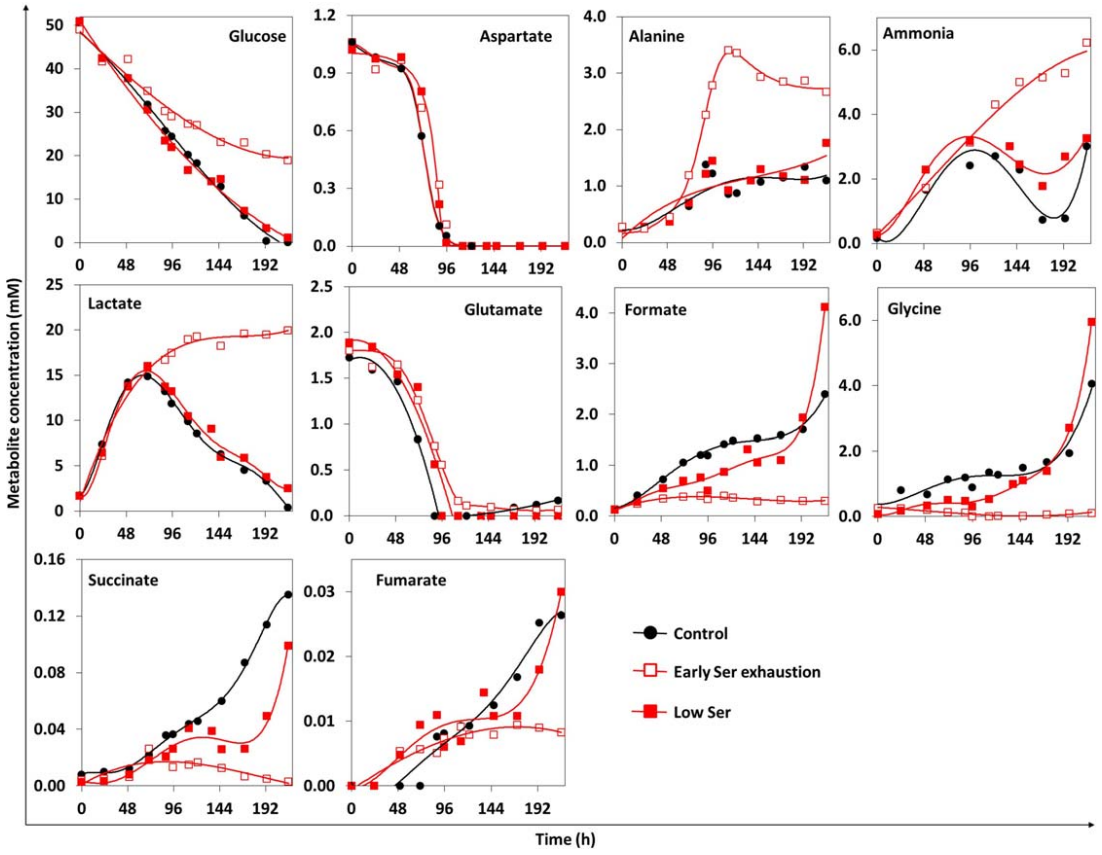

Figure 4.4 Time profiles of selected metabolites in the supernatants of control and serine modulated cultures (data from clone I).

4.3.2.2 Cultures with low serine concentration

When serine concentration was kept at low levels by daily feeding, substantial differences were not observed with respect to the control in terms of culture performance or metabolic behavior, except for a distinct reduction of nearly 50 % in formate and glycine production during the exponential phase (Figs. 4.1 and 4.5). Conversely, during the stationary phase, serine concentration progressively increased due to consumption slowdown (Fig. 4.1C), resulting in higher secretion of formate and glycine during this phase in relation to control cultures (Fig. 4.5). On the other hand, succinate is consumed contrasting with its release in control cultures. As in the case of

asparagine, these results suggest that serine feeding should be tightly controlled to minimize by-product formation and match cellular needs.

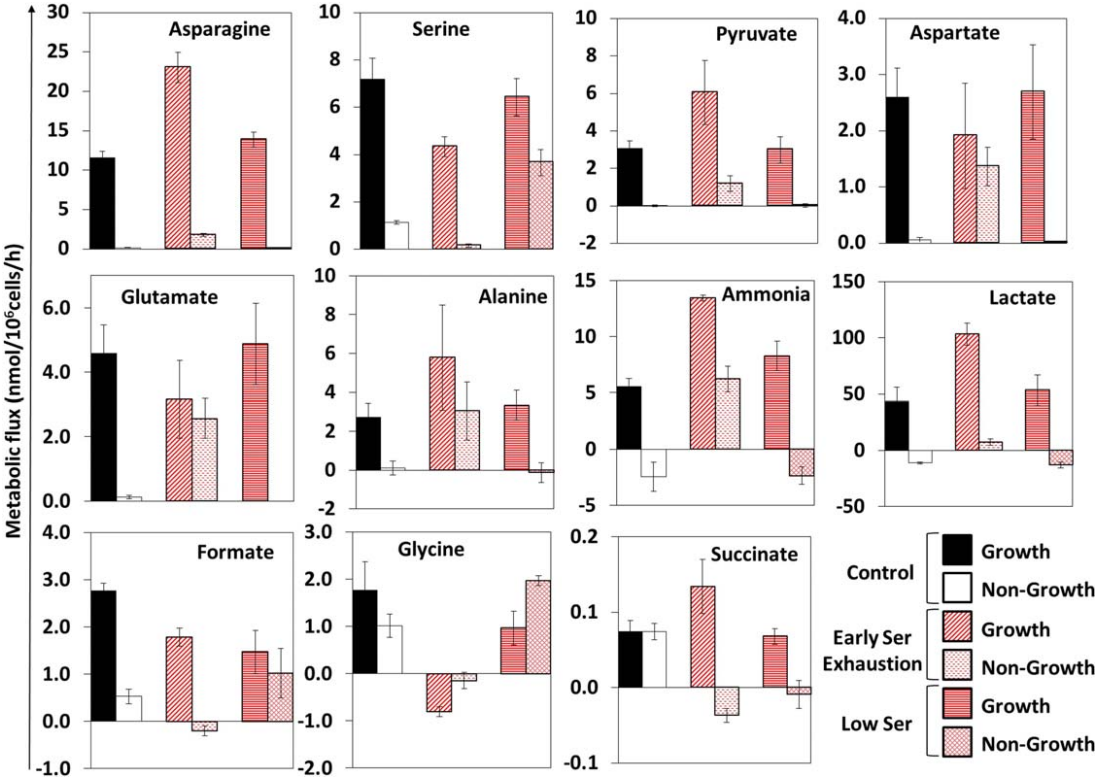

Figure 4.5 Overview of uptake/secretion rates in control and serine modulated cultures, represented in units of nmol/10^6cells/h. For asparagine, serine, pyruvate, aspartate and glutamate, a positive/negative value indicates consumption/secretion, respectively. For alanine, ammonia, lactate, formate, glycine and succinate, a positive or negative value indicates secretion or consumption, respectively. The growth and non-growth phases of "Control" and "Low Ser" cultures are from 0h to 96h and from 96h to 168h, respectively, whereas for "Early Ser Exhaustion" culture, the transition between phases is at 72h. Error bars are standard deviations from two independent cultures of clone I.

4.3.3 Evaluating asparagine and serine essentiality

The results obtained suggest both asparagine and serine are essential amino acids for GS-CHO cell growth in glutamine-free medium. However, residual initial concentrations of each amino acid allowed cells to grow up to a certain point at which other essential nutrients could have been depleted or reached limiting concentrations (Fig. 4.1). To verify this hypothesis, additional cultures were tested using centrifugation to remove

residual spent medium before inoculation. Cultures without supplementation of asparagine or both amino acids could not grow (Fig. 4.6A), implying that asparagine is indeed essential, whereas cultures without serine supplementation could still grow up to half the maximum viable cell density in the control. Moreover, 5 mM glycine addition (which in CDCHO medium is below 0.5 mM) could partially restore cell density and product formation observed in the absence of serine (Fig. 4.6A,B). Glycine is a key intervenient in the generation of tetrahydrofolate (THF)-bound one-carbon units and is synthesized through the activity of serine hydroxymethyl transferase. Interestingly, it has been found that some CHO cell mutants that are glycine auxotrophs only express the cytosolic, but not the mitochondrial, version of this enzyme (Tibbetts and Appling, 2010). This suggests most glycine needs in the GS-CHO clones here used are fulfilled by serine conversion in the mitochondria. In agreement, it was recently reported that cancer cell lines can inter-convert serine and glycine, but display better growth in glycine-free medium than is serine-free medium (Maddocks et al., 2013). This is due to the fact that serine conversion to glycine produces methyl-THF, whereas the reverse reaction inhibits proliferation by depleting the methyl-THF pool. At the same time, in our cultures formate is accumulated in the medium as a by-product from serine consumption, although not reaching previously reported toxic concentrations (Ihrig et al., 1995). Of note, when cells are cultured in the absence of serine with glycine supplementation, formate secretion is negligible (Fig. 4.6C).

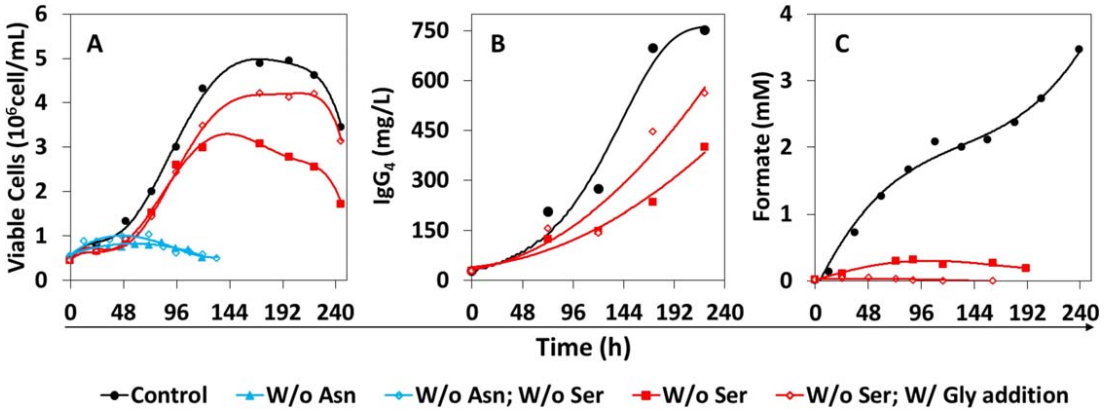

Figure 4.6 Cellular growth (A), IgG_4 (B) and formate (C) profiles in cultures of clone II, with/without serine or asparagine, and with/without glycine addition.

4.3.4 Pyruvate fate

To further evaluate pyruvate fates in the absence of asparagine or serine, in which pyruvate uptake is stimulated, a set of cultures was performed with initial 5 mM serine and asparagine or without either amino acid, supplemented with pyruvate labeled in the first carbon (1-^{13}C-Pyr). This labeled substrate allows to infer the ratio between the activities of pyruvate dehydrogenase (PDH) and pyruvate carboxylase (PC): in the former case, the ^{13}C label is lost to $^{13}CO_2$ release without integration in the TCA cycle, while through the carboxylation reaction labeled oxaloacetate is formed leading to appearance of ^{13}C-intermediates, as shown in Figure 4.7A.

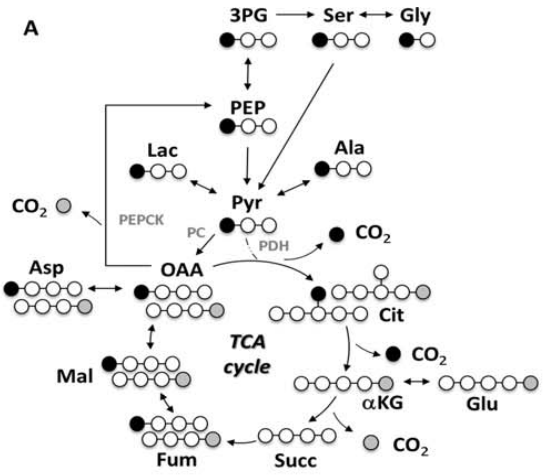

Figure 4.7A Schematic of carbon atom transitions in pyruvate metabolism. Isotopic label from 1-^{13}C-pyruvate is lost to CO_2 while entering the TCA cycle through pyruvate dehydrogenase (PDH), but is retained during the anaplerotic carboxylation to oxaloacetate (OAA) via pyruvate carboxylase (PC). Black and grey circles indicate different possibilities of label position after malate equilibration with fumarate. 3-phosphoglycerate (3PG); serine (Ser); glycine (Gly); phosphoenol-pyruvate (PEP); alanine (Ala); lactate (Lac); citrate (Cit); α-ketoglutarate (αKG); glutamate (Glu); fumarate (Fum); malate (Mal); aspartate (Asp).

The initial fraction of labeled pyruvate in the culture supernatant after 1-^{13}C-pyruvate addition was 50 %, and the time profiles of label distribution in intracellular metabolites during the ensuing 60 min are shown in Figures 4.7B and 4.7C. Interestingly, different M1 labeling levels of lactate (10 %) and alanine (40 %) were observed, suggesting different pyruvate sub-pools, one derived mainly from the catabolism of glucose and another mainly from extracellular pyruvate. Distinct labeling patterns in these two pyruvate-derived metabolites have been observed in other mammalian cell lines (Sheikholeslami et al., 2013; Walther et al., 2012). To better-fit experimental labeling data, researchers have assumed the presence of distinct pyruvate pools in the cytosol and the mitochondria, with alanine mainly derived from mitochondrial pyruvate containing more label originated from glutamine, and lactate primarily generated from cytosolic pyruvate coming from glycolysis.

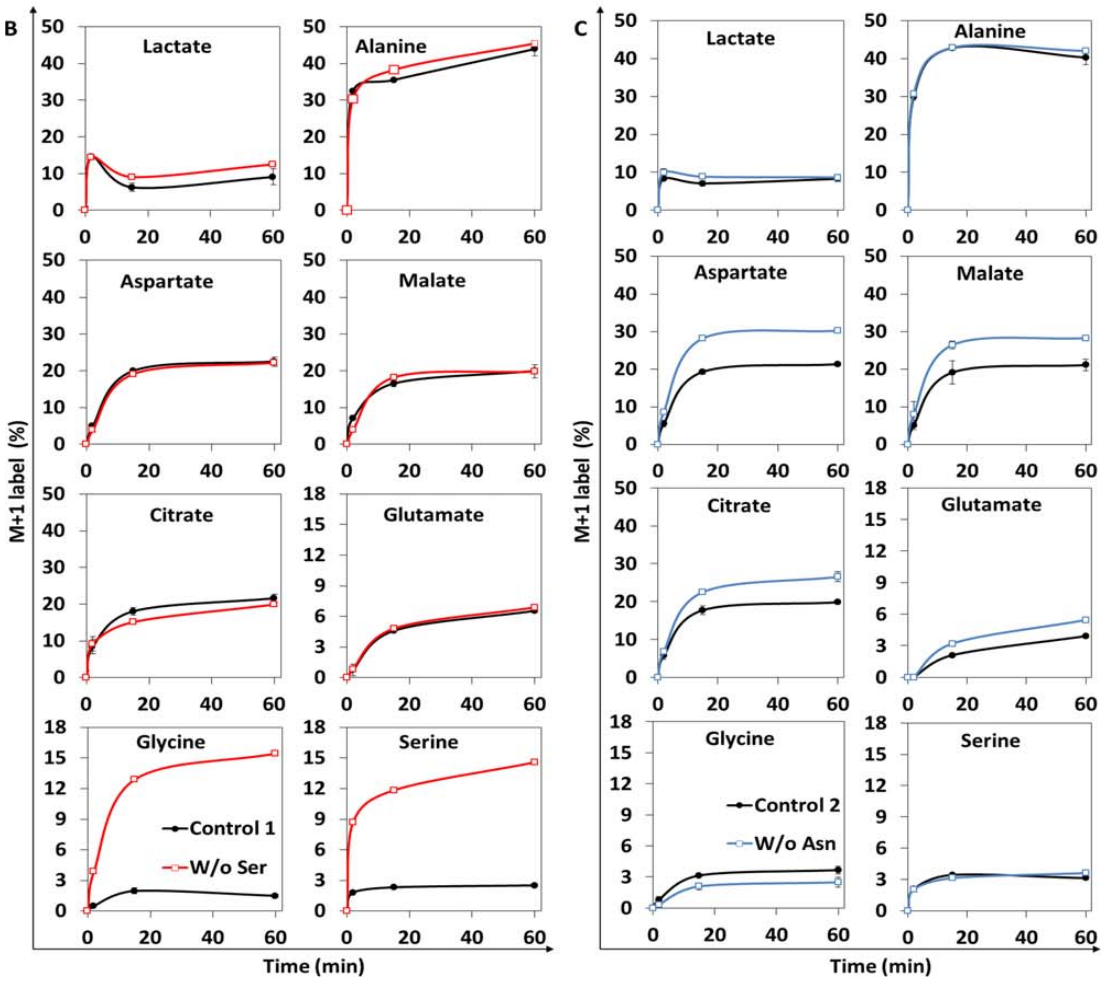

Figure 4.7B/C Time profiles of intracellular metabolites after the introduction of 1-^{13}C-pyruvate in cultures of clone II, in the absence of (B) serine, or (C) asparagine. Percentages of ^{13}C-labeled mass isotopomer (M1) were determined after correction for natural abundances. Error bars depict standard deviations from two biological replicates. The m/z values of M1 fragment ions are: lactate, 261; alanine, 260; aspartate, 418; malate, 419; citrate, 591; glutamate, 432; glycine, 246; serine, 390.

The pools of glutamate (M1 up to 6 %) and glutamine (similar; data not shown) were less enriched than aspartate, malate or citrate since the carboxylic group of oxaloacetate is lost as CO_2 in the formation of α-ketoglutarate from isocitrate. The appearance of label in glutamate and glutamine demonstrates equilibration of malate (formed through PC activity) with fumarate, which leads to randomization of the label between the two carboxylic groups (Fig. 4.7A). While fumarate was about 12% labeled,

we could not observe labeling of succinate in any culture (data not shown), confirming that the label from pyruvate is lost to CO_2 through clockwise TCA cycle activity, while being interrupted counterclockwise by the irreversibility of succinate dehydrogenase. After the initial 60 min of culture, the fraction of the labeled pools decreases in all cultures for all intracellular metabolites (data not shown). This is due to the much higher uptake rate of glucose from the culture medium, each molecule generating up to two intracellular non-labeled pyruvate molecules that will further dilute the half-labeled pyruvate flux. For this reason, the use of labeled pyruvate requires short-time sampling and is not suitable for isotopic steady-state flux analysis.

The M1 labeling patterns in cultures without serine were similar to the control for most metabolites analyzed (Fig. 4.7B,C). Aspartate, malate and citrate pools were significantly labeled, indicating activity through PC, in agreement with recent works (Ahn and Antoniewicz, 2011; Dean and Reddy, 2012; Templeton et al., 2013). Considering the 40 % M1 labeling of alanine and the 20 % of malate or aspartate, we can estimate that the PC/PDH ratio is approximately 1. The channeling of pyruvate into the TCA cycle during the initial growth period of a DHFR-CHO cell line was also reported to have similar fluxes through PC and PDH (Templeton et al., 2013). More interestingly, we observed that both serine and glycine pools displayed 15 % M1 labeling 1h after 1-^{13}C-pyruvate addition in cultures without serine, strongly contrasting with the minor fraction labeled (~3 %) in serine containing medium. This confirms that the serine synthesis pathway is activated under serine starvation conditions. The capability of several cancer cell lines to synthesize serine during the proliferative phase has previously been reported (Ye et al., 2012 and Maddocks et al., 2013), but in these studies labeled serine was derived from glucose. As the glycolytic reaction catalyzed by pyruvate kinase is irreversible, the appearance of label into serine and glycine coming from pyruvate in our study indicates activity through phosphoenolpyruvate carboxykinase (PEPCK) upon processing through PC (Fig. 4.7A). The role of PEPCK in serine synthesis from pyruvate has been recently highlighted (Kalhan et al., 2011; Kalhan and Hanson 2012); tracer isotopic studies in rat

hepatocytes showed that most of the carbon for *de novo* synthesis of serine is derived from pyruvate (Kalhan et al., 2011).

In cultures without asparagine, the fraction of ^{13}C-labeled TCA cycle intermediates (malate and citrate), as well as aspartate and glutamate was consistently higher than in control cultures (Fig. 4.7B,C). This indicates that the higher uptake flux of pyruvate under asparagine limitation is preferentially diverted through PC, resulting in a PC/PDH ratio of around 1.5, supporting the fact that cells re-rout carbon substrates to compensate the anaplerotic role of asparagine in addressing biosynthetic and energetic needs. Noteworthy, we could not observe the appearance of labeled asparagine in any of the cultures performed, suggesting that these cells do not synthesize asparagine even under starvation conditions. While negligible asparagine synthetase activity has been recently reported in DHFR-CHO cell lines by Dean and Reddy (2013), Fomina-Yadlin et al. (2013) showed the upregulation of transcript and protein levels of this enzyme following asparagine withdrawal in different parental and antibody-producing CHO cell lines, but growth suppression was still observed. Interestingly, in an earlier study, CHO cells could be adapted to grow in asparagine-free medium with increased uptake of other amino acids (Seewooster and Lehmann, 1995). Overall, it seems the dependency on asparagine for growth and the ability for its *de novo* synthesis is highly cell line-dependent and likely linked with the availability and metabolism of other amino acids, particularly glutamine.

4.4 Conclusions

The central roles of asparagine and serine in GS-CHO cells were investigated in terms of their essentiality and effect on cell physiology, namely their inter-relationships in nitrogen and carbon metabolism, biosynthesis and the impact on culture performance. Asparagine was confirmed as essential for growth and the main source of intracellular nitrogen and related alanine and ammonia formation. Moreover, the results revealed an interconnection between asparagine uptake and the flux of pyruvate in order to

maintain TCA cycle flux for biosynthesis and energy generation through increased anaplerotic PC activity. On the other hand, serine limitation activated its synthesis pathway, but also affected cell growth as well as the production of glycine and formate, highlighting the involvement in the metabolism of one-carbon units linked to purine biosynthesis and essential in methylation reactions. Interestingly, although asparagine and serine have distinct metabolic roles, their respective limitation triggered the up regulation of the consumption of the other, suggesting a compensatory mechanism. Furthermore, both amino acids were related to the production of specific TCA cycle intermediates, namely malate and fumarate associated with asparagine, and succinate associated with serine. Finally, the results presented suggest that feeding schemes of asparagine or serine should be tightly tuned to minimize by-product formation while assuring biosynthetic needs. Overall, this work contributed to enlighten the behavior of GS-CHO cells after modulating the availability of critical amino acids, and can be used as a basis for exploring bioprocess optimization strategies.

4.5 Acknowledgements

PTDC/BBB-BSS/0518/2012. Tiago Duarte acknowledges Fundação para a Ciência e a Tecnologia (FCT) for his Ph.D. grant (SFRH/BD/81553/2011). Nuno Carinhas acknowledges FCT for his post-doctoral fellowship grant (SFRH/BPD/80514/2011). FCT is also acknowledged for supporting the National NMR Network (RECI/BBB-BQB/0230/2012).

4.6 Author contribution

Tiago Duarte participated in the experimental design, performed the experiments, analyzed the data and participated in the writing of the chapter.

4.7 References

Ahn, W.S., Antoniewicz, M.R., 2011. Metabolic flux analysis of CHO cells at growth and non-growth phases using isotopic tracers and mass spectrometry. Metabol Eng. 13(5), 598-609

Bebbington, C.R., Renner, G., Thomson, S., King, D. Abrams, D., Yarranton, G.T., 1992. High-level expression of a recombinant antibody from myeloma cells using a glutamine synthetase gene as an amplifiable selectable marker. Nat. Biotechnol. 10, 169-75.

Birch, J.R., Racher, A.J., 2006. Antibody production. Adv. Drug Delivery Rev. 58, 671-85.

Butler, M., 2005. Animal cell cultures: recent achievements and perspectives in the production of biopharmaceuticals. Appl. Microbiol. Biotechnol. 68, 283-91.

Carinhas, N., Duarte, T.M., Barreiro, L.C., Carrondo, M.J.T., Alves, P.M., Teixeira, A.P. 2013. Metabolic signatures of GS-CHO cell clones associated with butyrate treatment and culture phase transition. Biotechnol. Bioeng. 110(12), 3244–3257.

Carinhas, N., Oliveira, R., Alves, P.M., Carrondo, M.J.T., Teixeira, A.P., 2012. Systems biotechnology of animal cells: the road to prediction. Trends Biotechnol, 30, 377-85.

Chaves das Neves, H.J., Vasconcelos, A.M. 1987, Capillary gas chromatography of amino acids, including asparagine and glutamine: Sensitivive gas chromatographic-mass spectrometric and selected ion monitoring gas chromatographic-mass spectrometric detection of the N,O(S)-tert-butyldimethylsilyl derivatives. J Chromatogr 392, 249-258.

Cockett, M.I., Bebbington, C.R., Yarranton, G.T., 1990. High level expression of tissue inhibitor of metalloproteinases in Chinese hamster ovary cells using glutamine synthetase gene amplification. Nat. Biotechnol. 8, 662-7.

Csibi, A., Fendt, S.-M., Li, C., Poulogiannis, G., Choo, A.Y., Chapski, D.J., Jeong, S.M., Dempsey, J.M., Parkhitko, A., Morrison, T., Henske, E.P., Haigis, M.C., Cantley, L.C., Stephanopoulos, G., Yu, J., Blenis, J., 2013. The mTORC1 Pathway Stimulates Glutamine Metabolism and Cell Proliferation by Repressing SIRT4. Cell 153, 840-54.

Cruz HJ, Freitas CM, Alves PM, Moreira JL, Carrondo MJ, 2000. Effects of ammonia and lactate on growth, metabolism, and productivity of BHK cells. Enzyme Microb Technol, 27:45-52.

Dean J., Reddy P., 2013. Metabolic analysis of antibody producing CHO cells in fed batch production, Biotechnol. Bioeng. 110(6), 1735-47

Duarte, T.M., Carinhas, N., Silva, A.C., Alves, P.M., Teixeira, A.P., 2014. ^{1}H-NMR protocol for exometabolome analysis of cultured mammalian cells, in: Pörtner, R. (Eds.), Animal Cell Biotechnology - Methods and Protocols, Methods in Molecular Biology 1104, 237-247.

Fomina-Yadlin, D., Gosink, J.J., McCoy, R., Follstad, B., Morris, A., Russell, C.B., McGrew, J.T., 2014. Cellular Responses to Individual Amino-Acid Depletion in Antibody-Expressing and Parental CHO Cell Lines. Biotechnol Bioeng. 111(5):965-79

Genzel, Y., Ritter, J.B., Konig, S., Alt, R., Reichl, U., 2005. Substitution of glutamine by pyruvate to reduce ammonia formation and growth inhibition of mammalian cells. Biotechnol. Prog. 21, 58-69.

Hassell, T., Butler, M., 1990. Adaptation to non-ammoniagenic medium and selective substrate feeding lead to enhanced yields in animal cell cultures. J. Cell Sci. 96, 501-8.

Hofmann, U., Maier, K., Niebel, A., Vacun, G., Reuss, M., Mach, K. 2007. Identification of metabolic fluxes in hepatic cells from transient 13C-labeling experiments: part I. Experimental observations, Biotechnol. Bioeng. 100(2), 344-354.

Ihrig, T.J., Maulawizada, M.A., Thomas, B.D., Jacobson, F.S., 1995. Formate Production by Cho Cells: Biosynthetic Mechanism and Potential Cytotoxicity, in: Beuvery, E.C., Griffiths, J.B., Zeijlemaker, W.P. (Eds.), Animal Cell Technology: Developments Towards the 21st Century. Kluwer Academic Publishers, Dordrecht, pp. 193-197.

Kalhan, S.C., Hanson, R.W., 2012. Resurgence of serine: an often neglected but indispensable amino acid. The Journal of Biological Chemistry, 287, 19786-19791.

Kalhan S.C., Uppal S.O., Moonman, J.L., Bennett, C., Gruca, L.L., Parimi, P.S., Dasarathy, S., Serre, D., Hanson, R.W., 2011. Metabolic and genomic response to dietary isocaloric protein restriction in the rat. *The Journal of Biological Chemistry,* 286, 5266-5277.

Maddocks O.D.L., Berkers C.R., Mason S.M., Zheng L., Blyth K., Gottlieb E., Vousden K.H. 2013, Serine starvation induces stress and p53-dependent metabolic remodeling in cancer cells, Nature 493, 542-548.

Neermann, J., Wagner, R., 1996. Comparative analysis of glucose and glutamine metabolism in transformed mammalian cell lines, insect and primary liver cells. J. Cell. Physiol. 166, 152-169.

Seewooster, T., Lehmann, J. 1995. Influence of targeted asparagine starvation on extra- and intracellular amino acid pools of cultivated Chinese hamster ovary cells. Appl Microbiol Biotechnol, 44, 344-350.

Sheikholeslami, Z., Jolicoeur, M., Henry, O., 2013. Probing the metabolism of an inducible mammalian expression system using extracellular isotopomer analysis. Journal of Biotechnology 164(4), 469–478.

Templeton N., Dean J., Reddy P., Young J.D. 2013. Peak antibody production is associated with increased oxidative metabolism in an industrially relevant fed-batch CHO cell culture, Biotechnol. Bioeng. 110(7), 2013-24.

Tibbetts, A.S., Appling, D.R., 2010. Compartmentalization of mammalian folate-mediated one-carbon metabolism. Annu. Rev. Nutr. 30, 57-81.

Walsh, G., 2010. Biopharmaceutical benchmarks 2010. Nat. Biotechnol. 28, 917-24.

Walther, J.L., Metallo, C.M., Zhang, J., Stephanopoulos, G. 2012. Optimization of (13)C isotopic tracers for metabolic flux analysis in mammalian cells. Metabolic Engineering, 14, 162–171.

Wurm, F.M., 2004. Production of recombinant protein therapeutics in cultivated mammalian cells. Nat. Biotechnol. 22, 1393-8.

Yang, M., Butler, M., 2000. Effects of ammonia on CHO cell growth, erythropoietin production, and glycosylation. Biotechnol. Bioeng. 68, 370-80.

Ye, J., Mancuso, A., Tong, X., Ward, P.S., Fan, J., Rabinowitz, J.D., Thompson, C.B. 2012. Pyruvate kinase M2 promotes de novo serine synthesis to sustain mTORC1 activity and cell proliferation. Proc. Natl. Acad. Sci. 109, 6904-6909.

Zhang, F., Sun, X., Yi, X., Zhang, Y., 2006. Metabolic characteristics of recombinant Chinese hamster ovary cells expressing glutamine synthetase in presence and absence of glutamine. Cytotechnology 51, 21-8.

Chapter 5

Discussion

CONTENTS

5.1 Discussion

The focus of this thesis was the characterization of the GS-CHO-K1 cell metabolism, a mammalian cell line that is widely adopted by the industry for the production of blockbuster biologics. The experimental approach was based on the comparison of cellular phenotypes under different productive states, either cell clones expressing different amounts of the same recombinant protein, cultured with or without productivity enhancers. The analysis of these scenarios enabled the identification of culture and cellular parameters that govern productivity, and to hypothesize new strategies in order to improve process performance.

Bioprocess development based on empirical knowledge and inefficient trial-and-error experiments to select ideal culture conditions to produce recombinant proteins has been evolving towards more balanced approaches. In the post-genomic era, Omics technologies allow us to holistically analyse cell components and study their interactions to then fully exploit the cell potential in the production of high-value biopharmaceuticals. While the fields of genomics and transcriptomics have had important contributions for cell line and bioprocess development, metabolomics is still

maturing in its effort to cover the whole cell metabolome. NMR and MS based methods keep evolving, providing increasingly comprehensive datasets.

In what concerns fluxome analysis of mammalian cells, MFA methods have been widely adopted, where the most simple application takes only metabolite transport rates as experimental data and balances them in the metabolic network in order to estimate intracellular fluxes (Quek et al. 2010). Flux resolution can be further improved using of isotopic tracers coupled with MFA. Several studies have shown that a careful choice of labelled tracers is essential to achieve optimal flux resolution of specific pathways (Crown and Antoniewicz 2012; Metallo et al. 2009). Thus, the use of specific isotopic tracers became a fundamental method in this work allowing increasing metabolic network resolution and the precision necessary to distinguish metabolic activity through cyclic and parallel pathways. This way it was possible to estimate the recycling of phosphates between PPP and glycolysis, and to investigate the bridge between glycolysis and TCA cycle (PC, PDH and ME activities) under different culture conditions.

The main aims, approaches followed, major outcomes and suggestions for future studies based on the outcomes of this thesis are summarized in Figure 5.1.

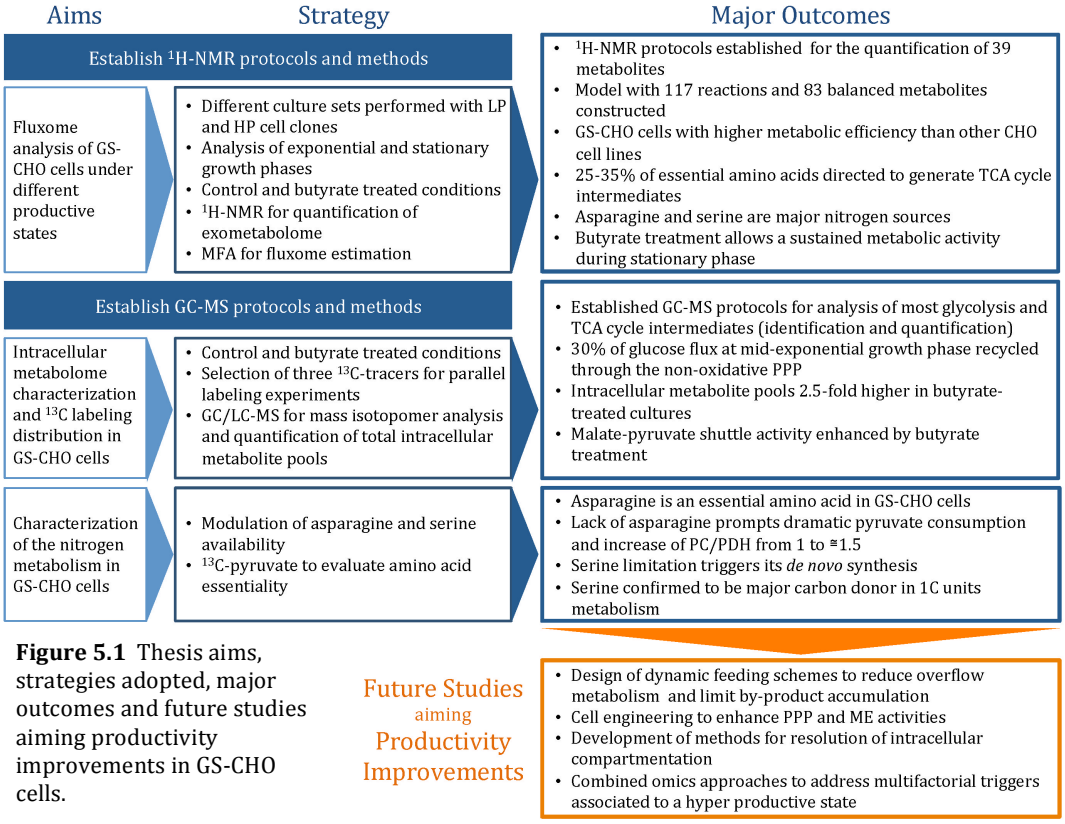

Figure 5.1 Thesis aims, strategies adopted, major outcomes and future studies aiming productivity improvements in GS-CHO cells.

5.1.1 GS-CHO-K1 characterization

We initially compared the metabolism of two GS-CHO cell clones producing different levels of an IgG_4 (the productivity per cell is 2.5-fold different between clones). ^{1}H-NMR spectroscopy of the cell culture supernatant allowed the quantification of an extensive number of metabolites over time. Besides the main substrates (glucose and amino acids) and lactate, usually analyzed in mammalian cell cultures, it was possible to quantify pyruvate, acetate, the phospholipid precursor choline, as well as several by-products (Chapter 2). From this analysis we observed that in batch cultures, the depletion of asparagine coincides with the start of the stationary phase. Glucose and serine were also almost depleted by the end of the stationary phase. The ability to directly measure the depletion of key nutrients makes exometabolomics a common

method for rational media design. As a first approach to tackle the depletion of these nutrients, a strategy based on a bolus-feeding containing the limiting nutrients was attempted. Although we could prolong cell viability for 80h (data not shown), this attempt did not lead to higher cell densities and protein titers (Chapter 2), suggesting the depletion of additional nutrients not measured by our ^{1}H-NMR protocol, and/or the accumulation of (un)measured growth inhibiting by-products.

We constructed a GS-CHO-K1 metabolic network, including 117 reactions and 83 balanced metabolites, to contextualize the exometabolome data, and estimate by MFA *in vivo* fluxes in the low and high producer clones. Despite the difference in specific productivities between clones (about 2.5-fold), they exhibited minor metabolic differences in the estimated fluxes. This might be explained in part by the low resolution of the estimated fluxomes of each clone. These cultures were conducted without resorting to labelled substrates, which prevented discriminating the fluxes through parallel/cyclic pathways and reversible reactions.

The quest for improved production of complex biologics in CHO cells has been accompanied by attempts to improve metabolic efficiency, mainly the channelling of glucose-derived carbons from glycolysis into the TCA cycle, avoiding the formation of by-products (e.g. lactate) while maximizing the ATP produced per glucose consumed. Therefore, one approach to improve the efficiency of CHO cells has been through altering energy metabolism by controlling glucose concentration, keeping it at levels that sustain cell proliferation and maintenance but limit the amount of glucose-derived undesired by-products (Dean and Reddy 2013; Kim et al. 2012). However, this approach needs to be fine-tuned otherwise it might have a negative impact on the glycosylation patterns of antibodies produced in CHO cells (Liu et al. 2014). For instance, Seo and co-workers (2014) observed aglycosylated antibodies in fed-batch cultures of a human cell line (F2N78) when glucose was depleted or exhibited high ammonia accumulation. Thus, a balanced stoichiometric feeding can significantly increase cell viability, reduce by-product formation and improve glycosylation quality

(Xie et al. 1997). Several cell engineering approaches have also been conducted to improve the metabolic efficiency of CHO cells, in particular the down-regulation of specific genes to reduce lactate formation (Chen et al. 2001; Kim and Lee 2007).

Nevertheless, in the cancer metabolism field the most accepted explanation for the high lactate secretion rate despite plenty of oxygen availability (Warburg effect), suggests that it better serves the anabolic demands of rapidly proliferating cells (Vander Heiden et al. 2009). Although ATP generation from glycolysis is much less efficient than oxidative metabolism, producing only two ATP molecules compared with 36 for the complete oxidation of glucose, lactate production allows glycolysis to be accelerated because the conversion of pyruvate to lactate recycles the NAD^+ necessary for glycolysis. Rather than undergoing complete oxidation to CO_2 and water in the TCA cycle, the partial conversion of glucose into lactate allows more glycolytic intermediates upstream to pyruvate to be available for the biosynthesis of cellular building blocks (nucleic acids, amino acids, and fatty acids), which are required for proliferation. This might explain why the down-regulation of lactate production has allowed only marginal improvements in cell culture performance.

The manipulation of energy metabolism in mammalian cells has moved beyond controlling glucose and glutamine concentrations towards the analysis of the contributions of several amino acids and their interactions with cellular metabolism (Zhou et al. 1997). In the work presented in this thesis, further investigations were made into the amino acid metabolism that differentiates GS-CHO cells from other CHO cell lines. GS-CHO cells can synthetize glutamine above endogenous levels, allowing them to thrive in a glutamine-free media. Through modulations of asparagine we found that this amino acid was the main nitrogen source for the cell and used for energy generation in the TCA cycle, essential for cell growth (Chapter 4). Additionally, asparagine and serine were associated with the production of by-products, including not only ammonia but also formate, alanine or glycine. These results suggest that

feeding strategies can be designed and fine-tuned in order to minimize by-product formation, while maintaining biosynthesis requirements.

5.1.2 Advantages of using isotopic tracers

Labelled tracers provide accurate information about carbon transitions that become especially relevant in estimating parallel and cyclic fluxes (Niklas and Heinzle 2012). In particular, the use of isotopic tracers allows to distinguish PPP activity from glycolysis or the partitioning between PC and PDH enzymatic activities. Thus, ^{13}C-MFA ensures a more realistic representation of *in vivo* cellular metabolism (Ahn and Antoniewicz 2011; Niklas and Heinzle 2012).

In this work, we used [1,2-^{13}C]-glucose to characterize the flux partitioning between glycolysis and pentose phosphate pathways (Chapter 3) in exponentially-growing cultures of the high producer clone. Importantly, it was possible to quantify PPP activity, rendering up to 30% of all glucose-derived carbons, as 70% continued directly throughout glycolysis. This is particularly relevant as non-oxidative PPP activity is often described as negligible during exponential phase in the literature (Ahn and Antoniewicz 2011). Additionally, a high cycling activity between PPP and glycolysis was demonstrated by the abundance of heavier isotopomers. Unfortunately, due to the high costs associated to cultures with labelled substrates and MS analysis, we could not compare the fate of labelled glucose between the low and high producer clones. It would be of interest to quantify this feature in the low producer clone as well to investigate its correlation with productivity.

As stated before, the estimation of fluxes through parallel and cyclic pathways cannot be resolved without the use of labelled tracers. Goudar et al (2010) showed that the lack of isotopic tracer information does not have a significant impact on most fluxes in the network, but estimations obtained through classical MFA and ^{13}C-MFA only matched when ox-PPP fluxes and PC activity were fixed at the values obtained through ^{13}C-MFA. Bonarius et al (1996) had quite different results while using the two

techniques to estimate metabolic fluxes in hybridoma cells at different physiological states: using classical MFA (without the use of labelled tracers) 90% of all glucose-derived carbons were estimated to go through PPP instead of only 20% when calculated through ^{13}C-MFA. These contrasts translate the potential of using labelled tracers in order to deepen our knowledge of net fluxes in the CHO metabolic network.

We also used fully-labelled (^{13}C and ^{15}N) asparagine and fully-labelled serine to investigate further the fate of these two amino acids in GS-CHO cells. This way, it was possible to confirm asparagine and serine as important nitrogen sources, fuelling other amino acids and TCA cycle intermediates. Using 1-^{13}C-pyruvate it was possible to distinguish the fate of pyruvate in case of asparagine or serine unavailability – conditions which dramatically increased pyruvate uptake rates (Chapter 4). This allowed us to differentiate the activities of PC and PDH, both sharing 50% of the metabolic fluxes derived from pyruvate into the TCA cycle. Therefore, pyruvate carboxylase is also an important anaplerotic route in these cells. The lack of asparagine increased pyruvate carboxylation, showing the metabolic flexibility of these cells to optimize their metabolism to this perturbation (Olson et al. 2016).

In the light of current knowledge, the results obtained appear to be cell-line dependent, in agreement with the notion that a thorough characterization of major cell lines will be required to identify the features that confer them a hyperproductive phenotype (Seth et al. 2007). We can anticipate that the use of labelled tracers and metabolic flux analysis will continue to be explored as a powerful way to uncover these "superior attributes" of host cells lines.

5.1.3 Butyrate effects on GS-CHO cell metabolism

Butyrate is thought to induce an open chromatin state, as a result of hyper acetylation of histones, and these alterations favour higher transcription rates (Kruh 1982; Palermo et al. 1991). Moreover, it has been shown that butyrate interrupts cell cycle at G1 phase, where protein synthesis could be highest (Kruh 1982). Rapid improvements

in protein production, avoiding time-consuming and laborious gene amplification and cell engineering steps, explains butyrate application in industry. Furthermore, it has been shown that butyrate does not compromise glycosylation of recombinant antibodies, while it may alter sialic acid content (Mimura et al. 2001; Sung et al. 2004).

We used butyrate treatment to study how metabolism is rearranged in such higher recombinant protein productive phenotype. Butyrate treatment led to improving mAb productivity by 3-fold in the stationary phase, and remarkably allowed maintaining a high transport of glucose-derived carbons into the TCA cycle, sustaining a high nutrient consumption throughout culture time (Chapter 2). Additionally, butyrate treatment seems to induce an increased malate-pyruvate cycle activity, revealed by the use of isotopic tracers (Chapter 4). Importantly, it could compensate for insufficient pyruvate transport from the cytosol into the mitochondria that might limit the energetic capacity of GS-CHO cells. The interaction between cytosolic glycolysis and mitochondrial TCA cycle is a well known bottleneck in production processes and, despite being pivotal in metabolism, the control mechanisms remain rather unknown (Wahrheit et al. 2014). These results point out the need to further clarify these mechanisms surrounding this metabolic hub, possibly through enzymatic studies with the capability to distinguish cellular compartments. Moreover, the evaluation on how the availability of pyruvate may limit the performance of high producing clones seems to be crucial to further detail the interconnectivity between such metabolic pathways.

Interestingly, CHO cells under butyrate treatment conditions presented also an increase of 2.5-fold, in average, in intracellular metabolite pools through glycolysis, PPP and TCA cycle intermediates, fitting well with the observation that butyrate-treated cells were in fact larger and with higher dry cell weights measured. Glutamine was the metabolite with highest difference in intracellular metabolite pools at around 4-fold, which correlates well with the hypothesis that butyrate allows higher expression levels of glutamine synthetase, in addition to the genes of interest, as discussed in Chapter 3.

5.2 Outlook for future research

At the moment, our group is working on the data obtained from parallel labelling experiments using different isotopic tracers to be integrated into a single model allowing the comparison of the fluxome of GS-CHO cells with different productive phenotypes. It is expected that the result from this comparison will reveal insights about the metabolism that may allow media design optimization, also providing important clues for process and cell engineering strategies.

Future efforts should be directed towards the incorporation of compartmentalization in metabolic models. The regulation of energy metabolism is intimately connected to the structural organization of the cells. Several studies have revealed that molecular overcrowding restricts the mobility of large and small molecules inside the cells, impacting cellular features such as the intracellular diffusion of ATP or the transport of metabolites across different compartments (Ovádi and Saks 2004). Compartmentalization can be also a hurdle to the analysis of metabolic fluxes, increasing the number of alternative pathways, reversible transport reactions and the number of degrees of freedom. Nevertheless, the ability to separately measure metabolite concentrations in different intracellular compartments remains a bottleneck (Wahrheit et al. 2011). The metabolome is the cellular information layer which quicker responds to perturbations; changes in the concentration of metabolites can occur in seconds. Therefore, efficient separation of compartments before metabolite analysis is technically complex. Alternative approaches must be developed to deal with this challenge. For instance, Lewis et al (2014) proposed to trace hydrogen in compartmentalized reactions that use NADPH as a cofactor, allowing to discern metabolic pathway activity in both the cytosol and the mitochondria.

MS-based metabolomics approaches are in expansion allowing to uncover metabolic bottlenecks for recombinant protein production in CHO cells. A big step in this direction was recently given by Link and coworkers (2015); these authors developed a

method for real-time metabolome profiling using high-resolution MS, which allows measuring the dynamic behavior of 300 metabolites upon a perturbation.

Integration of all levels of Omics data is a priority towards a global understanding of any biological system (Lewis et al. 2016). Little effort has been done so far on the simultaneous integration of the information from the genome, transcriptome, proteome and metabolome. Genome-scale models (GEMs) that aim to provide a comprehensive representation of the link between genotype and phenotype, while integrating data from all Omics layers have started to be developed for mammalian cells. These models include a collection of all known metabolic processes, involving metabolites, enzymes catalysing each reaction and the genes that code for the machinery required in these processes. Moreover, these models aim to accurately predict cellular behavior in culture, including growth rates, auxotrophies of cell lines and production titres. Quek et al (2014) used Recon 2, the human genome-scale metabolic network (Thiele et al. 2013), for the metabolic characterization of Human Embryonic Kidney (HEK) cells when L-alanyl-L-glutamine dipeptide was depleted. These genome-scale models have been developed also for *Saccharomyces cerevisiae*, *Pichia pastoris*, as well as *Mus musculus*, for industrial, medical and drug design applications (Gutierrez and Lewis 2015). With the recent publication of several CHO genomes, a specific GEM for CHO cells can now be reconstructed (Lewis et al. 2013; Xu et al. 2011).

Next generation sequencing is stimulating a genomic revolution in how we can approach the issue of productivity improvements (Kremkow et al. 2015; Monger et al. 2015). These advances will enable the modification of target DNA sequences and thus overcoming limitations imposed by secretory pathways or inefficient nutrient metabolism (Wurm and Hacker 2011). Likewise, the availability of the CHO genome sequence has allowed to use microRNAs for regulating gene expression. Through miRNA binding to specific mRNA sequences in the host cell it will be possible to impact

cell growth, apoptosis, metabolism, secretion and specific productivity of recombinant proteins (Datta et al. 2013).

Either by comparing clones with different productivity levels or by comparing clones in conditions that induce enhanced productivities (optimal temperature, pH or osmotic pressure, butyrate exposure, feeding strategies), common features of hyperproductivity are starting to be unveiled. These features are being revealed through several Omics levels, among four main functions: growth control, energy metabolism, redox balance and protein secretion (Seth et al. 2007). Instead of a few "master switches" that could dictate hyperproductivity, the data integrated through Systems Biology approaches suggests that a myriad of features may be responsible for that phenotype.

5.3 Final Remarks

Over the last three decades typical antibody titers obtained in bioreactors have increased by up to 100-fold. Further advances will depend upon improved understanding of metabolic flux regulation in producer cell lines, to provide the environmental and genetic conditions favourable to high product titer and quality. Resorting to complementary analytical techniques based on NMR and MS, isotopic tracer studies and MFA modeling approaches, the work developed in this thesis is a step forward in this direction, representing the most comprehensive characterization of GS-CHO cells metabolism to date. Nevertheless, there is still much to be learned and we anticipate ^{13}C-MFA studies using parallel experiments will continue to contribute to elucidate metabolic fluxes in relevant experimental settings.

5.4 Author contribution

Tiago Duarte wrote this chapter.

5.5 References

Ahn WS, Antoniewicz MR. 2011. Metabolic flux analysis of CHO cells at growth and non-growth phases using isotopic tracers and mass spectrometry. Metab Eng 13(5):598-609.

Bonarius HPJ, Hatzimanikatis V, Meesters KPH, Gooijer CD, Schmid G, Tramper J. 1996. Metabolic flux analysis of hybridoma cells in different culture media using mass balances. Biotechnology & Bioengineering 50:20.

Chen K, Liu Q, Xie L, Sharp PA, Wang DIC. 2001. Engineering of a mammalian cell line for reduction of lactate formation and high monoclonal antibody production. Biotechnology & Bioengineering 72(1):7.

Crown SB, Antoniewicz MR. 2012. Selection of tracers for 13C-metabolic flux analysis using elementary metabolite units (EMU) basis vector methodology. Metab Eng 14(2):150-61.

Datta P, Linhardt RJ, Sharfstein ST. 2013. An 'omics approach towards CHO cell engineering. Biotechnol Bioeng 110(5):1255-71.

Dean J, Reddy P. 2013. Metabolic analysis of antibody producing CHO cells in fed-batch production. Biotechnology & Bioengineering 110(6):13.

Goudar C, Biener R, Boisart C, Heidemann R, Piret J, de Graaf A, Konstantinov K. 2010. Metabolic flux analysis of CHO cells in perfusion culture by metabolite balancing and 2D [13C, 1H] COSY NMR spectroscopy. Metab Eng 12(2):138-49.

Gutierrez JM, Lewis NE. 2015. Optimizing eukaryotic cell hosts for protein production through systems biotechnology and genome-scale modeling. Biotechnology Journal 10:13.

Kim JY, Kim YG, Lee GM. 2012. CHO cells in biotechnology for production of recombinant proteins: current state and further potential. Appl Microbiol Biotechnol 93(3):917-30.

Kim SH, Lee GM. 2007. Down-regulation of lactate dehydrogenase-A by siRNAs for reduced lactic acid formation of Chinese hamster ovary cells producing thrombopoietin. Appl Microbiol Biotechnol 74(1):152-9.

Kremkow BG, Baik JY, MacDonald ML, Lee KH. 2015. CHOgenome.org 2.0: Genome resources and website updates. Biotechnol J 10(7):931-8.

Kruh J. 1982. Effects of sodium butyrate, a new pharmacological agent, on cells in culture. Molecular and Cellular Biochemistry 42:18.

Lewis AM, Abu-Absi NR, Borys MC, Li ZJ. 2016. The use of 'Omics technology to rationally improve industrial mammalian cell line performance. Biotechnol Bioeng 113(1):26-38.

Lewis CA, Parker SJ, Fiske BP, McCloskey D, Gui DY, Green CR, Vokes NI, Feist AM, Vander Heiden MG, Metallo CM. 2014. Tracing compartmentalized NADPH metabolism in the cytosol and mitochondria of mammalian cells. Mol Cell 55(2):253-63.

Lewis NE, Liu X, Li Y, Nagarajan H, Yerganian G, O'Brien E, Bordbar A, Roth AM, Rosenbloom J, Bian C and others. 2013. Genomic landscapes of Chinese hamster ovary cell lines as revealed by the Cricetulus griseus draft genome. Nat Biotechnol 31(8):759-65.

Link H, Fuhrer T, Gerosa L, Zamboni N, Sauer U. 2015. Real-time metabolome profiling of the metabolic switch between starvation and growth. Nat Methods 12(11):1091-7.

Liu B, Spearman M, Doering J, Lattova E, Perreault H, Butler M. 2014. The availability of glucose to CHO cells affects the intracellular lipid-linked oligosaccharide distribution, site occupancy and the N-glycosylation profile of a monoclonal antibody. J Biotechnol 170:17-27.

Metallo CM, Walther JL, Stephanopoulos G. 2009. Evaluation of 13C isotopic tracers for metabolic flux analysis in mammalian cells. J Biotechnol 144(3):167-74.

Mimura Y, Lund J, Church S, Dong S, Li J, Goodall M, Jefferis R. 2001. Butyrate increases production of human chimeric IgG in CHO-K1 cells whilst maintaining function and glycoform profile. Journal of Immunological Methods 247:12.

Monger C, Kelly PS, Gallagher C, Clynes M, Barron N, Clarke C. 2015. Towards next generation CHO cell biology: Bioinformatics methods for RNA-Seq-based expression profiling. Biotechnol J 10(7):950-66.

Niklas J, Heinzle E. 2012. Metabolic flux analysis in systems biology of mammalian cells. Adv Biochem Eng Biotechnol 127:109-32.

Ovádi J, Saks V. 2004. On the origin of intracellular compartmentation and organized metabolic systems. Molecular and Cellular Biochemistry 256/257:8.

Palermo DP, DeGraaf ME, Marotti KR, Rehberg E, Post LE. 1991. Production of analytical quantities of recombinant proteins in Chinese hamster ovary cells using sodium butyrate to elevate gene expression. Journal of Biotechnology 19:13.

Quek LE, Dietmair S, Hanscho M, Martinez VS, Borth N, Nielsen LK. 2014. Reducing Recon 2 for steady-state flux analysis of HEK cell culture. J Biotechnol 184:172-8.

Quek LE, Dietmair S, Kromer JO, Nielsen LK. 2010. Metabolic flux analysis in mammalian cell culture. Metab Eng 12(2):161-71.

Seo JS, Min BS, Kim YJ, Cho JM, Baek E, Cho MS, Lee GM. 2014. Effect of glucose feeding on the glycosylation quality of antibody produced by a human cell line, F2N78, in fed-batch culture. Appl Microbiol Biotechnol 98(8):3509-15.

Seth G, Charaniya S, Wlaschin KF, Hu WS. 2007. In pursuit of a super producer-alternative paths to high producing recombinant mammalian cells. Curr Opin Biotechnol 18(6):557-64.

Sung YH, Song YJ, Lim SW, Chung JY, Lee GM. 2004. Effect of sodium butyrate on the production, heterogeneity and biological activity of human thrombopoietin by recombinant Chinese hamster ovary cells. J Biotechnol 112(3):323-35.

Thiele I, Swainston N, Fleming RM, Hoppe A, Sahoo S, Aurich MK, Haraldsdottir H, Mo ML, Rolfsson O, Stobbe MD and others. 2013. A community-driven global reconstruction of human metabolism. Nat Biotechnol 31(5):419-25.

Vander Heiden MG, Cantley LC, Thompson CB. 2009. Understanding the Warburg effect: the metabolic requirements of cell proliferation. Science 324(5930):1029-33.

Wahrheit J, Nicolae A, Heinzle E. 2011. Eukaryotic metabolism: measuring compartment fluxes. Biotechnol J 6(9):1071-85.

Wahrheit J, Niklas J, Heinzle E. 2014. Metabolic control at the cytosol-mitochondria interface in different growth phases of CHO cells. Metab Eng 23:9-21.

Wurm FM, Hacker D. 2011. First CHO genome. Nat Biotechnol 29(8):718-20.

Xie L, Nyberg G, Gu X, Li H, Möllborn F, Wang DIC. 1997. Gamma-Interferon Production and Quality in Stoichiometric Fed-Batch Cultures of Chinese Hamster Ovary (CHO) Cells under Serum-Free Conditions. Biotechnology & Bioengineering 56(5):6.

Xu X, Nagarajan H, Lewis NE, Pan S, Cai Z, Liu X, Chen W, Xie M, Wang W, Hammond S and others. 2011. The genomic sequence of the Chinese hamster ovary (CHO)-K1 cell line. Nat Biotechnol 29(8):735-41.

Zhou W, Rehm J, Europa A, Hu WS. 1997. Alteration of mammalian cell metabolism by dynamic nutrient feeding. Cytotechnology 24:10.

APPENDIX

Table A1 List of CHO metabolic reactions considered in the model (Chapter 2)

#	Reversilibity	Reaction	Measured
		Glycolysis	
1	0	Glc+ATP=G6P+ADP	yes
2	-1	G6P=F6P	no
3	0	F6P+ATP=DHAP+GAP+ADP	no
4	-1	DHAP=GAP	no
5	-1	GAP+NAD+ADP=3PG+NADH+ATP	no
6	0	3PG+ADP=Pyr+ATP	no
		TCA cycle	
7	0	Pyr+NAD+CoASH=AcCoA+CO_2+NADH	no
8	0	AcCoA+Oxal=Cit+CoASH	no
9	0	Cit+NAD(P)=αKG+CO_2+NAD(P)H	no
10	0	αKG+CoASH+NAD=SucCoA+CO_2+NADH	no
11	-1	SucCoA+GDP=Succ+GTP+CoASH	no
12	-1	Succ+FAD=Fum+$FADH_2$	no
13	-1	Fum=Mal	no
14	-1	Mal+NAD=Oxal+NADH	no
		Pyruvate fates	
15	-1	Pyr+NADH=Lac+NAD	yes
16	-1	Pyr+Glu=Ala+αKG	no
		Pentose Phosphate Pathway	
17	0	3G6P+6NADP=3CO_2+3R5P+6NADPH	no
		Anaplerotic Reaction	
18	-1	Mal+NAD(P)=Pyr+HCO_3+NAD(P)H	no
		Amino Acid Metabolism	
19	-1	Glu+NAD(P)=αKG+NH_4+NAD(P)H	no
20	-1	Oxal+Glu=Asp+αKG	no
21	-1	Gln+ADP=Glu+ATP+NH_4	no
22	0	Thr+NAD+CoASH=Gly+NADH+AcCoA	no
23	-1	Ser+THF+NADP=Gly+NADPH+N10FTHF	no
24	-1	N_{10}FTHF+ADP=ATP+Formate+THF	yes
25	0	Ser=Pyr+NH_4	no
26	0	Thr= αKb+NH_4	no

27	0	αKb+CoASH+NAD+HCO_3+ATP=SucCoA+ADP+NADH+CO_2	no
28	0	Trp=Ala+2CO_2+αKa	no
29	0	Lys+2αKG+3NAD(P)+FAD=αKa+2Glu+3NADPH+$FADH_2$	no
30	0	αKa+2CoASH+2NAD=2AcCoA+2NADH+2CO_2	no
31	0	Val+αKG+CoASH+NAD=IsobutCoA+Glu+CO_2+NADH	no
32	0	IsobutCoA+FAD+2NAD+HCO_3+ATP=SucCoA+ADP+$FADH_2$+2NADH+CO_2	no
33	0	IsobutCoA=Isobut	yes
34	0	Ile+αKG+2CoASH+2NAD+FAD+HCO3+ATP=AcCoA+SucCoA+ADP+Glu+CO_2+2 NADH+$FADH_2$	no
35	0	Leu+αKG+CoASH+NAD=IsovalCoA+Glu+CO_2+NADH	no
36	0	IsovalCoA+FAD+ATP+CO_2+SucCoA+CoASH=3AcCoA+Succ+$FADH_2$+ADP	no
37	0	IsovalCoA=Isoval	yes
38	0	Phe+NADH=Tyr+NAD	no
39	0	Tyr+αKG+SucCoA+CoASH=Fum+2AcCoA+Succ+Glu+CO_2	no
40	0	Met+Ser+ATP=αKb+NH_4+AMP	no
41	-1	Asn=Asp+NH_4	no
42	-1	Pro+NAD(P)=Glu+NAD(P)H	no
43	0	Arg+αKG+NAD(P)=2Glu+NAD(P)H+Urea	no
44	0	His=Glu+NH_4	no
		Glycogen Synthesis	
45	0	G6P=G1P	no
46	0	G1P+UMPRN+2ATP=UDPG+2ADP	no
47	0	UDPG=Glycogen+UDP	no
		Nucleotide Synthesis	
48	0	R5P+ATP=PRPP+AMP	no
49	0	PRPP+2Gln+Gly+Asp+5ATP+CO_2+2N_{10}FTHF=IMP+2Glu+Fum+5ADP+2THF	no
50	0	IMP+Asp+GTP=AMPRN+Fum+GDP	no
51	0	IMP+Gln+ATP+NAD=GMPRN+Glu+AMP+NADH	no
52	0	HCO_3+NH_4+Asp+2ATP+NAD=Orotate+2ADP+NADH	no
53	0	Orotate+PRPP=UMPRN+CO2	no
54	0	UMPRN+Gln+ATP=CMPRN+Glu+ADP	no
55	0	AMPRN=dAMP	no
56	0	GMPRN=dGMP	no
57	0	CMPRN=dCMP	no
58	0	UMPRN=dTMP	no
		Lipid Synthesis	

59	0	Choline+ATP=Pcholine+ADP	no
60	0	Pcholine+18AcCoA+Glyc3P+22ATP+33NADH=PC+16ADP+6AMP+33NAD	no
61	-1	PC+Ser=PS+Choline	no
62	0	PS=PE+CO_2	no
63	-1	Choline+Glyc3P=Glyc3PC	no
64	0	G6P=Inositol	no
65	0	Inositol+18AcCoA+Glyc3P+22ATP+33NADH=PI+16ADP+6AMP+33NAD	no
66	0	18AcCoA+2Glyc3P+22ATP+33NADH=PG+16ADP+6AMP+33NAD	no
67	0	2PG=DPG+Glyc	no
68	0	16AcCoA+Ser+Choline+16ATP+29NADPH=SM+2CO_2+14ADP+2AMP+29NADP	no
69	0	18AcCoA+18ATP+14NADPH=Cholesterol+9CO_2+18ADP+14NADP	no
		Biomass Formation	
70	0	160.1015Ala+235.2056Glu+70.3787Gln+174.6799Gly+114.9787Ser+147.4132Lys+157.4070Leu+82.6648Ile+91.8543Arg+169.4920Asp+95.7754Thr+118.3569Val+40.0354Met+67.4027Phe+47.4956Tyr+36.2551His+55.5590Pro+70.3787Asn+11694463ATP+8.943AMPRN+4.878Cholesterol+14.9321CMPRN+4.0108dAMP+2.6829dCMP+2.6829dGMP+4.0108dTMP+0.8130DPG+75.6090Glycogen+16.9104GMPRN+18.6990PC+7.046PE+0.271PG+2.71PI+0.813PS+2.168SM+8.943UMPRN+9.2297Trp=1Biomass+11694463ADP	yes
		Other by-products	
71	-1	AcCoA+AMP=Acetate+CoASH+ATP	yes
72	-1	DHAP+NADH=Glyc3P+NAD	no
73	-1	Glyc3P=Glyc	no
		IgG Glycosylation	
74	-1	UDPG=UDPGal	no
75	0	Glc+ATP+GTP=GDPMann+ADP	no
76	0	F6P+Gln+AcCoA+UTP=UDPNAG+Glu+CoASH	no
77	0	UDPNAG+ATP+3PG+CTP=CMPSialic+UDP+ADP	no
78	0	GDPMann+NADPH=GDPFuc+NADP	no
		IgG Formation	
79	0	428.7 Ala + 362.75 Glu + 351.76 Gln + 516.64 Gly + 934.36 Ser + 472.67 Lys + 516.64 Leu + 175.88 Ile + 307.79 Arg + 296.8 Asp + 626.57 Thr + 714.51 Val + 65.954 Met + 285.8 Phe + 285.8 Tyr + 164.89 His + 505.65 Pro + 263.82 Asn + 142.9 Trp + 10.992 GDPFuc + 54.962 UDPNAG + 32.977 GDPMann + 21.985 UDPGal + 21.985 CMPSialic = 32.977 GDP + 21.985 UDP + 21.985 CMP + 1 IgG	yes
		Transport Reactions	
80	-1	=Asp	yes
81	-1	Gly=	yes
82	-1	=Ser	yes
83	-1	=Glu	yes

84	-1	=Tyr	yes
85	-1	Ala=	yes
86	-1	=Arg	yes
87	-1	=Asn	yes
88	-1	=Gln	yes
89	0	=His	yes
90	0	=Ile	yes
91	0	=Leu	yes
92	0	=Lys	yes
93	0	=Met	yes
94	0	=Phe	yes
95	-1	=Pro	yes
96	0	=Thr	yes
97	0	=Trp	yes
98	0	=Val	yes
99	-1	=Choline	yes
100	-1	NH4=	yes
101	0	CO2=	no
102	-1	Cit=	yes
103	-1	Fum=	yes
104	-1	Pyr=	yes
105	-1	Succ=	yes
106	-1	Mal=	yes
107	-1	Glyc=	yes
108	-1	Pcholine=	yes
109	-1	Glyc3PC=	yes
110	-1	Formate=	yes
111	-1	Acetate=	yes
112	0	Isobut=	yes
113	0	Isoval=	yes
114	0	Biomass=	yes
115	0	=Glc	yes
116	-1	Lac=	yes
117	0	IgG=	yes

Notes to reactions:

21: Considered reversible to include glutamine synthetase activity in GS-CHO cells; ATP is taken in account since this is the main direction of flow.

42: Considered reversible and simplified to include Pro synthesis (1 ATP and another NAD(P)H is missing for the Pro synthesis direction).

70: Metabolic requirements reflect the nmol content in 10^6 cells with a CDW of 271 pg/cell. For butyrate-treated cultures during stationary phase, the coefficients were adjusted to a CDW of 368 pg/cell.

73: Considered reversible to include Glyc kinase activity; ATP not considered since Glyc is produced.

79: Metabolic requirements reflect the nmol content in 1 mg of IgG.

Experience

Creator of the website/hub Sciencemotionology.com 2014 to present

- Promoting the fields of scientific animation, illustration and visual communication

PhD in Systems Biology | Portugal, Netherlands 2012 to 2016

- PhD thesis: *Probing CHO cells metabolism using metabolomics and fluxomics tools*
- Institution: iBET/ITQB-UNL (Instituto de Biologia Experimental e Tecnológica/Instituto de Tecnologia Química e Biológica – Universidade Nova de Lisboa), Oeiras, Portugal
- Experience: mammalian cell cultures; from shake flasks up to 2L bioreactors; enzymatic assays; SDS-PAGE; development of quantitative assays/protocols using: ^{1}H-NMR; ^{13}C-isotopes; GC-MS; LC-MS
- Collaborative work: Cell Systems Engineering group – TU Delft, 2014, The Netherlands
  - Application of GC and LC-MS methods for the analysis of the metabolome and fluxome of CHO cells

Research Assistant | iBET | Portugal 2010 to 2011

- Project: *2D fluorometry: a powerful tool to improve mammalian cell process development*
- iBET (Instituto de Biologia Experimental e Tecnológica)

Research Technician | iBET | Portugal, Germany 2009 to 2010

- Set up of the Bayer Schering Pharma Satellite lab @ iBET
- Project concerning high throughput clone selection, enzymatic assays
- Formal training at Bayer Healthcare, Cologne, Germany

Young Researcher | Genentech | USA 2008 to 2009

- Process Research and Development Department
- Project related to downstream – mAb purification

Analyst | Bank BPI | Portugal 2007 to 2008

- Project: Internal Processes Optimization aiming Paper Consumption Reduction

MSc. in Biological Engineering | Portugal, Germany 2001 to 2007

- Master thesis: *Gas-liquid mass transfer in elevated viscosity Corynebacterium glutamicum DM1730 culture medium*
- Institution: IST/UL (Instituto Superior Técnico/ Universidade de Lisboa), Portugal
- Collaboration: AVT group, RWTH Aachen, Germany (ERASMUS Program)

Volunteer Work

- Research assistant: Studies aiming vaccine production against *Burkholderia cepacia* infections in patients with cystic fibrosis, 2006, BSRG/IST-UL, Lisboa, Portugal

Scientific Publications

- Sá JV, Duarte TM, Carrondo MJT, Alves PM, Teixeira AP, 2014, Metabolic Flux Analysis: A Powerful Tool in Animal Cell Culture, Animal Cell Culture, Springer, Cell Engineering 9:521-539
- Duarte TM/Carinhas N, Barreiro LC, Carrondo MJT Alves PM, Teixeira AP, 2014, Metabolic responses of CHO cells to limitation of key amino acids. Biotechnol. Bioeng 111(10):2095–2106
- Giese H, Azizan A, Kümmel A, Liao A, Peter CP, Afonso J, Hermann R, Duarte TM, Büchs J, 2013, Liquid films on shake flask walls explain increasing maximum oxygen transfer capacities with elevating viscosity, Biotechnol. Bioeng. 111(2):295-308
- Duarte TM/Carinhas N, Barreiro LC, Carrondo MJT, Alves PM, Teixeira AP, 2013, Metabolic signatures of GS CHO cell clones associated with butyrate treatment and culture phase transition, Biotechnol. Bioeng. 110(12):3244-57
- Duarte TM, Carinhas N, Silva AC, Alves PM, Teixeira AP. 2013. 1H-NMR protocol for exometabolome analysis of cultured mammalian cells. Animal Cell Biotechnology - Methods and Protocols, 3rd Edition, Springer, Part III:237-247
- Liu HF, McCooey B, Duarte T, Meyers DE, Hudson T, Amanullah A, Reis R, Kelley BD, 2011, Exploration of overloaded cation exchange chromatography for monoclonal antibody purification, Journal of chromatography. A, 1218(39):6943-52.
- Teixeira AP, Duarte TM, Carrondo MJTC, Alves PM, 2011, Synchronous Fluorescence Spectroscopy as a Novel Tool to enable PAT Applications in Bioprocesses, Biotechnol. Bioeng, 108(8):1852-61
- Teixeira AP, Duarte TM, Oliveira R, Carrondo MJTC, Alves PM, 2011, High-throughput analysis of animal cell cultures using two dimensional fluorometry, J. Biotechnology, 151:255-260
- Duarte TM, Carrondo MJT, Alves PM, Teixeira AP 2011, Fluorescence-based tools to improve biopharmaceutical process development, ESACT Conference Proceedings, Vienna, Austria, 5(8):O5
- Azizan A, Duarte T, Liao A, Peter CP, Büchs J, 2007, Gas-liquid Mass Transfer in Elevated Viscosity Medium with *Corynebacterium glutamicum* DM 1730 Culture Medium, Chemie Ingenieur Technik, 79(9):1473

Scientific Conferences

- Duarte TM, 2016, Sciencemotionology: a 4ª dimensão da ciência, 4th Science Communication Congress, Pavilhão do Conhecimento, Lisboa, Portugal

- Duarte TM, 2016, Sciencemotionology: Promoting the fields of scientific animation and illustration, EMBO Conference: Visualizing Biological Data (VIZBI), EMBL Heidelberg, Germany
- Teixeira AP, Duarte TM, Carinhas N, Seifar R, Wahl AS, Alves PM, 2015, Metabolic profiling of mAb-producing CHO cells using parallel labeling experiments, 8th Conference on Recombinant Protein Production, Palma, Mallorca, Spain
- Teixeira AP, Duarte TM, Carinhas N, Carrondo MJT, Alves PM, 2015, Comprehensive view of CHO cells metabolism using key ^{13}C-substracts, ESACT 24th meeting, Barcelona, Spain
- Duarte TM, Carinhas N, Carrondo MJT, Alves PM, Teixeira AP, 2014, Insights into the metabolism of CHO cells under key nutrient limitations, Cell Engineering XIV, Quebec City, Canada
- Carinhas N, Duarte TM, Barreiro LC, Carrondo MJT, Alves PM, Teixeira AP, 2013, Assessing the exometabolome and fluxome of CHO cells for predictive bioprocess improvement, ESACT 23rd meeting, Lille, France
- Duarte TM, Carinhas N, Barreiro LC, Carrondo MJT, Alves PM, Teixeira AP, 2013, Metabolic characterization of MAb producing CHO cells for predictive bioprocess improvement, 7th Conference on Recombinant Protein Production, Laupheim, Germany
- Duarte TM, Alves PM, Teixeira AP, 2012, Fluxome profiling of CHO cells under different productive states, Metabolic Engineering IX, Biarritz, France
- Duarte TM, Carrondo MJT, Alves PM, Teixeira AP, 2011, Fluorescence-based tools to improve biopharmaceutical process development, ESACT 22nd meeting, Vienna, Austria
- Duarte TM, Fernandes F, Vidigal J, Fernandes P, Bandeira V, Silva C, Sousa M, Portugal C, Crespo JP, Alves PM, Teixeira AP, 2011, Development of fluorescence-based PAT enabling tools for animal cell processes, 10th Conference on Protein Expression in Animal Cells, Cascais, Portugal
- Duarte TM, Fernandes F, Vidigal J, Fernandes P, Bandeira V, Sousa M, Portugal C, Crespo JP, Alves PM, Teixeira AP, 2011, Application of synchronous fluorescence spectroscopy to monitor animal cell processes, Chempor, Caparica, Portugal
- Teixeira AP, Duarte TM, Carrondo MJT, Alves PM, 2010, Improving animal cells process development with fluorescence-based methods, ETW 5th, Ittingen, Switzerland

Scientific Workshops

- 4th CERMAX practical course on basic NMR spectroscopy, 2011, ITQB/IBET, Oeiras, Portugal
- Visualizing Molecular Processes with 3D Animation, 2010, Harvard Medical School Portugal, IPATIMUP, Porto, Portugal
- Sea Life Scientific Illustration Course, 2007, Oceanário de Lisboa, Portugal

Awards

- EMBL Advanced Training Centre Partnership Programme Fellowship, 2016, EMBL Heidelberg, Germany
- PhD Scholarship (SFRH/BD/81553/2011), FCT Portugal

Languages

- Portuguese | mother tongue
- English | Very good working knowledge | TOEFL iBT 2013 100/120
- French | Basic conversational knowledge
- Spanish | Basic conversational knowledge
- German | Basic conversational knowledge

Other Skills

- 3D graphics, 2015, SAE Institute Amsterdam; Certificate of Accomplishment
- Scientific Writing: Writing in the Sciences, 2014, Stanford University Online; Certificate of Accomplishment
- Entrepreneurship: Bioentrepreneurship, 2013, Nova School of Business, Certificate of Accomplishment (18 out of 20)
- Organization:
  - InTeraQB, 2013 and 2014, promoting interaction between researchers and students across ITQB campus
  - Conference 2005: *Cloning – Human Genome: a psychological approach*, IST/UL – ISPA
  - Bioempresas 2004, Conferences on Biological Engineering, IST/UL, Portugal
- Software:
  - MATLAB
  - MS Office (PowerPoint; Excel; Word; Visio)
  - Autodesk Maya
  - After Effects
  - Blender
  - Photoshop

ITQB-UNL | Av. da República, 2780-157 Oeiras, Portugal
Tel (+351) 214 469 100 | Fax (+351) 214 411 277

www.itqb.unl.pt